IJOER
RESEARCH JOURNAL

International Journal
of
Engineering Research & Science

Preface

We would like to present, with great pleasure, the inaugural volume-3, Issue-4, April 2017, of a scholarly journal, *International Journal of Engineering Research & Science*. This journal is part of the AD Publications series *in the field of Engineering, Mathematics, Physics, Chemistry and scienc Research Development*, and is devoted to the gamut of Engineering and Science issues, from theoretical aspects to application-dependent studies and the validation of emerging technologies.

This journal was envisioned and founded to represent the growing needs of Engineering and Science as an emerging and increasingly vital field, now widely recognized as an integral part of scientific and technical investigations. Its mission is to become a voice of the Engineering and Science community, addressing researchers and practitioners in below areas

Chemical Engineering	
Biomolecular Engineering	Materials Engineering
Molecular Engineering	Process Engineering
Corrosion Engineering	
Civil Engineering	
Environmental Engineering	Geotechnical Engineering
Structural Engineering	Mining Engineering
Transport Engineering	Water resources Engineering
Electrical Engineering	
Power System Engineering	Optical Engineering
Mechanical Engineering	
Acoustical Engineering	Manufacturing Engineering
Optomechanical Engineering	Thermal Engineering
Power plant Engineering	Energy Engineering
Sports Engineering	Vehicle Engineering
Software Engineering	
Computer-aided Engineering	Cryptographic Engineering
Teletraffic Engineering	Web Engineering
System Engineering	
Mathematics	
Arithmetic	Algebra
Number theory	Field theory and polynomials
Analysis	Combinatorics
Geometry and topology	Topology
Probability and Statistics	Computational Science
Physical Science	Operational Research
Physics	
Nuclear and particle physics	Atomic, molecular, and optical physics
Condensed matter physics	Astrophysics
Applied Physics	Modern physics
Philosophy	Core theories

Chemistry	
Analytical chemistry	Biochemistry
Inorganic chemistry	Materials chemistry
Neurochemistry	Nuclear chemistry
Organic chemistry	Physical chemistry
Other Engineering Areas	
Aerospace Engineering	Agricultural Engineering
Applied Engineering	Biomedical Engineering
Biological Engineering	Building services Engineering
Energy Engineering	Railway Engineering
Industrial Engineering	Mechatronics Engineering
Management Engineering	Military Engineering
Petroleum Engineering	Nuclear Engineering
Textile Engineering	Nano Engineering
Algorithm and Computational Complexity	Artificial Intelligence
Electronics & Communication Engineering	Image Processing
Information Retrieval	Low Power VLSI Design
Neural Networks	Plastic Engineering

Each article in this issue provides an example of a concrete industrial application or a case study of the presented methodology to amplify the impact of the contribution. We are very thankful to everybody within that community who supported the idea of creating a new Research with IJOER. We are certain that this issue will be followed by many others, reporting new developments in the Engineering and Science field. This issue would not have been possible without the great support of the Reviewer, Editorial Board members and also with our Advisory Board Members, and we would like to express our sincere thanks to all of them. We would also like to express our gratitude to the editorial staff of AD Publications, who supported us at every stage of the project. It is our hope that this fine collection of articles will be a valuable resource for *IJOER* readers and will stimulate further research into the vibrant area of Engineering and Science Research.

Mukesh Arora

(Chief Editor)

Board Members

Dr. S.R.Boselin Prabhu

Ph.D, Wireless Sensor Networks, M.E. Network Engineering, Excellent Professional Achievement Award Winner from Society of Professional Engineers Biography Included in Marquis Who's Who in the World (Academic Year 2015 and 2016). Currently Serving as Assistant Professor in the department of ECE in SVS College of Engineering, Coimbatore.

Dr. Maheshwar Shrestha

Postdoctoral Research Fellow in DEPT. OF ELE ENGG & COMP SCI, SDSU, Brookings, SD Ph.D, M.Sc. in Electrical Engineering from SOUTH DAKOTA STATE UNIVERSITY, Brookings, SD.

Zairi Ismael Rizman

Senior Lecturer, Faculty of Electrical Engineering, Universiti Teknologi MARA (UiTM) (Terengganu) Malaysia Master (Science) in Microelectronics (2005), Universiti Kebangsaan Malaysia (UKM), Malaysia. Bachelor (Hons.) and Diploma in Electrical Engineering (Communication) (2002), UiTM Shah Alam, Malaysia

Dr. D. Amaranatha Reddy

Ph.D.(Postdocteral Fellow,Pusan National University, South Korea), M.Sc., B.Sc. : Physics.

Dr. Dibya Prakash Rai

Post Doctoral Fellow (PDF), M.Sc.,B.Sc., Working as Assistant Professor in Department of Physics in Pachhuncga University College, Mizoram, India.

Dr. Pankaj Kumar Pal

Ph.D R/S, ECE Deptt., IIT-Roorkee.

Dr. P. Thangam

BE(Computer Hardware & Software), ME(CSE), PhD in Information & Communication Engineering, currently serving as Associate Professor in the Department of Computer Science and Engineering of Coimbatore Institute of Engineering and Technology.

Dr. Pradeep K. Sharma

PhD., M.Phil, M.Sc, B.Sc, in Physics, MBA in System Management, Presently working as Provost and Associate Professor & Head of Department for Physics in University of Engineering & Management, Jaipur.

Dr. R. Devi Priya

Ph.D (CSE),Anna University Chennai in 2013, M.E, B.E (CSE) from Kongu Engineering College, currently working in the Department of Computer Science and Engineering in Kongu Engineering College, Tamil Nadu, India.

Dr. Sandeep

Post-doctoral fellow, Principal Investigator, Young Scientist Scheme Project (DST-SERB), Department of Physics, Mizoram University, Aizawl Mizoram, India- 796001.

Mr. Abilash

MTech in VLSI, BTech in Electronics & Telecommunication engineering through A.M.I.E.T.E from Central Electronics Engineering Research Institute (C.E.E.R.I) Pilani, Industrial Electronics from ATI-EPI Hyderabad, IEEE course in Mechatronics, CSHAM from Birla Institute Of Professional Studies.

Mr. Varun Shukla

M.Tech in ECE from RGPV (Awarded with silver Medal By President of India), Assistant Professor, Dept. of ECE, PSIT, Kanpur.

Mr. Shrikant Harle

Presently working as a Assistant Professor in Civil Engineering field of Prof. Ram Meghe College of Engineering and Management, Amravati. He was Senior Design Engineer (Larsen & Toubro Limited, India).

Table of Contents

Mycelium-bound lipase production of immobilized whole cell from a wild-type *Penicilium citrinum* strain

R. T. Lima[1], P. M. Sato[2], R. M. Pereira[3], G. S. S. Andrade[4]

Institute of Science and Technology, University of Alfenas, Poços de Caldas-MG

Abstract— Pencillium citrinum whole cell was cultivated and immobilized in a low cost support aiming to be used as an active and stable biocatalyst for modification of oil and fats. PUF (polyurethane foam) coated in 6mm was used as support and the immobilization occurred as a natural consequence of cell growth. Olive oil was the mycelium-bound lipase inductor and the production was optimized by statistical analysis of pH and temperature effects in culture broth. Immobilized whole cell was characterized as a natural immobilized lipase and all the assays were made using olive oil hydrolysis. The mycelium-bound lipase production was improved by adjustment the culture broth to pH 7.5 and 35°C of incubation temperature. The SEM micrographs showed the entangled cells morphology and a high adhesion in support matrix. Biochemical characterization revealed maximum values of lipase activity in pH 8 and 40°C and a half-life time at 60°C was 2.2h. Results from kinetics study indicated the biocatalyst follow the Michaelis-Menten kinetic. The potential catalytic of immobilized whole cells was assessed in soybean oil hydrolysis and 55.7% of degree of hydrolysis was attained in 12h.

Keywords— whole cell, mycelium-bound lipase, immobilization, hydrolysis, oil.

I. INTRODUCTION

Generally, enzymes associated with the mycelia are referred to as mycelium-bound enzymes. Mycelium-bound enzymes are economically attractive because they can be produced at low cost and considered as naturally immobilized enzymes that may be used without the laborious operations of isolation, purification and addition of co-factors, *etc* [1]. The whole-cell biocatalyst includes the cell wall- or the cell membrane-bound lipase (i.e., intracellular enzyme), which can be used instead of extracellular lipase [2]. Over the past decades, mycelium-bound lipase of filamentous fungus has been extensively studied as an alternative biocatalyst in biotransformation processes [3].

Mycelium-bound lipase can be used directly as suspended free cells or immobilized within biomass support particles as whole cells biocatalyst [4]. Immobilization of whole cells provides stability as well as improves reusability [5]. The concept of immobilized whole cells is different for those applied in fermentation process, since whole cells keep the enzymes in active state, without cell replication. Whole cell immobilization requires the same techniques applied to conventional enzyme immobilization, such as adsorption, covalent attachment, cross-link and entrapment, although the most useful for filamentous fungi is the entrapment in porous support, due to its morphology [3].

The literature has shown that whole cells immobilization in reticulated polyurethane foam (PUF) is a convenient way to spontaneously obtain immobilized whole cells. So far, a few strains were studied as potential mycelium-bound lipase producers, such as *Rhizopus* sp. [6, 7, 8], *Aspergillus* sp. [9, 10, 11] and *Mucor* sp. [12, 13, 14]. The genus *Penicillium* is also a known fungal producer of lipases which are employed in the dairy industry and in a number of bioconversions of industrial importance [15], nevertheless its potential as whole cells biocatalyst were not enough explored.

In this context the present work aims to investigate the potential of a wild-type *Penicillium citrinum* strain as a mycelium-bound lipase producer and its immobilization in PUF. The objective was to evaluate the catalytic potential of the immobilized whole cells in enzymatic modification of fats and oils, such as hydrolysis, transesterification and interesterification processes. For this, firstly, the physicochemical parameters were optimized to enhance the production of mycelium-bound lipase and then the immobilized whole cells produced were characterized as a conventional immobilized lipase. Additionally, the efficiency biocatalytic process of soybean hydrolysis with immobilized whole cells was evaluated on batch reaction.

II. MATERIALS AND METHODS

2.1 Materials

PUF (Esfrebon^{MR}) with an average porosity of 0.76 ± 0.11mm and a density of 0.02 ± 0.01 g cm^{-3} was purchased from a local market, cut into 6mm cubes [13], and treated with nitric acid solution (0.1mol L^{-1}) to remove impurities. The PUF was then

washed twice with distilled water and dried in an oven at 60 ∘C for 24h. Olive and soybean oils were purchased locally. Arabic gum (Synth), ethanol (Synth) and acetone (Synth) were of analytical grade.

2.2 Microorganism and growth media

Fungal strain *P. citrinum* URM 4216 was purchased from culture collection URM (University Recife Mycologia) at Federal University of Pernambuco (Pernambuco, Brazil). PDA (Potato Dextrose Agar—Difco) was used as solid culture medium for fungi propagation. The culture medium used for cell growth contained soy peptone (Himedia) 70 g L^{-1}, $NaNO_3$ (Vetec) 1.0 g L^{-1}, KH_2PO_4 (Synth) g L^{-1}, $MgSO_4 \cdot 7H_2O$ (Vetec) 0.5 g L^{-1}, and olive oil (Carbonell) 30 g L^{-1}.

2.3 Preparation of immobilized whole cells biocatalyst

Whole cells immobilized were prepared by inoculating a suspension of fungal cells spores (10 – 50 mL L^{-1}) into 250 mL conical flasks containing 100 mL of culture medium (pH adjusted) and 0.6 g of cuboidal PUF sterilized previously. The system was incubated at controlled temperature for a maximum period of 120 h. The immobilized whole cell biocatalyst was separated from the liquid medium by filtration, washed twice with distilled water and acetone, and dried under vacuum for 24h.

2.4 Experimental design

A 2^2 full experimental design with three replicates at the center point was used to evaluate the effect of physic-chemical parameters pH (X_1) and temperature (X_2) in the mycelium-bound lipase production. The lipase activities were the response variable of the design experiment and assayed by the hydrolysis of olive oil emulsion [13]. The experimental design results were analyzed using Statistica version 7 (StatSoft Inc., USA).

2.5 Determination of morphological, biochemical and kinetics properties

Surface morphology of immobilized whole cells was observed by Scanning Electron Microscopy (SEM) (LEO 440i Oxford). The pH and temperature optimal of the immobilized whole cell lipase was studied within the 6.0 – 8.5 and 30–55°C range, respectively. The influence of substrate concentration (olive oil) on the hydrolytic activities was also analyzed in the hydrolysis assay varying the proportion of oil in the emulsion from 5 to 70% wt. Michaelis-Menten constant (K_m) and the maximum velocity (V_{max}) were calculated using OriginPro version 8 (Originlab Corporation). The thermal stability of lipase was determined by incubating the whole cells at 60∘C for 150 min with periodical withdrawals every 30 min to quantification the residual lipase activity and calculation the denaturation rate constant (k_D) and half-life time ($t_{1/2}$). In all the experiments, the lipase activities were assayed by the hydrolysis of olive oil emulsion 10 % wt [13].

2.6 Soybean oil hydrolysis

Batch hydrolytic reactions were performed in 250mL conical flasks in an orbital shaker (170 rpm) at 37°C and atmospheric pressure for 24 h, containing 50 g emulsion soybean oil (oil/water ratio = 1/4; 2.5% Arabic gum). After addition of 10% wt. of immobilized whole cells, small samples were removed from the reactor periodically to quantify the free fatty acids formed. The degree of hydrolysis was calculated according to Equation (1) [16].

$$\% \, Hidrólise = \frac{(V_a - V_b) * M * 10^{-3} * MWm}{Wt * f} * 100 \tag{1}$$

where Va is the volume of potassium hydroxide solution (KOH) required during titration of sample; Vb is the volume of potassium hydroxide solution (KOH) required during titration of control; M is the KOH molarity (0.02 M); MWm is the average molecular weight of fatty acids (278.6 $gmol^{-1}$); Wt is the weight of the sample taken and f is the fraction of oil at start of reaction.

III. RESULTS AND DISCUSSION

3.1 Mycelium-bound lipase immobilization

P. citrinum whole cell was prepared and immobilized in PUF in a medium containing olive oil at 30°C for 120h of incubation time. The biomass growth kinetic and lipase activity of mycelium and extract broth are showed in Fig.1. As observed, there was no expressive growth up to 48 h of incubation time. After that, biomass growth curve followed typical microorganism growth and the highest biomass concentration (49.3 ± 1.5 g L^{-1}) was attained in 96 h of incubation. Mycelium-bound lipase production was confirmed by the high lipase activity reached, in order to 105.5 ± 3.0 U g^{-1}, in

comparison with low value obtained by extract broth. In addition, it was also verified a proportional relation between the fungal growth and mycelium-bound lipase activity.
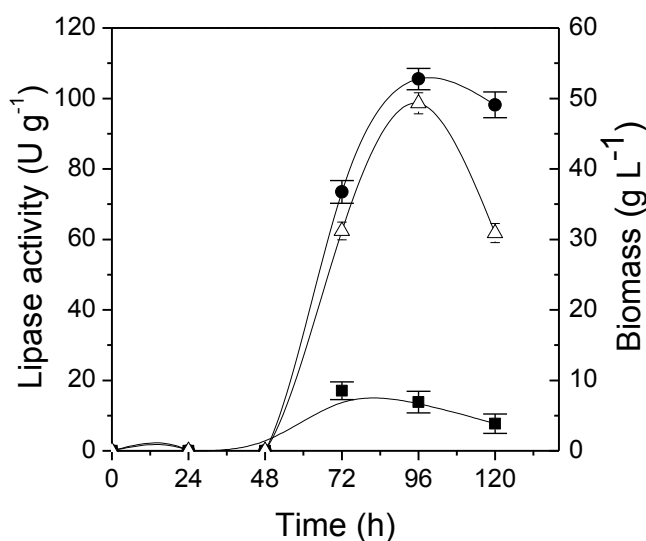
FIGURE 1: PROFILE OF BIOMASS GROWTH (-△-), MYCELIUM-BOUND LIPASE ACTIVITY (-●-) AND EXTRACT BROTH LIPASE ACTIVITY (-■-). CULTIVATION CONDITIONS: PH 6.8 (WITHOUT ADJUSTMENT), 30 °C, 0.3 L INOCULUM

Previous work [12] reported an unsatisfactory mycelium-bound lipase activity using *P. citrinum* whole cells immobilized in PUF, with only 10.53 ± 0.67 U g^{-1} lipase activity. However, a study about the profile of biomass growth was not performed, adopting 72h of incubation time. As can be observed in Fig. 1, 72h is considered to be insufficient since the biomass growth was still at the lag phase. Therefore, the incubation time of 96h was adopted in all followed experiments.

3.2   Experimental design

Optimization of culture conditions is very important as they affect the enzyme production and the ratio between mycelium-bound and extracellular lipases produced by the microorganism [3]. Studies of temperature and pH effects on growth and metabolite production are scare with respect to filamentous fungi, mainly *P. citrinum* cells. In this work, a full factorial 2^2 design with three replicates in the center points was used to study the combined effect of the pH and temperature in the culture medium to enhance the mycelium-bound lipase production by *P. citrinum* immobilized whole cells. In all runs olive oil was used as a lipase inductor and an incubation time of 96 h was assumed. The experimental design is shown in Table 1 together with the experimental results in terms of lipase activity.

TABLE 1
EXPERIMENTAL DESIGN AND RESULTS ACCORDING TO A FULL 2^2 FACTORIAL DESIGN TO EVALUATE THE INFLUENCE OF THE VARIABLES PH AND TEMPERATURE IN MYCELIUM-BOUND LIPASE PRODUCTION BY *P. CITRINUM* IMMOBILIZED WHOLE CELLS

Runs	Independent variables (coded values in parenthesis)		Response variable
	pH (X_1)	Temperature (°C) (X_2)	Lipase activity (U g^{-1})
1	6.5 (-1)	25 (-1)	67.92
2	6.5 (-1)	35 (+1)	100.83
3	7.5 (+1)	25 (-1)	130.16
4	7.5 (+1)	35 (+1)	162.78
5	7.0 (0)	30 (0)	71.10
6	7.0 (0)	30 (0)	64.53
7	7.0 (0)	30 (0)	67.33

Results in Table 1 showed the strong influence of pH and temperature in mycelium-bound lipase production. Lipase activity were varied about $67 - 163$ U g^{-1} and the maximum value was attained at the highest pH level (7.5) and temperature (35°C) as shown in run 4. Much lower values were found at center points (pH 7.0 and 30°C) and at the lowest level (pH 6.5 and 25°C), indicating the positive effects of pH and temperature on the mycelium-bound activity. Similar results are found in literature, since most of the lipases from *Penicillia* are reported to be most active and stable in neutral to alkaline pH range and high temperatures [15, 17].

This hypothesis was confirmed by the statistical analysis of these results that showed significant and positive effects for both studied variables at a 95 % confidence level, unlike interaction, as described in Table 2.

TABLE 2
ESTIMATED EFFECTS, STANDARD ERRORS AND STUDENT'S T TEST FOR MYCELIUM-BOUND LIPASE PRODUCTION BY *P. CITRINUM* IMMOBILIZED WHOLE CELLS USING A FULL 2^2 FACTORIAL DESIGN

Variable	Effects	Standard error	p
Mean	119.27	± 1.70	0.0002*
X1	64.16	± 3.41	0.0028*
X2	33.86	± 3.41	0.0099*
X1.X2	-0.15	± 3.41	0.9645

* Significant at 95 % confidence level. X_1 and X_2 represent the variables pH and temperature, respectively.

The main effects (Table 2) were fitted by multiple regression analysis to a linear model and the best fitting response function can be written by Equation (2), in which A= Lipase activity (U g^{-1}); X_1= coded value of temperature (°C) and X_2 = coded value of pH.

$$A = 119.27 + 32.08X_1 + 16.93X_2 \qquad (2)$$

The statistical significance of this model was evaluated by the F test (Table 3), which revealed that this regression is statistically significant at 95 % probability level. The model did not show lack of fit and the determination coefficient (R^2 = 0.9975) indicates that the model can explain 99.75 % of the variability. Thus, the fitted equation displayed was considered to be suitable for describing the lipase activity as a function of the studied variables and was used to plot the response surfaces as showed in Figure 2.

TABLE 3
ANALYSIS OF VARIANCE (ANOVA) FOR THE REGRESSION OF THE MODEL THAT REPRESENTS MYCELIUM-BOUND LIPASE PRODUCTION BY *P. CITRINUM* IMMOBILIZED WHOLE CELLS USING A FULL 2^2 FACTORIAL DESIGN

Variables	Sum of squares	Degree of freedom	Mean square	F	p
X_1	4116.79	1	4116.79	354.75	0.0028*
X_2	1146.48	1	1146.48	98.80	0.0099*
$X_1.X_2$	0.022	1	0.022	0.002	0.9694
Pure error	23.21	2	11.61		
R²	0.9975				

* Significant at 95 % confidence level. X_1 and X_2 represent the variables pH and temperature, respectively.
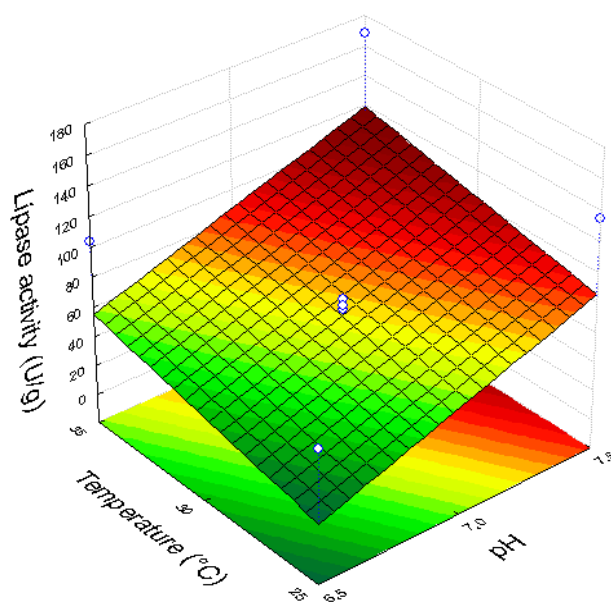
FIGURE 2. SURFACE RESPONSES FOR THE MYCELIUM-BOUND LIPASE PRODUCTION BY *P. CITRINUM* IMMOBILIZED WHOLE CELLS AS A FUNCTION OF pH AND TEMPERATURE ACCORDING TO THE FITTED MATHEMATICAL MODEL

Data showed the best conditions to enhance mycelium-bound lipase production is at pH 7.5 and temperature of 35°C. To validate the model (Equation 2), cultivation runs were performed under the optimal predicted conditions and the differences between the experimental and theoretical values were lower than 2%.

The spore concentration of the inoculum appears to be a critical factor for the process outcome and also in the immobilized cells and lipase activity [13]. Under the establishment conditions in terms of pH and temperature, the effect of inoculum in mycelium-bound lipase production was evaluated and illustrated by Figure 3.

Figure 3 shows, except 10 mL L^{-1}, there were no expressive difference between mycelium-bound lipase production in range of 20 to 50 mL L^{-1} of inoculum concentration. The highest lipase activity value was attained with 30 mL L^{-1} that corresponds to about 1×10^6 spores mL^{-1} medium concentration. Similar behavior was obtained in a previous study using *Mucor circinelloides* whole cells immobilized in PUF, in which high lipase activity was found with the same spore concentration [13].
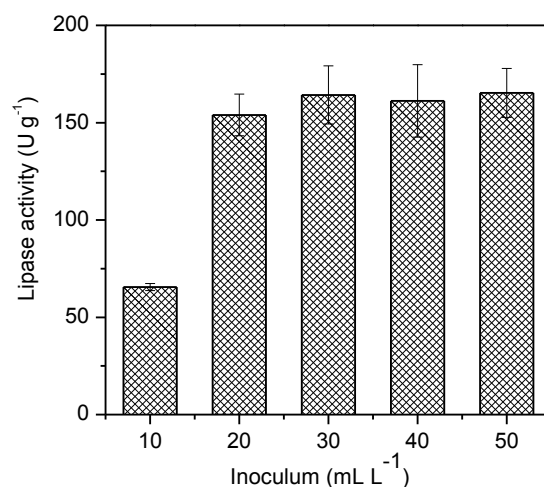
FIGURE 3. THE EFFECT OF INOCULUM SPORES IN THE MYCELIUM-BOUND LIPASE PRODUCTION BY *P. CITRINUM* IMMOBILIZED WHOLE CELLS

Wolski et al. [17] evaluate the effect of inoculum concentration in lipase activity from *Penicillium* sp. and found that 40 mL L^{-1} was the best inoculum concentration. Some reports related the effect of inoculum in fungal morphology, since the biomass growth in fully entangled filaments are obtained with lower inoculum concentration, thus enhancing the lipase production [18].

3.3 Morphological, biochemical and kinetics properties

Figure 4 (a-b) shows the SEM images of a cross sectional of whole cells immobilized in 6-mm cubic PUF particle. As can be observed in Fig. (4a), the cells have formed a dense film inside the reticulated fiber of PUF, which means the strong adhesion of cells into the support. This is very important and indicated that the cells would not release from the support even under vigorous agitation. With 5 times magnification (Fig. 4b), it is possible to see fully entangled morphology of cells around the fiber of PUF.

(a) **(b)**
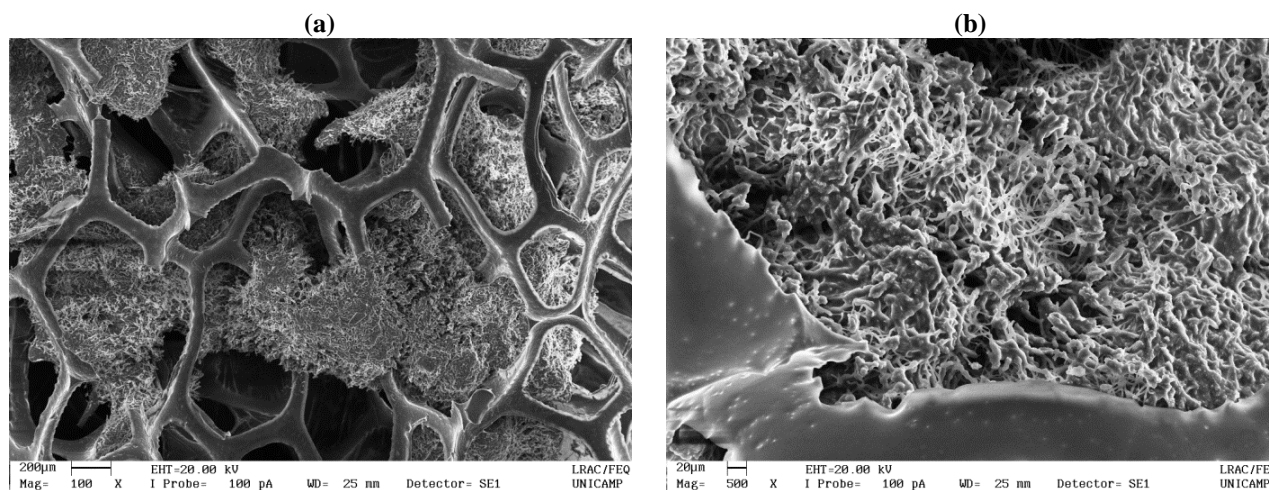
FIGURE 4. SEM IMAGES OF *P. citrinum* WHOLE CELLS IMMOBILIZED IN PUF WITH MAG OF (A) 100 X (B) 500X

The effect of the pH and temperature on mycelium-bound lipase activity was investigated by varying the buffer pH from 6.0 to 8.5 and temperature from 30 to 55 °C. The higher values of lipase activity was on average 166.8 ± 3.2 U g^{-1} and, as illustrated in Fig. 5a, the lipase activity increase proportionally with pH, achieving the maximum value in pH 8.0. For temperature, the optimal lipase activity was attained at 40 °C (Fig. 5b).

(a) **(b)**
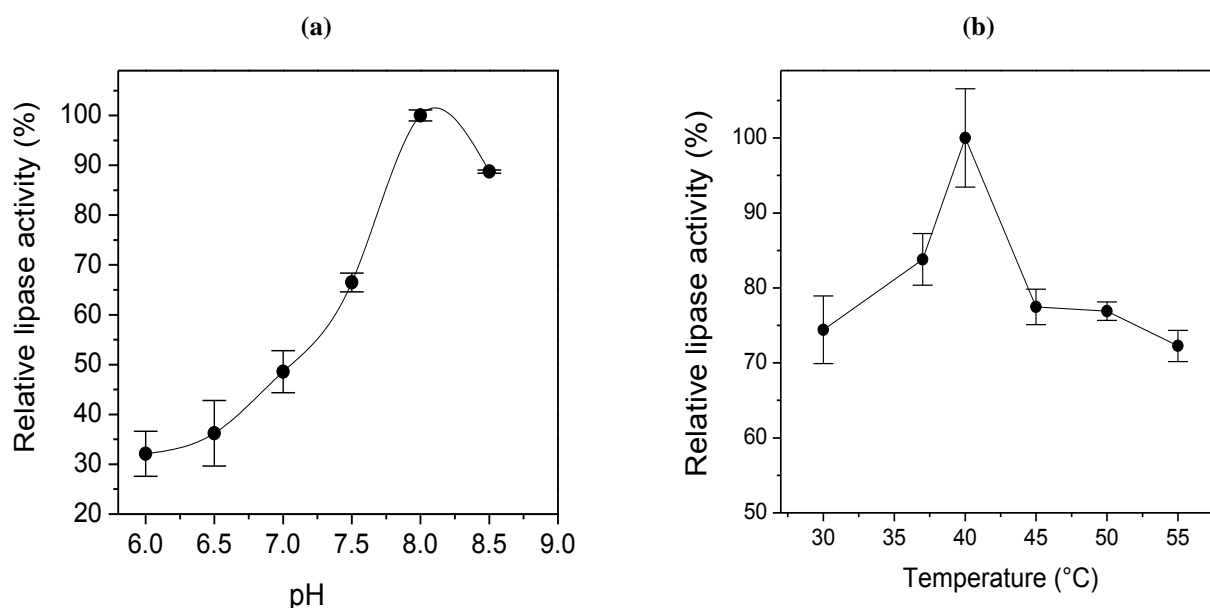
FIGURA 5. PH (A) AND TEMPERATURE (B) OPTIMAL OF *P. CITRINUM* IMMOBILIZED WHOLE CELLS

The thermal stability of mycelium-bound lipase from immobilized whole cells was determined aiming to evaluate the irreversible loss of enzymatic activity on exposure to high temperature. Figure 6 shows the denaturation kinetic of lipase activity at 60 °C for 150 min. After this period, the mycelium-bound lipase remained lower than 50% of its original activity. Based on these results, by fitting a model of first order deactivation, the thermal deactivation constant (k_d) and half-life time ($t_{1/2}$) of immobilized whole cells were determined and the values achieved were 8.62×10^{-5} h^{-1} and 2.23h, respectively. The half-life time is the time which takes for the activity to reduce to a half of the original activity and inversely proportional to the rate of deactivation.
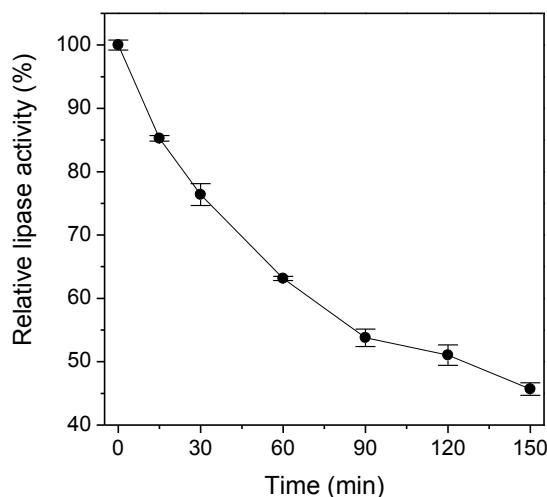
FIGURE 6. RESIDUAL LIPASE ACTIVITY OF *P. CITRINUM* IMMOBILIZED WHOLE CELLS AT 60°C

The enzyme kinetics parameters K_m and V_{max} were measured from nonlinear regression technique aiming to determine the catalytic effectiveness of the immobilized whole cells. The apparent V_{max} value indicated the maximum reaction rate and the K_m value indicated the substrate affinity and enzyme conformational changes, while the catalytic efficiency (V_{max}/K_m) indicated the overall cumulative effect of V_{max} and K_m on enzyme activity [19]. The lipase activity of immobilized whole cells at different substrate concentrations was determined, as illustrated in Figure 7, and the maximum reaction rate obtained (V_{max}) was 123.2 U g^{-1}. The lower affinity of the mycelium-bound lipase-substrate was revealed by its elevated K_m value of 158.10 mM, confirmed by catalytic efficiency of 0.78. This behavior can be due to the presence of support matrix associated to mycelium, which would cause diffusional effects in mass transfer between lipase and substrate [8].
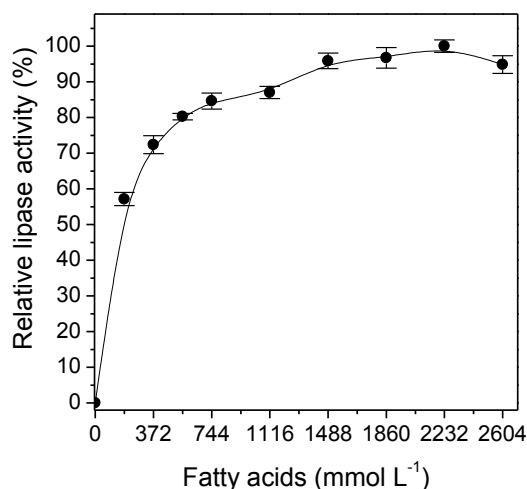
FIGURE 7. EFFECT OF SUBSTRATE CONCENTRATION IN LIPASE ACTIVITY OF *P. CITRINUM* IMMOBILIZED WHOLE CELLS (EXPRESSED BY TOTAL FATTY ACIDS INTO OIL EMULSION)

3.4 Soybean oil hydrolysis

The catalytic potential of immobilized whole cells was evaluated in the hydrolysis of vegetable oil with long-chain polyunsaturated fatty acids such as soybean. Soybean oil hydrolysis was performed in a stirred-tank reactor for 24 h at 37 ◦C with Arabic gum as emulsifier in oil emulsion (25% wt.) at pH 7.0 buffer phosphate 0.1mol L^{-1}. The kinetic profile of the soybean oil hydrolysis is displayed in Figure 8.
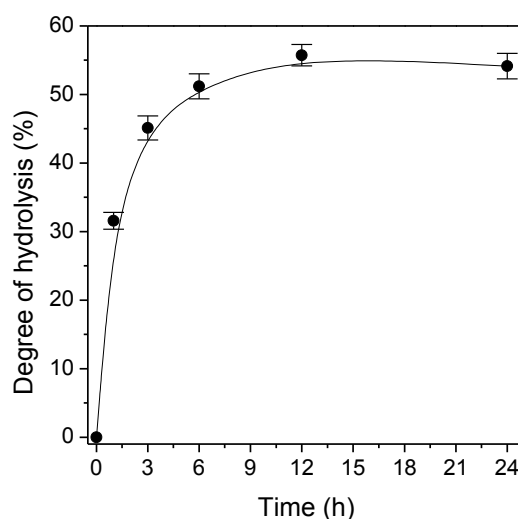
FIGURE 8- KINETIC OF SOYBEAN OIL HYDROLYSIS CATALYZED BY *P. CITRINUM* IMMOBILIZED WHOLE CELLS (T=37 ºC, PH 7.0)

Under these conditions, soybean oil was efficiently hydrolyzed by immobilized whole cells achieving almost 50% of hydrolysis degree in 3h of reaction time. Maximum hydrolysis degree of 55.7 ± 1.6% was attained in 12h of reaction time, which remained stable for a further 12 h. These results evidenced the potential of immobilized whole cells as biocatalyst in reaction of hydrolysis, since the literature reports similar results employing commercial preparations lipase. Aarthy et al. [20] investigate the hydrolysis of cod liver, salmon, sardine and shark oils using *Cryptococcus* sp. lipase and found in 24h hydrolysis degree in a range of 28.6 to 36.4 %. After an optimization of reaction conditions such as time, emulsifier and loading lipase, the hydrolysis ratio was enhanced to 83.7%, but in 72h of reaction time. Avelar et al. [21] tested soybean, canola and olive oils in the hydrolysis reactions employing lipase from dormant castor bean seed and found in 3h of reaction about 88.2% degree of hydrolysis for canola oil. They optimized the parameters mass ratio oil:buffer, temperature and $CaCl_2$, and achieved full hydrolysis of canola oil in 3h of reaction time.

IV.   CONCLUSION

P. citrinum whole cells were successfully immobilized in PUF and suitable conditions to enhance the mycelium-bound lipase production were determined. Maximum lipase activity was achieved in 96 h incubation time in medium at pH=7.5 at 30 °C using inoculum size of 30 mL L^{-1}. SEM images showed strong adhesion of cells into the support matrix under the establishment conditions. The immobilized whole cells were characterized and revealed optimum lipase performance in pH 8.0 at 37 °C, with V_{max} 123.24 U g^{-1} and satisfactory thermal stability at 60° C (half-life time =2.23 h). Enzymatic soybean hydrolysis was carried out by immobilized whole cells, which obtained maximum hydrolysis degree of 55.7± 1.56% in 12h of reaction time. These results suggest the use of immobilized whole cells as biocatalyst are promising and economically attractive in oils and fats industry.

REFERENCES

[1] J. L. Loo, A. Khoramnia, O. M. Lai, K. Long, H. M. Ghazali, Mycelium-bound lipase from a locally isolated strain of Geotrichum candidum, Molecules, 19, 8556-8570 (2014).

[2] G. Jin, T. J. Bierma, C. G. Hamaker, R. Mucha, V. Schola, J. Stewart, C. Wade, Use of a whole-cell biocatalyst to produce biodiesel in a water-containing system, Journal of Environmental Science and Health, 44, 21-28 (2009).

[3] D. V. Cortez, H. F. de Castro, G. S. S. Andrade, Potencial catalítico de lipases ligadas ao micélio de fungos filamentosos em processos de biotransformação, Química Nova, 40, 1, 85-96 (2017).

[4] H. Fukuda, A. Kondo, S.Tamalampudi, Bioenergy: Sustainable fuels from biomass by yeast and fungal whole-cell biocatalysts. Biochemical Engineering Journal, v. 44, 2-12 (2009).

[5] Guldhe, P. Singh, S. Kumari, I. Rawat, K. Permaul, F. Bux, Biodiesel synthesis from microalgae using immobilized *Aspergillus niger* whole cell lipase biocatalyst, Renewable Energy, 85, 1002-1010 (2016).

[6] Arumugam, V. Ponnusami, Biodiesel production from *Calophyllum inophyllum* oil using lipase producing *Rhizopus oryzae* cells immobilized within reticulated foams, Renewable Energy, 64, 276-282 (2014).

[7] J. S. Kyeong, S. H.Yeom, Preparation of immobilized whole cell biocatalyst and biodiesel production using a packed-bed bioreactor, Bioprocess and Biosystems Engineering, 37, 2189-2198 (2014).

[8] D. Wang, Z. Zhu, X. Wang, M. Bustamante, Y. Xu,Y. Liu, W. Liao, Improving mycelium-bound lipase production by aggregating *Rhizopus chinensis* on a draft tube in a modified stirred tank fermentor, Process Biochemistry, 50, 2019-2028 (2015).

[9] Solarte, E. Yara-Varón, J. Eras, M. Torres, M. Balcells, R. Canela-Garayoa, Lipase activity and enantioselectivity of whole cells from a wild-type *Aspergillius flavus* strain, Journal of Molecular Catalysis B: Enzymatic, 100, 78-83 (2014).

[10] Li, L. Li, H. Zhou, C. Xia, L. He, Improving yield of 1,3-diglyceride by whole-cell lipase from *A. Niger* GZUF36 catalyzed glycerolysis via medium optimization, Journal of the Brazilian Chemical Society, 26, 2, 247-254 (2015).

[11] H. Yan, H. C. Liu, Z. Wang, Optimization of the fermentation conditions and substrate specifity of mycelium-bound ester hydrolases of *Aspergillus oryzae* Cs007, Journal of the Serbian Chemical Society, 80,1, 1-8 (2015).

[12] G. S. S. Andrade, L. Freitas, P. C. Oliveira, H. F. De Castro, Screening, immobilization and utilization of whole cell biocatalysts to mediate the ethanolysis of babassu oil. Journal of Molecular Catalysis B: Enzymatic, 84,183-188 (2012).

[13] G.S.S. Andrade, A. K. F. Carvalho, C. M. Romero, P. C. Oliveira, H. F. De Castro, *Mucor circinelloides* whole-cells as a biocatalyst for the production of ethyl esters based on babassu oil, Bioprocess and Biosystems Engineering, 37, 2539-2548, (2014).

[14] A. K. F. Carvalho, E. L. P. Faria, J. D. Rivaldi, G.S.S. Andrade, P. C. Oliveira, H. F. De Castro, Performance of whole-cells lipase derived from *Mucor circinelloides* as a catalyst in the ethanolysis of non-edible vegetable oils under batch and continuous run conditions, Industrial Crops and Products, 67, 287-294 (2015).

[15] S. Dheeman, S. Antony-Babu, J. M. Frías, G. T. M. Henehan, Purification and characterization of an extracellular lipase from a novel strain Penicillium sp. DS-39 (DSM 23773), Journal of Molecular Catalysis B: Enzymatic, 72, 3-4, 256-262 (2011).

[16] L. Freitas, T. Bueno, V. H. Perez, J. C. Santos, H. F. De Castro, Enzymatic hydrolysis of soybean oil using lipase from different sources to yield concentrated of polyunsaturated fatty acids, World Journal of Microbiology and Biotechnology, 23,1725-1731 (2007).

[17] E. Wolski, M. Rigo, J. V. Di Luccio, D. de Oliveira, H. Treichel, Production and partial characterization of lipases from a newly isolated *Penicillium* sp. using experimental design, Letters in Applied Microbiology, 49, 60-66, (2009).

[18] Y. Teng, Y. Xu,; D. Wang, Changes in morphology of *Rhizopus chinensis* in submerged fermentation and their effect on production of mycelium-bound lipase, Bioprocess and Biosystems Engineering, 3, 1615-7591 (2009).

[19] K. C. Badgujar, B. M. Bhanage, Lipase immobilization on hyroxypropyl methyl cellulose support and its applications for chemoselective synthesis of β-amino ester compounds, Process Biochemistry, 51, 1420-1433 (2016).

[20] M. Aarthy, P. Saravanan, N. Ayyadurai, M. K. Gowthamana, N. R. Kamini, A two-step process for production of omega 3-polyunsaturated fatty acid concentrates from sardine oil using Cryptococcus sp. MTCC 5455 lipase, Journal of Molecular Catalysis B: Enzymatic, 125, 25-33 (2016).

[21] M. H.M. Avelar, D. M.J. Cassimiro, K. C. Santos, R. C.C. Domingues, H. F. de Castro, A. A. Mendes, Hydrolysis of vegetable oils catalyzed by lipase extract poder from dormant castor bean seeds, Industrial Crops and Products, 44, 452-458 (2013).

Correlation between Non-Destructive Testing (NDT) and Destructive Testing (DT) of Concrete for Linear, Quadratic and Cubic Relation

Sanket Uniyal[1], Susanta Kumar Sethy[2]

[1]M.tech Student: Structural Engineering with Specialization in Offshore Structures University of Petroleum and Energy Studies, Dehradun India.
[2]Asst. Professor Civil Engineering Department U.P.E.S, Dehradun

Abstract— *This work present a correlation and comparison between Non- Destructive test (Rebound Hammer) & Destructive test of testing the compressive strength of concrete cubes for Linear, Quadratic & Cubic Relation. Concrete cubes of 150mm×150mm×150mm were cast of M-20, M-25, M-30 and M-35 grades and each grade cured for 7days, 14days and 28days. A total 120 cubes were cast. When analyses were carried out, there are a relation between the results of rebound number obtained from rebound hammer and compressive strength obtained from compression machine. These results i.e. rebound number and compressive strength value of cubes M-20, M-25, M-30 and M-35 grades were correlate and compared with Linear, Quadratic & Cubic Equation and checked from which equations among these three gives a more accurate results with compressive strength. After analyses it was found that among three of them predicted strength of cube only the linear and quadratic equation gave more accurate relationships with compressive strength of concrete. And at the end it also gave statistical analysis of the results which shows that there were a significant difference between the rebound number and compressive strength.*

Keywords— *Concrete, Compressive Strength, Destructive Testing (DT), NON-Destructive Testing (NDT), Correlation.*

I. INTRODUCTION

Concrete is a composite material which is produced from the combination of fine aggregates, coarse aggregates and water with proper proportion. The strength of concrete is most important along with its durability. Therefore it is important to check or find out the compressive strength of concrete before used in structural purpose. Therefore, it is very important to check the compressive strength of concrete before subjecting it to its anticipated loads. Compressive strength of a hardened concrete can be determine using destructive & non- destructive test (NDT) methods. The (DT) is carried out by crushing the cast specimen to failure while the NDT method is carried out without destroying the cast specimen. The Rebound Hammer (Schmitz) is one of the most popular NDT methods used to test the strength of concrete. The aim of this project is to compare the concrete compressive strengths measured using destructive method and those measured using the NDT for Linear, Quadratic & Cubic Relation and to check from which equations among these three gives a more accurate results with compressive strength.

II. MATERIALS & METHODS

Materials: Throughout the project work CCI brand of PPC is used. The coarse aggregates and fine aggregates used for experiments are taken from laboratory of college. Portable drinking water is used in concrete.

Methods: Concrete of grades M-20, M-25, M-30, M-35 was used for the study. The mix design was done in accordance with IS: 10262 (2009) specification. Mixing was done in concrete mixer. Concrete cube 150mm×150mm×150mm were cast. The specimen were demoulded after 24 hours and immersed into curing tank filled with water and cured for 7days, 14days & 28days.

NDT of concrete using Rebound Hammer: The NDT of compressive strength of concrete was carried out using rebound (Schmitz) hammer. The test was based on the principle that the rebound of an elastic mass depend on the hardness of the surface against which the mass impinges.

Destructive Testing (DT) using the Compression Machine: The compressive strength test was carried out using the compression machine. The test was carried out in accordance with IS: 516 (1959) specification. 30 concrete specimens for each concrete grade of M-20, M-25, M-35, and M-40 were tested after curing for 7, 14and 28 days.

III.   RESULTS AND DISCUSSION

Materials Cement: Table 1 shows the test results of CCI brand of PPC. The cement test results obtained meets the standard values in IS: 1489 (Part 1):1991. Hence it is good for concrete works.

Coarse Aggregate: Table 1 shows the results of the test conducted on the coarse aggregate. The aggregate impact value (AIV) of the aggregate used was 19%. These values are less than the IS: 2386 (Part IV)-1963, and specific gravity 2.73, the coarse aggregate used was good for concrete works.

Fine Aggregate: Specific gravity of fine aggregates 2.67. This is good for concrete works.

TABLE 1
RESULTS OF PRELIMINARY TEST ON MATERIALS

TEST	RESULTS	STANDARD CODE	LIMIT IN CODE
Specific Gravity of Cement	3.15		3.15
Initial Setting Time of Cement(Min)	54	IS :1489 (Part 1) -1991	Greater than 30min
Final Setting Time of Cement(Min)	210	IS :1489 (Part 1) -1991	Less than 600min
Specific Gravity of Fine Aggregate	2.67	IS :2386 (Part III)-1963	2.5 to 3
Specific Gravity of Coarse Aggregate	2.73	IS :2386 (Part III)-1963	2.5 to 3
AIV	19%	IS:2386 (Part IV)-1963	Good aggregate (10% to 20%)

Relationship between compressive strength and Rebound Number: The results of both DT and NDT are presented in Tables 2, Table 3 and Table 4 for concrete cubes of ages 7, 14 and 28 days respectively. The results show that a higher rebound number result gives high compressive strength value and vice versa. Table 5 and Table 6 and Table 7 shows the results of compressive strength and rebound number with predicted values of linear, quadratic and cubic relation of different mix M-20, M-25, M-35, and M-40 for 7, 14 and 28days respectively. So the results are shown given below:

TABLE 2
COMPRESSIVE STRENGTH AND REBOUND NUMBER FOR DIFFERENT CONCRETE CURED FOR 7DAYS

M-20		M-25		M-30		M-35	
C.S	R.No	C.S	R.No	C.S	R.No	C.S	R.No
11	12.5	16.52	18.01	16	17.45	20.5	22.12
10	11.5	15.3	17.01	13.5	14.7	18.6	19.65
10	11.5	14	15.26	14.5	16.23	20.5	22.53
11.5	13	16.42	17.92	17	17.97	19	21.51
12	13.54	17.25	18.95	15.5	16.92	17.5	18.54
13.5	14.28	15.24	17.21	16.5	17.94	16.5	18
12	13.25	15.98	17.45	14.1	16.12	17	18.05
11.7	13.11	16.47	18.02	16	17.081	18	19.88
11.6	12.7	17.48	18.23	14	15.98	18.5	20
12.5	13.4	16.24	18.82	14.5	16.31	19	21.21

TABLE 3
COMPRESSIVE STRENGTH AND REBOUND NUMBER FOR DIFFERENT CONCRETE CURED FOR 14 DAYS

M-20		M-25		M-30		M-35	
C.S	R.No	C.S	R.No	C.S	R.No	C.S	R.No
17	18.01	22.5	22.68	17.3	18.5	22	25.9
14.2	15.04	21.3	22.47	20.6	22.92	22.5	26.8
13.6	14.48	23.45	25.01	18.6	19.75	19.5	21.47
15	16.47	24.02	26.04	17.5	18.9	23	27.5
14.7	15.33	23.40	24.92	22.2	26.34	23.5	29.05
13.9	14.95	22.10	23.45	19	21	24	31
14.3	15.12	21.01	22.31	18.5	20.02	25.5	34.25
15.3	16.9	24.10	26.31	19	21.34	17.5	19.05
16	17.43	21.98	23.01	20.2	22.56	20	21.98
13.8	14.72	22.97	24.45	17	18.14	21	23.7

TABLE 4
COMPRESSIVE STRENGTH AND REBOUND NUMBER FOR DIFFERENT CONCRETE CURED FOR 28 DAYS

M-20		M-25		M-30		M-35	
C.S	R.No	C.S	R.No	C.S	R.No	C.S	R.No
23.5	27.2	28.2	34.50	33.3	44.23	38	51.9
20.5	22.8	30.1	37.00	34.	46.18	36.5	47
20	22.5	27	33.98	31.5	41.67	41	54.5
24	28.83	25.12	33.01	32	42.5	42.5	55.6
23.5	26.5	26.87	33.45	34	46.25	38.5	52.4
21.5	24.87	29.45	36.47	36.5	47.52	37.5	50
28.5	34.5	26.57	33.25	37.5	50.02	35.5	46.75
24.5	29.84	27.00	33.98	29.5	29.5	38.8	53
22	25.4	29.21	36.25	33.7	45.45	40	54.11
21	23.05	25.01	33.00	37	49	43.5	60.3

Data Analysis: The above results are compared with Linear, Quadratic & Cubic Equations respectively.

TABLE 5
CORRELATION BETWEEN COMPRESSIVE STRENGTH & REBOUND NUMBER WITH PREDICTED CONCRETE STRENGTH FOR 7 DAYS.

C.S	R. NO.	PREDICTED CONCRETE STRENGTH		
		LINEAR EQUATION	QUADRATIC EQUATION	CUBIC EQUATION
11	12.5	11.21	11.12	11.13
10	11.5	10.26	10.09	10.16
10	11.5	10.26	10.09	10.16
11.5	13	11.68	11.64	11.62
12	13.54	12.20	12.18	12.15
13.5	14.28	12.90	12.93	12.88
12	13.25	11.92	11.89	11.86
11.7	13.11	11.79	11.75	11.73
11.6	12.7	11.40	11.33	11.32
12.5	13.4	12.07	12.04	12.01
14	15.26	13.83	13.89	13.85
16.42	17.92	16.36	16.43	16.44
17.25	18.95	17.34	17.38	17.41
15.24	17.21	15.69	15.77	15.76
15.98	17.45	15.92	15.99	15.99
16.47	18.02	16.46	16.52	16.54
17.48	18.23	16.66	16.72	16.74
16.24	17.82	16.27	16.34	16.35
16	17.45	15.92	15.99	15.99
13.5	14.7	13.30	13.34	13.30
14.5	16.23	14.76	14.83	14.81
17	17.97	16.41	16.48	16.49
15.5	16.92	15.41	15.49	15.48
16.5	17.94	16.38	16.45	16.46
14.1	16.12	14.65	14.73	14.70
16	17.81	16.26	16.33	16.34
14.5	16.31	14.83	14.91	14.89
20.5	22.12	20.35	20.17	20.13
18.6	19.65	18.01	18.01	18.04
19	21.51	19.77	19.64	19.64
17.5	18.54	16.95	17.00	17.03
16.5	18	16.44	16.50	16.52
17	18.05	16.49	16.55	16.57
18	19.88	18.23	18.21	18.25
18.5	20	18.34	18.32	18.35
19	21.21	19.49	19.39	19.39

FIG 1. LINEAR RELATION BETWEEN COMPRESSIVE STRENGTH & REBOUND NUMBER

FIG 2. QUADRATIC RELATION BETWEEN COMPRESSIVE STRENGTH & REBOUND NUMBER

FIG 3. CUBIC RELATION BETWEEN COMPRESSIVE STRENGTH & REBOUND NUMBER

TABLE 6

CORRELATION BETWEEN COMPRESSIVE STRENGTH & REBOUND NUMBER WITH PREDICTED CONCRETE STRENGTH FOR 14 DAYS.

C.S	R. NO.	PREDICTED CONCRETE STRENGTH		
		LINEAR EQUATION	QUADRATIC EQUATION	CUBIC EQUATION
17	18.01	16.94	17.00	16.69
14.2	15.048	14.11	13.91	13.87
13.6	14.48	13.64	13.26	13.31
15	16.47	15.30	15.45	15.26
14.7	15.33	14.35	14.22	14.15
14.3	15.12	14.17	13.99	13.95
15.3	16.9	15.66	15.90	15.66
16	17.43	16.11	16.43	16.16
13.8	14.72	13.84	13.53	13.55
22.5	23.68	22.31	21.53	21.07
21.3	22.47	21.39	20.72	20.27
23.45	25.01	23.32	22.34	21.84
24.02	26.04	24.11	22.89	22.36
23.40	24.92	23.26	22.28	21.79
22.10	23.45	22.14	21.38	20.93
24.10	26.31	24.31	23.02	22.49
17.3	18.5	17.41	17.46	17.12
20.6	22.92	20.26	21.03	20.58
18.6	19.75	18.22	18.58	18.19
17.5	18.9	17.67	17.83	17.47
22.2	26.34	22.46	23.04	22.50
19	21	19.02	19.61	19.19
18.5	20.02	18.39	18.81	18.42
19	21.34	19.24	19.88	19.45
20.2	22.56	20.03	20.78	20.33
17	18.14	17.18	17.12	16.80
22	25.9	21.76	22.82	22.30
22.5	26.8	22.22	23.26	22.70
23	27.5	22.57	23.57	22.97
23.5	29.05	23.35	24.16	23.43
24	31	24.33	24.72	23.73
25.5	34.25	25.97	25.17	23.43
17.5	19.05	18.32	17.96	17.60
20	21.98	19.79	20.36	19.93

FIG 4. LINEAR RELATION BETWEEN COMPRESSIVE STRENGTH & REBOUND NUMBER

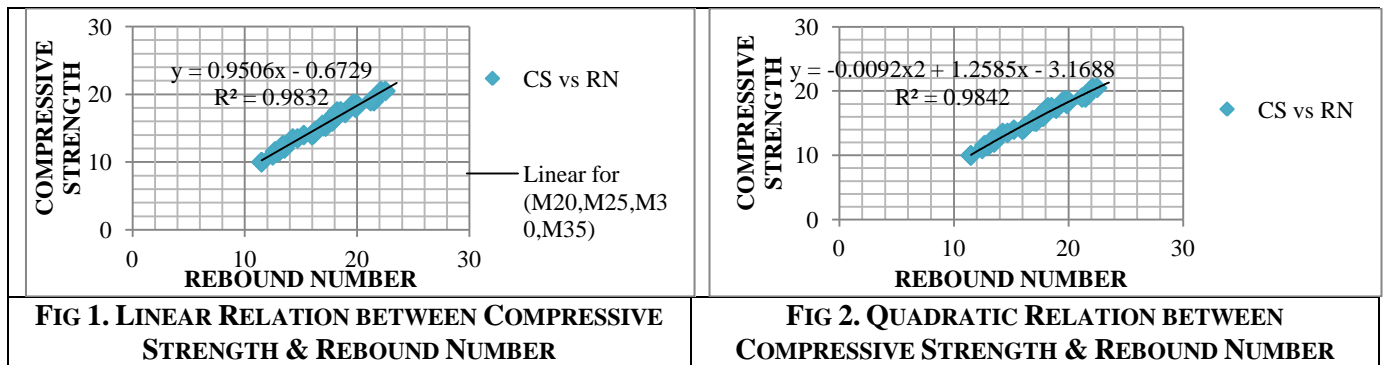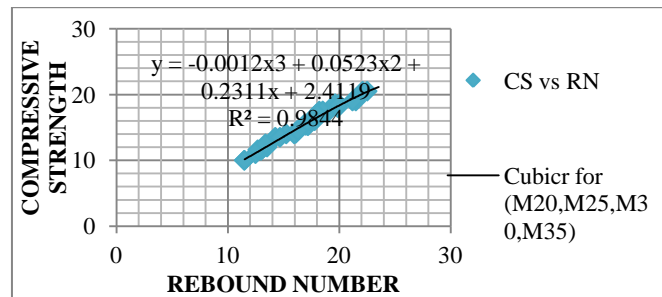**FIG 5. QUADRATIC RELATION BETWEEN COMPRESSIVE STRENGTH & REBOUND NUMBER**

FIG 6. CUBIC RELATION BETWEEN COMPRESSIVE STRENGTH & REBOUND NUMBER

TABLE 7

CORRELATION BETWEEN COMPRESSIVE STRENGTH & REBOUND NUMBER WITH PREDICTED CONCRETE STRENGTH FOR 28 DAYS.

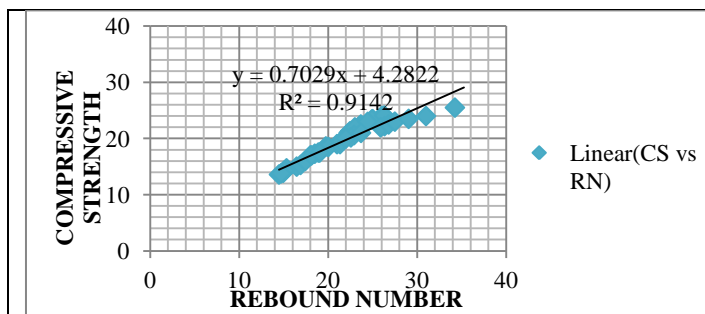| C.S	R. NO.	PREDICTED CONCRETE STRENGTH		
		LINEAR EQUATION	QUADRATIC	CUBIC EQUATION
23.5	27.2	23.01	23.08	23.12
20.5	22.8	20.24	20.54	20.63
20	22.5	20.06	20.37	20.47
24	28.83	24.03	24.03	24.07
23.5	26.5	22.57	22.67	22.71
28.5	34.5	27.59	27.42	27.50
24.5	29.84	24.66	24.63	24.66
22	25.4	21.88	22.03	22.08
21	23.05	20.40	20.69	20.77
28.2	34.50	27.59	27.42	27.50
30.1	37.00	29.16	28.95	29.06
27	33.98	27.26	27.10	27.17
25.12	33.01	26.65	26.52	26.58
26.87	33.45	26.93	26.78	26.85
29.45	36.47	28.83	28.62	28.73
26.57	33.25	26.80	26.66	26.73
29.21	36.25	28.69	28.49	28.59
25.01	33.00	26.65	26.51	26.57
33.3	44.23	33.70	33.49	33.74
34	46.18	34.92	34.75	35.03
31.5	41.67	32.09	31.86	32.06
32	42.5	32.61	32.39	32.60
34	46.25	34.97	34.79	35.08
37.5	50.02	37.33	37.26	37.61
29.5	39.5	30.73	30.50	30.66
33.7	45.45	34.46	34.28	34.55
37	49	36.69	36.59	36.92
36.5	47	35.44	35.28	35.58
41	54.5	40.14	40.25	40.65
38.5	52.4	38.83	38.84	39.22
37.5	50	37.32	37.25	37.59
35.5	46.75	35.28	35.12	35.41
40	54.11	39.90	39.99	40.39
43.5	60.3	43.79	44.23	44.64
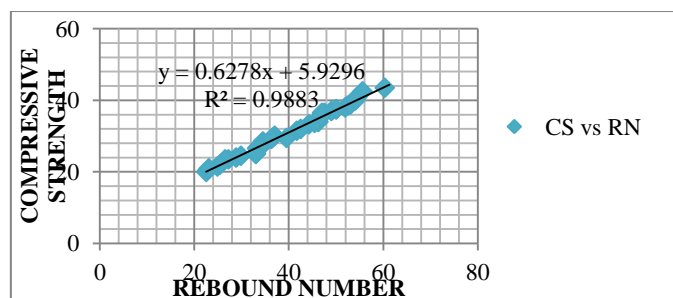
FIG 7. LINEAR RELATION BETWEEN COMPRESSIVE STRENGTH & REBOUND NUMBER

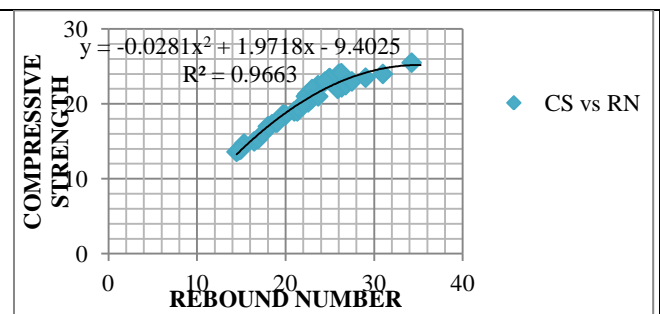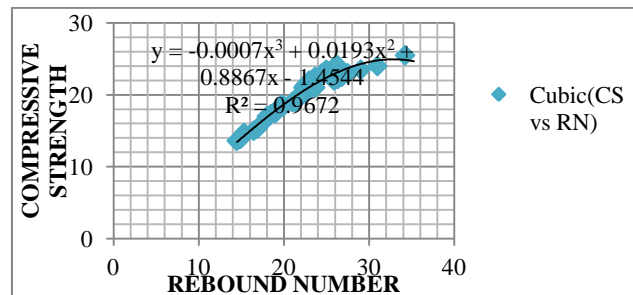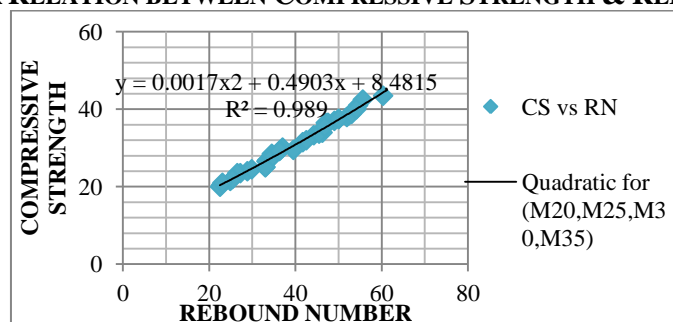**FIG 8. QUADRATIC RELATION BETWEEN COMPRESSIVE STRENGTH & REBOUND NUMBER**
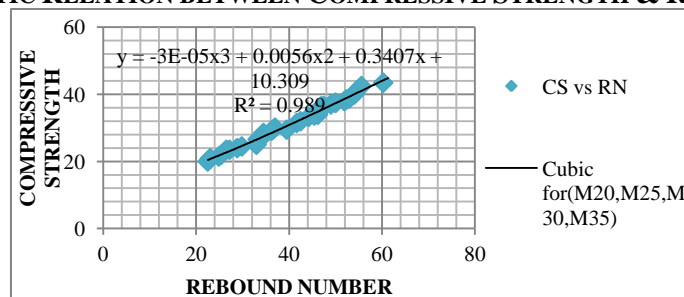
FIG 9. CUBIC RELATION BETWEEN COMPRESSIVE STRENGTH & REBOUND NUMBER

IV. CONCLUSION

The correlation among the strength values obtained by destructive and NDT test methods on

Concrete cubes have been established. Schmidt Hammer test method is used as a non-destructive test. The following principal conclusions have been drawn:-

- The use of rebound hammer test method on concrete cubes is not suitable to estimate its strength.

- Direct use of rebound hammer demonstrates high variations, which makes engineering judgment quite difficult.

- The Schmidt Hammer method could only be used as a reliable instrument to calculate the compressive strength.

- This project gives a useful mathematical linear and non-linear relationship that help the engineer to predict confidently the crushing strength of standard concrete cubes, by measuring the rebound index by means of Schmidt hammer.

- The linear and quadratic equations give perfect relationships with the compressive strength of concrete whereas there is a much difference in cubic equation results. It means only linear and quadratic mathematical expression is applicable for a wide range of concrete strengths.

REFERENCES

[1] J.C. Agunwambaa , T. Adagbab , A comparative analysis of the rebound hammer and   ultrasonic pulse velocity in testing concrete, Nigerian Journal of Technology (NIJOTECH) Vol. 31, No. 1, March, 2012, pp. 31{39}.

[2] IS-13311 (Part1): 1992 non-destructive testing of concrete - methods of test part 1 (ultrasonic pulse velocity).

[3] IS-13311 (Part2): 1992 non-destructive testing of concrete - methods of test part 2 (rebound hammer).

[4] *Jedidi Malek* Higher Institute of Technological Studies of Sfax, Department of Civil Engineering. *Machta Kaouther* Higher Institute of Technological Studies of Rades, Department of Civil Engineering, *(Destructive and Non-destructive Testing of Concrete Structures).*

[5] Guidebook on non-destructive testing of concrete structures.

An Efficient Voltage and Frequency Division Methods for Multiprecision Multiplier on FPGA

Mrs. N.S.Labhade (Assistant Prof.)[1], Sandip Chougule[2], Santosh Gadikar[3], Sunil Sharma[4]

(Dept. of E&TC, ICOER Wagholi, Pune)

Abstract— *In this paper, we present a reconfigurable multiprecision(MP) multiplier that contains variable precision ,parallel processing, Dynamic voltage scaling (DVS)and dedicated MP operands scheduling to provide desired performance for various operating conditions. The proposed reconfigurable multiplier works independent smaller precision also it works in parallel to perform higher precision multiplications according to conditions or user requirements of voltage or frequency the dynamic voltage/frequency scaling unit configures to works at proper precision and frequency. In this paper we design a multiplier circuit that consumes less power and reduces area overhead by parallel processing .for this instead of using 16bit or 32bit operands we used single 8bit or twin parallel bit multiplication operation . in multipresicion multiplier small multiplications causes complex structures which results in unwanted signal generation and increases complexity of circuitary ,for this we used 8bit multiplier for 16 bit and 32bit multiplication hence to reduce power consumption and acconding to runtime workload we combine multiprecision multiplier with dynamic voltage scaling(DVS).The DVS technique consists look up tables(LUT) and on chip critical path replica approach .The LUT allows the supply voltage according to the voltage frequency relationship stored in LUT.*

Keywords— *Multiprecision, Reconfigurable.*

I. INTRODUCTION

A nowadays Consumer demand for increasingly portable and high performance multimedia and communication products imposes strong constraints on the power consumption of individual internal components [1]. Of these multipliers perform one of the most frequently encountered arithmetic operations in digital signal processors (DSPs) [2]. For embedded applications, it has become essential to design more power-aware multipliers. Given that the fairly complex structure and interconnections, multipliers can exhibit a large number of unbalanced paths, resulting in glitch generation and propagation [3]. This unwanted switching activity can be overcomed by balancing internal paths through the combination of architectural and transistor-level optimization techniques. In addition to that equalizing internal path delays, dynamic power reduction can also be achieved by monitoring the effective dynamic range of the input operands so as to disable unused sections of the multiplier, and/or shorten the output product at reduced precision. It is possible because, in most sensor applications, the actual inputs do not always occupy the entire magnitude of its word-length. The operations in lower precisions are the most frequently required. In contrast to that most of today's full-custom DSPs and application-specific integrated circuits (ASICs) are designed for a fixed maximum word-length so as to accommodate for the worst case scenario. Therefore, an 8-bit multiplication computed on a 32-bit Booth multiplier would result in unnecessary switching activity and power loss.

Several works had been done on this word-length optimization. [1] Proposed system of multipliers of different precisions with each optimized to cater for a particular scenario. Each pair of incoming operands is routed to a smallest multiplier that can compute the result to take advantage of the lower energy consumption of the smaller circuit. This ensemble of point systems is reported to consume the least power but this can increase the chip area. for this, [5] proposed to share and reuse some functional modules within the ensemble. In [3], an 8-bit multiplier is reused for 16-bit multiplication, adding scalability without large area coverage. [5] Extended this method by implementing pipelining to further improve the multiplier's performance. A more flexible approach is proposed in [15], with several multiplier elements grouped together to provide higher precisions and reconfigurability. Reference [7] analyzed that the overhead associated to such reconfigurable multipliers. Combining multiprecision (MP) with dynamic voltage scaling (DVS) can provide reduction in power consumption by adjusting the supply voltage according to circuit's run-time workload rather than fixing it to cater for the worst case scenario [4]. Conventional DVS techniques consist of lookup table (LUT) and on-chip critical path replica approaches [17]–[19]. In addition, the critical path may change as a result of the varying supply voltage or process or temperature variations. Recent DVS approaches can overcome the limitations of the conventional DVS [24], because it completely removes worst case safety margins and error-tolerant DVS techniques can further aggressively reduce power consumption. In this paper, we propose a lower power reconfigurable multiplier architecture which combines MP with an error-tolerant DVS approach. [25]

II.   WORK FLOW

The objective of this paper is to implement an efficient Dynamic voltage and frequency scaling (DVFS) for multi precision multiplier on reconfigurable FPGA (spartan3).

To Implement of DVFS for multiplier block is on FPGA and which is offering good performance at low power supply voltage 3.3V to 1.8V and frequency 32MHz to 8MHz.To avoid unnecessary switching activity dynamic voltage and frequency scaling is performed.

To generate control signal, Scanning of input data is carried out.

To Address the issues of fix length ASIC's.

The following figure shows the operation flow of the system.
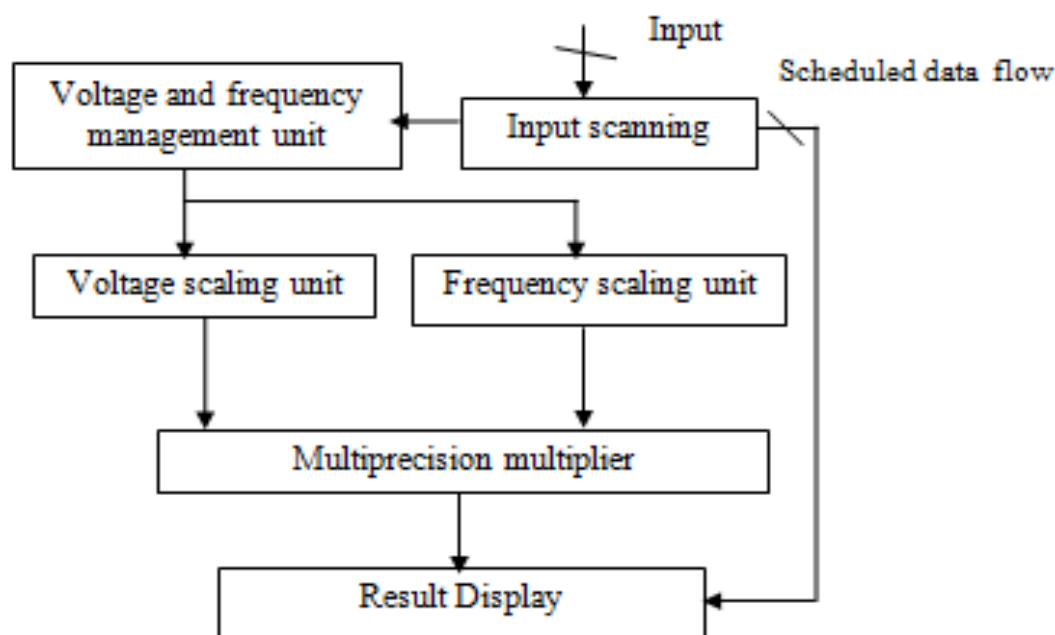
FIG. 1 WORK FLOW OF MULTIPRECISION MULTIPLIER

III.   METHODOLOGY

3.1   Scanning

Scanning is vital step for making system dynamic. This is the first and important step, by this step range of input is detected. After the scanning it will generate the control signal 1, 2, 3 for 8bit, 16bit, and 32bit data.

3.2   Voltage Scaling

 Here, frequency scaling is used to conserve the power. For stable operation of voltage required is determined by the frequency at which circuit is clocked, and can be reduced by if the frequency of the system is reduce.

3.3   Frequency Scaling

In an integrated circuits(IC) at the time of implementation manufacturer kept the fixed word length that is not used in all the application. To avoid this voltage scaling is important according to workload to system.

3.4   Multiplication

The Multiplier is controlled by three external signals. Once the input is scanned and detected the operating voltage and frequency are tuned automatically. The voltage range and frequency of 1.2-3.3V and 32-8MHz is achieved for full functionality respectively

IV.   RESULTS

TABLE 1
VOLTAGE AND FREQUENCY DIVISION

Scanning range	Voltage(v)	Frequency(MHz)
8*8	1.8	25
16*16	2.8	50
32*32	3.3	100

TABLE 2
MULTIPLICATION RESULTS

	8*8	16*16	32*32
A	10	290	70000
B	20	41	20
Result	200	11890	1400000

4.1   8 * 8 Bit Multiplication
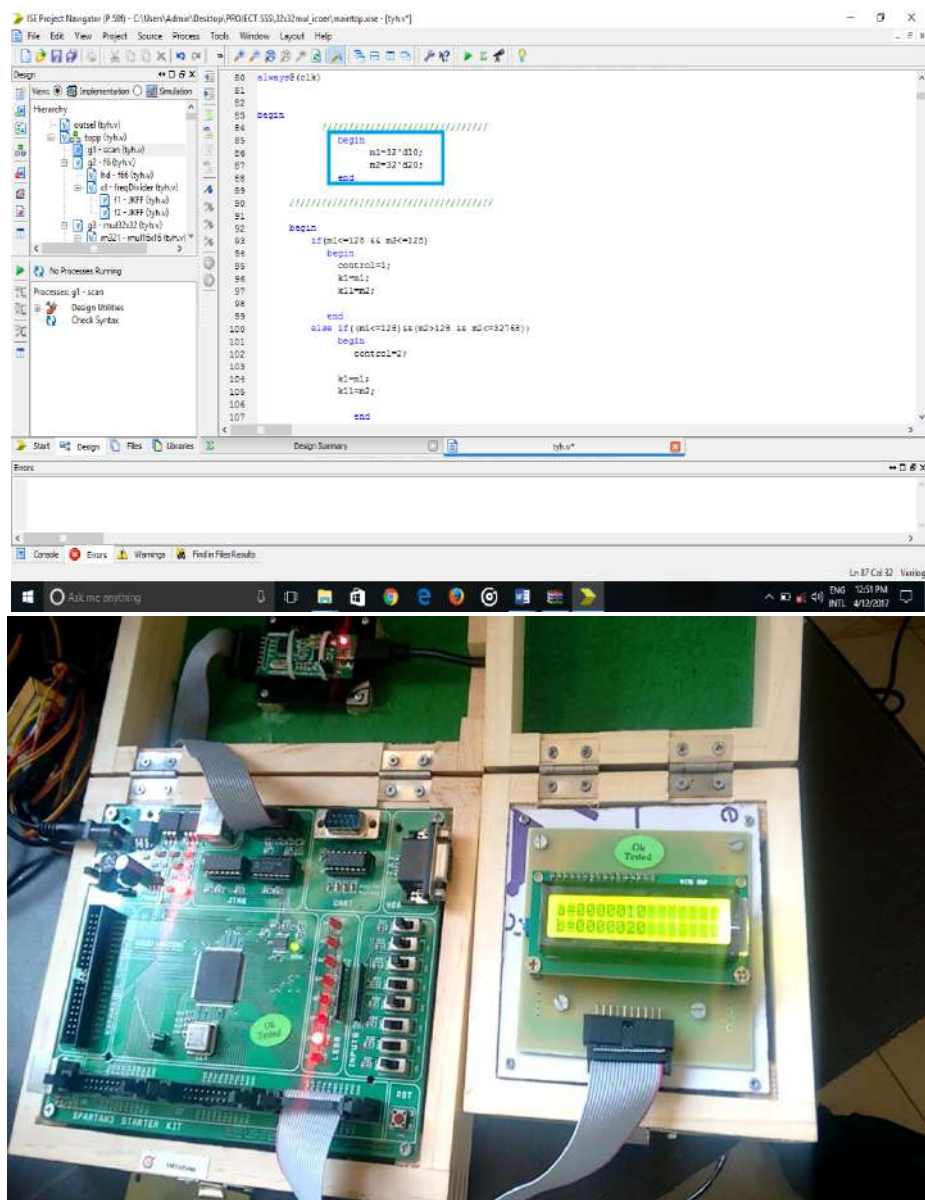
4.2   16 * 16 Bit Multiplication
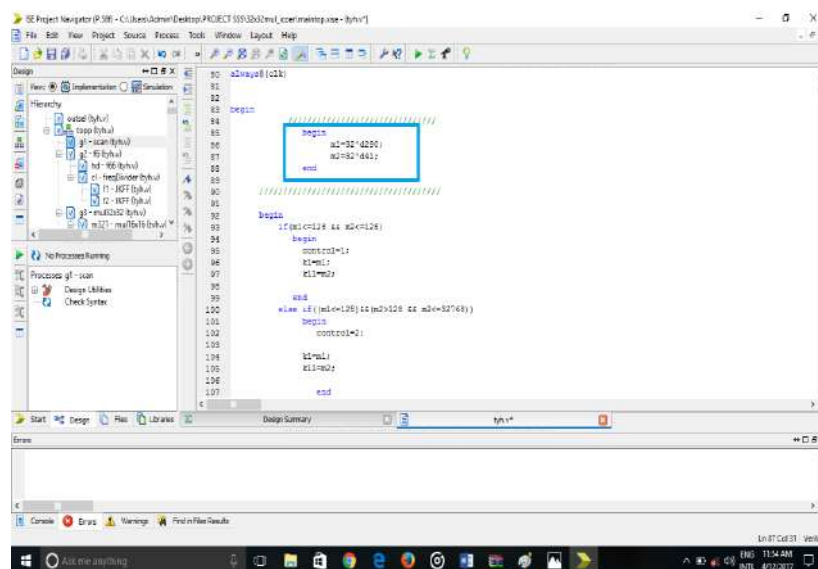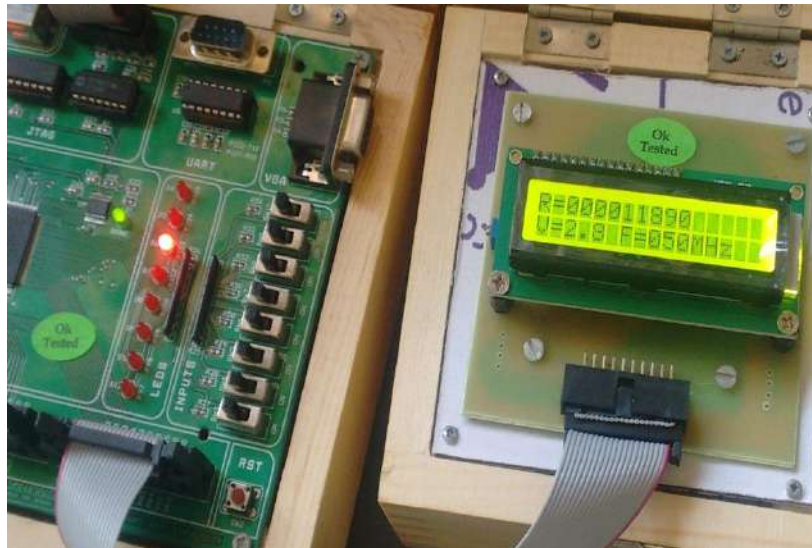
4.3   32 * 32 Bit Multiplication
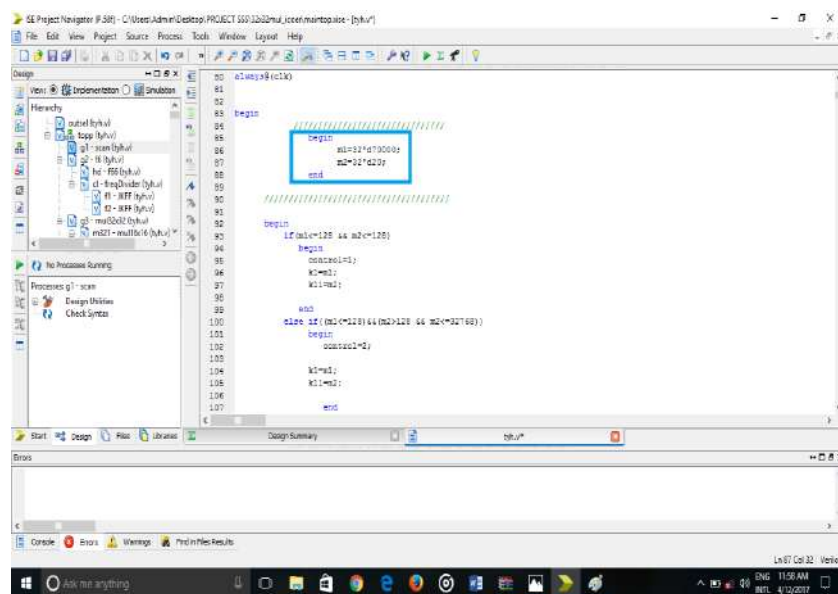
V.   CONCLUSION

Today energy efficient devices are the world's necessity. This paper presented techniques for efficient use of hardware resources power on FPGA. Here dynamically adjusting the frequency and voltage   according to bit width of input data by scaling technique. As input is known the system can save the power by disabling the unused selection of multiplier

REFERENCES

[1]   R. Min, M. Bhardwaj, S.-H. Cho, N. Ickes, E. Shih, A. Sinha, A. Wang, and A. Chandrakasan, "Energy-centric enabling technologies for wireless sensor networks," IEEE Wirel. Commun., vol. 9, no. 4, pp. 28–39, Aug. 2002.

[2]   T. Kuroda, "Low power CMOS digital design for multimedia processors," in Proc. Int. Conf. VLSI CAD, Oct. 1999, pp. 359–367

[3]   F. Carbognani, F. Buergin, N. Felber, H. Kaeslin, and W. Fichtner, "Transmission gates combined with level-restoring CMOS gates reduce glitches in low-power low-frequency multipliers," IEEE Trans. Very Large Scale Integer. (VLSI) Syst., vol. 16, no. 7, pp. 830–836, Jul. 2008.

A Novel Approach to Communicate with Deaf Dumb and Blind Person

Prof. M.S.Ghute[1], Prof.S.Soitkar[2], Prof.K.P.Kamble[3], Mr. A. Kalbande[4]

[1,3,4]Department of Electronics and Telecommunication, Yeshwantrao Chavan College of Engg, Nagpur
[2]Department of Electronics Engineering, Nagpur

Abstract— In day to day life communication is major issue for deaf, dumb people and for Blind person it is difficult to take notes of particular things. So, for removing the barrier of communication a glove is designed for mute people with preloaded messages and a Braille embosser for Blind person to read notes in Braille language.

The main objective of this paper is to design a portable and reasonably sized Device that is easy to use. The design for this Device was made keeping in mind all different kind of disabilities. This paper is valuable to a disable person who is having difficulty in communicating with others. The hardware implemented in this paper can be used remotely to give notes to blind by imprinting on Braille Embosser. To implement this paper the main components are PIC18F886, APR33A3, Bluetooth Transceiver HC-05, Flex Sensor, Servo motors SG-90.

Keywords— Bluetooth, Braille Embosser, Glove, LCD, PIC.

I. INTRODUCTION

In real word, there are many people who are deaf and dumb cannot communicate easily. Hence in this paper a glove is designed using flex sensor to communicate between Dumb and normal people and assigning particular message for each gesture .The gestures created by the glove will be sent to normal person's phone and will also be displayed on LCD. In this paper a Braille Embosser is designed to communicate with blind person having servomotors to imprint Braille characters with the advancement in the technology, there have been many innovations in regards with this disabled people but person with moderate income would not afford it. So the first and the foremost need of a society is to develop a system through which a person with disabilities can live a life that a normal person does.

Disabilities like blind, deaf, dumb are more of serious concern. Science and Technology have made Human life addictive to comfort but still there exists an underprivileged group of people who are fighting for finding a innovative way that can make the process of communication easier for them. According to the World Health Organization, about 285 million people in the world are blind, 300 million are deaf and 1 million are dumb. In day to day life communication is major issue for deaf, dumb, blind people. This paper "A Novel Approach to Communicate with Deaf, Dumb and Blind Person" removes the barrier of communication between them and normal person.

II. SYSTEM FUNCTIONALITY

2.1 PART I: FOR BLIND

First, For Blind people it is very difficult to talk notes and read books like others .This paper developed and designed a Braille Embosser for blind by which the blind will be able to read the alphabets one by one with the help of Braille characters which are in 2*3 Matrix .The input to the Braille embosser can be given remotely using any device using Bluetooth connectivity. In this paper Servo Motors (SG-90) is used for imprinting the Braille characters in 2*3 matrixes. as shown in the fig1.Initially all the pointers of the Servo's are in parallel to the surface of the ground and when some character is being made the shaft is pointed at 90 degrees i.e. perpendicular to the ground surface. Different characters are imprinted with proper delay between each character .In this way we can provide all the reading material to the blind people in Braille Language remotely. For Wireless connectivity Bluetooth Transceiver HC-05 is used.
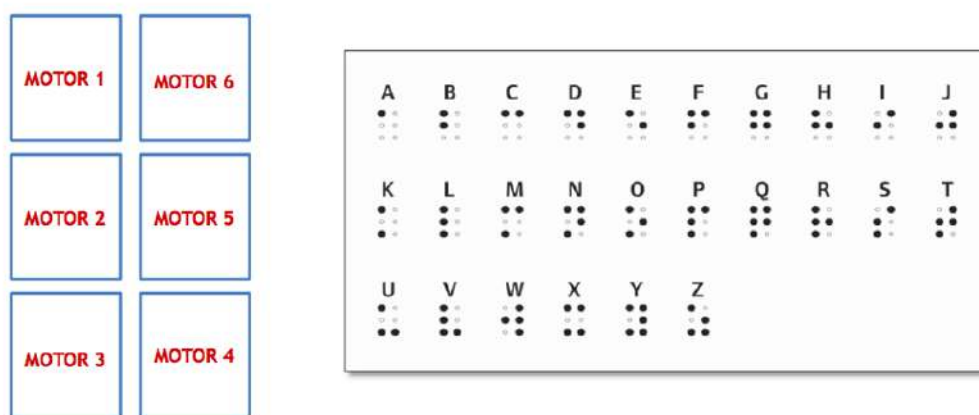
FIG. 1: ARRANGEMENT OF SERVO MOTORS (SG-90) FOR IMPRINTING THE BRAILLE CHARACTERS

2.2   PART II: FOR DUMB

For Mute/Dumb Person input is given through Glove which is having Flex Sensor is shown in fig.2 which is connected to PIC .Output of the glove is computed according to the gesture and a specific preloaded audio clip/message is played via speaker and for this Apr33A3 is used. This output is also sent to the Mobile Device using the Bluetooth Module wirelessly and is displayed on a LCD screen too. For different flex different resistance values were tested at Normal position and at Bend Position and accordingly the program was written using conditions. Like this the different hand gestures were recognized. The Analog to Digital Convertors i.e. ADC are inbuilt in PIC Hence it is not used externally

2.3   PART III : FOR DEAF

Finally, For Deaf Person if we want to convey something to the Deaf person. Input is given via Bluetooth Device Such as Mobile .Which has preloaded messages which can be displayed in front of the LCD screen remotely which lies in front of the Deaf Person.
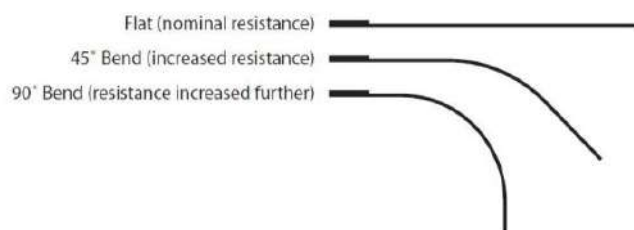
FIG. 2: BENDING OF FLEX SENSOR

III.   WORKING PRINCIPLE

For blind people input is given remotely through Mobile device which is connected via Bluetooth and Output can be sensed via braille embosser. Servo Motors SG90 is being used as a Braille Embosser to give the sense of the Braille characters which are in the form of 2*3 Matrix. Bluetooth Transceiver HC-05is used to communicate with the Embosser via PIC16F886.Then, For Mute/Dumb person. Input is given through Glove which is having Flex Sensor which is connected to PIC. Output of Glove is computed according to the gesture specific preloaded audio clip/message is played via speaker and for that APR33A3 module is used. This output is sent through the mobile device using the Bluetooth module wirelessly and is displayed on the LCD screen as shown in fig.3. For different flex resistance values were tested at Normal position and at Bend Position and accordingly the program was written using condition. Then Finally for Deaf person if we want to convey something to the deaf person. Input is given via Bluetooth device such as mobile which has pre loaded messages which can be displayed on LCD screen remotely which lies in front of the deaf person.
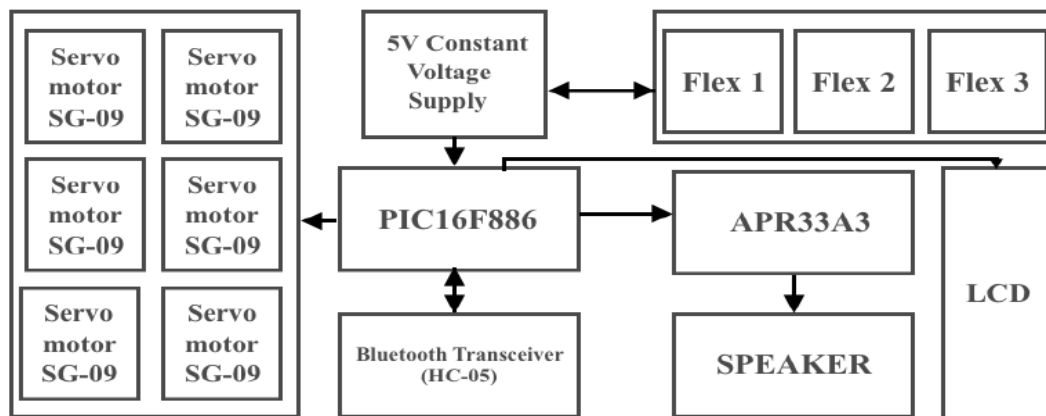
FIG. 3: BLOCK DIAGRAM FOR COMMUNICATION

Fig. 4 circuit diagram used for implementation of hardware part consist of six servo motors arranged in a fashion to imprint braille characters ,which are then connected to PIC at PORTC0-5 , LCD is also connected to PORTB 2-7 of PIC ,Three flex sensor for the gloves are also connected in this diagram to PORTA 0-2 of PIC ,Bluetooth module for wireless communication is connect to PORTC6-7 Audio Playback module is connected to PORT3-7.Pull down Transformer is also connected for prevention the circuit from voltage overloading.
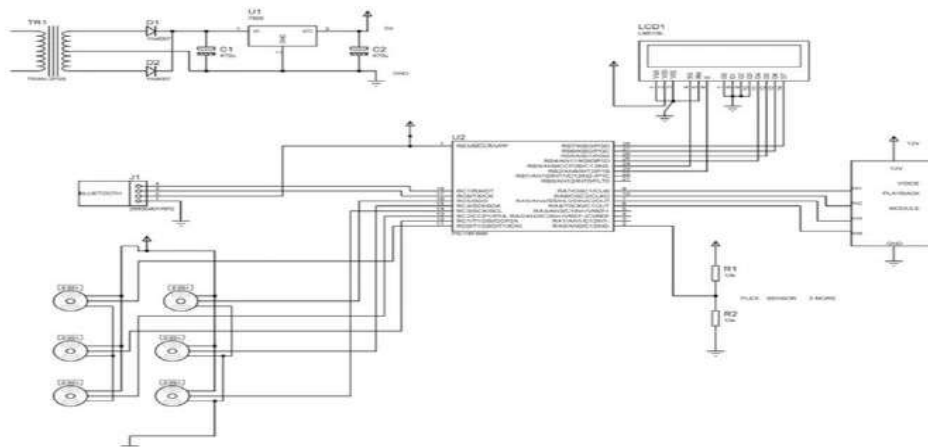
FIG. 4: CIRCUIT DIAGRAM USED FOR IMPLEMENTATION OF HARDWARE
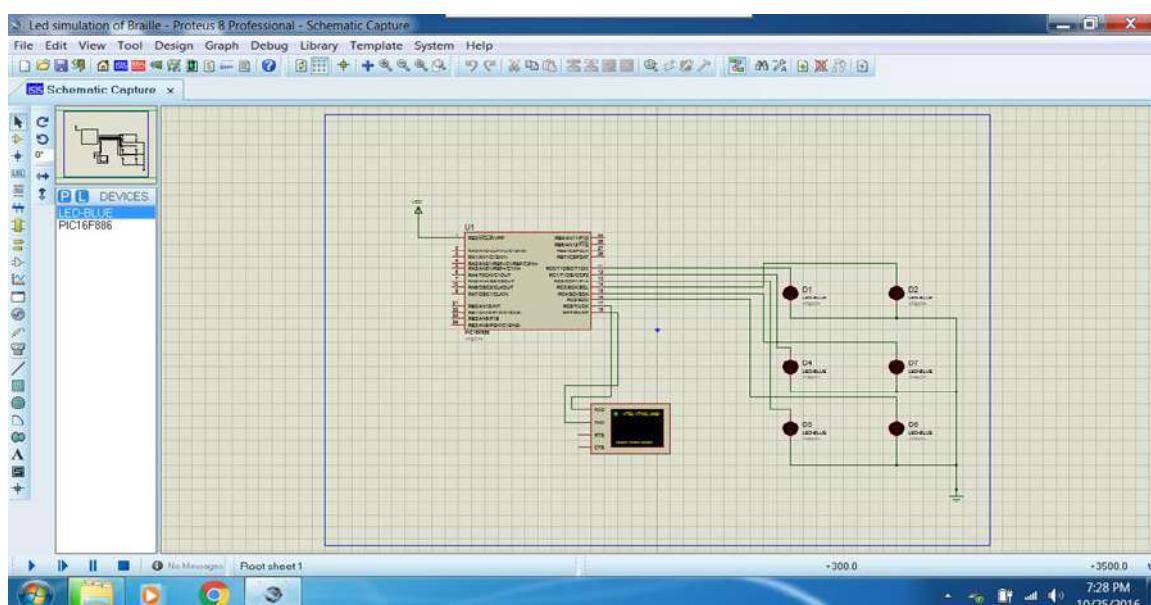
FIG. 5: SIMULATION RESULT
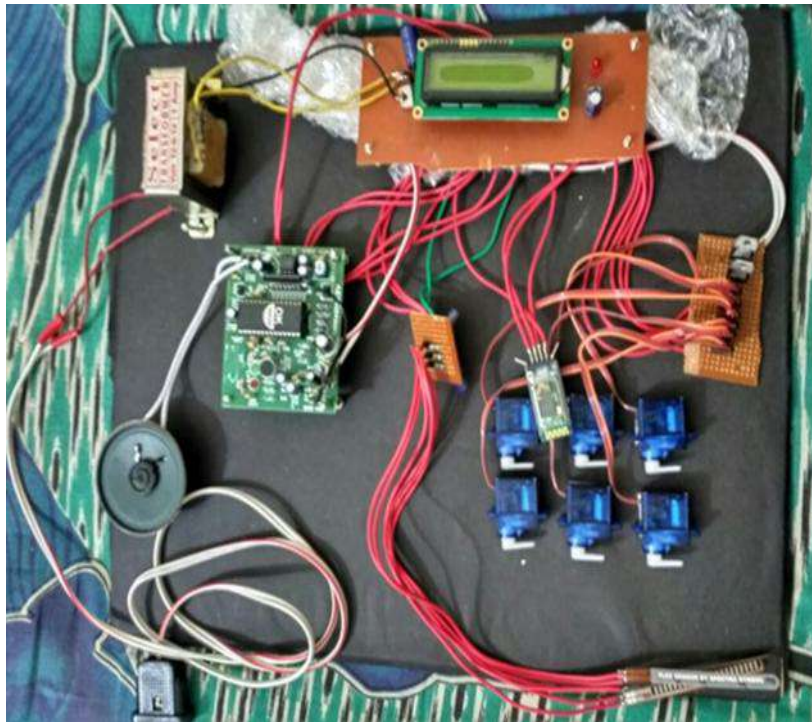
FIG. 6: HARDWARE IMPLEMENTED FOR COMMUNICATION WITH DEAF, DUMB AND BLIND PERSON

IV.   CONCLUSION

After working on this noble idea this paper successfully build a device to remove the barrier of communication between deaf, dumb and blind person and a disable person .People can use Bluetooth device for the communication whose range is descent for now i.e. 30 meters. Hence this device can work wirelessly used for around 30 meters. Simulation result &hardware implemented shown in figure 5 & 6 respectively.As per the design and application of this device, if properly manufactured in small size and in large amount this device can be manufactured at a very low price with high usability .This is a very noble approach to communicate bidirectionally between normal and disable person. This is very useful for the blind person as with the help of this device he can read anything which is written in normal English language and can be imprinted on the Braille embosser. People can also communicate wirelessly using this Braille embosser to blind person .Flex sensor results can also be displayed on mobile screen wirelessly using Bluetooth , in future WIFI technology will be use to increase the range of the device.

REFERENCES

[1] Indian Sign Languages using Flex Sensor Glove - International Journal of Engineering Trends and Technology (IJETT) - Volume4 Issue6- June 2013.

[2] Implementation of Flex sensor and Electronic Compass for Hand Gesture Based Wireless Automation of Material Handling Robot - International Journal of Scientific and Research Publications, Volume 2, Issue 12, December 2012 1 ISSN 2250-3153

[3] Novel Approaches for Robotic Control Using Flex Sensor - Sangeetha.P et al. Int. Journal of Engineering Research and Applications www.ijera.com ISSN : 2248-9622, Vol. 5, Issue 2, (Part -2) February 2015, pp.79-81

Comparison of Self Compacting Concrete (SSC) containing Fly Ash, Ground Granulate Blast Furnace Slag

Akash Goyal

College of Engineering Studies, University of Petroleum and Energy Studies, Dehradun, Uttarakhand

Abstract— *This research work includes the comparison of compressive strength of two different mineral admixtures namely Fly ash and blast furnace slag. It also comprises of comparison of workability of both the mineral admixtures. This is obtained by performing slump test, L box test, U box test and T50 test. The method adopted to perform the workability is by replacing 30%, 40% and 50% of Portland cement with the particular mineral admixture and then compared. The influence of these mineral admixtures on the properties of these mixtures is also investigated. The mix proportion is made as per the guidelines of European federation of contractors and producers for structure. The mixture comprises of Ordinary Portland cement (grade 43). Local rivers were used to obtain the sand lying under zone 2 was used. The specific gravity of the sand is kept 2.65 and that of cement 3.15. Coarse aggregates of nominal size of size 12.5mm conforming IS 383-1970 were used. The specific gravity of coarse aggregate being 2.77. The size of the coarse aggregate is to be checked in order to check that it does not cause a blocking effect in self compacting concrete. In case of self compacting concrete the ratio of coarse aggregate is much lower than that in case of ordinary Portland cement. Fine aggregate ratio in self compacting concrete is kept higher in comparison to Ordinary Portland cement so that flowing viscosity is high and the stability of the mixture is maintained and also bleeding is kept at bay and segregation of coarse material is also avoided (Boukendakdji et al., 2009). The specific gravity of the sand is kept 2.65 and that of cement 3.15 . Fly ash being industrial by product was obtained from Uttarakhand Power Corporation, Dehradun whereas Ground Granulate Blast Furnace Slag (GGBS) was obtained from local vendors for cheap prices.*

From this view point it can be incorporated that the cost of self compacting concrete can be considerably reduced by replacing Portland cement with industrial by-products and also reducing the amounts of chemical admixtures and hence their cost.

Keywords: *Fly ash, Ground granulated blast furnace slag, Ordinary Portland cement, self compacting concrete.*

I. INTRODUCTION

Concrete is the most important and the most used construction material across the globe. Numerous efforts are being made at this very time also in order to modify and enhance the properties of concrete, be it its compressive strength, tensile and flexural strength, aesthetic looks, and compaction and consolidation properties. These decades of research can be classified into four stages. First came the conventional concrete that comprised of materials - water, cement, coarse aggregates, and fine granular aggregates. Then as the population grew, there grew a need of more infrastructure and with the advancements over the decades engineers created high compressive strength concrete (HCSC). In initial stages this was obtained by reducing the amount of water per cement ratio. In later years the fifth ingredient was discovered, they being chemical admixtures. They fall into these categories.

- Air entrainers
- Water reducers
- Set retarders

The main objective of these chemical admixtures was to enhance the properties of the concrete mixture in both the fresh state as well as hardened state. But in recent years mineral admixtures is the new addition in concrete technology which performs really well. With the addition of mineral admixtures to the concrete mixture Self Compacting Concrete is obtained which is cheap in cost and the same time does not compromise with the other properties of the concrete. Some common mineral admixtures used are.

- Rice husk ash
- Metakolin
- Silica fume
- Fly ash
- Blast furnace slag

Self compacting concrete (SCC) is a concrete which does not require any mechanical or dynamic vibrations in order to compact it. It flows under its own weight to achieve the desired compactness and placement even without bleeding and segregation. Self compaction concrete was first developed in Japan in late 1980s in order to tackle the problem of use of vibrators in congested reinforced constructions. But the only problem with the self compacting concrete is the cost as it amounts to large volumes of Portland cement and chemical admixtures to be manufactured and maintain the desired freshness and hardness. But to reduce the cost of the mixture. It has been proved economical due to number of reasons.

- Faster manufacturing
- Reduction in manpower on site
- Better surface finish
- Easy to place
- Improved durability
- Greater freedom in design
- Thin concrete sections
- Reduction in noise level
- Absence of vibrating machines
- Skilled labour for placement not required
- Safer working conditions

The way to achieve the desired freshness and performance of the SCC is the use of mineral admixtures such as silica fumes, ground granulated blast furnace slag, fly ash which is finely granulated and mixed into the concrete mixture. By the usage of mineral admixtures it reduces the amount of Portland cement. the cost will be automatically reduced if the admixtures used are industrial by products. They also tend to reduce the heat of hydration of the concrete mixture hence giving it a good performance as lower water content leads to higher durability in addition to better mechanical properties of the structure. With the use of mineral admixture the requirement for chemical adhesives is eliminated.

II.   EXPERIMENTAL INVESTIGATION

2.1   Mix Proportion

In this study one control mix whereas six mixtures with different composition and different mineral admixtures were prepared and studied in order to study the behaviour of the self compacting concrete. The replacement of 30%, 40%, 50% of Portland cement with the respective mineral admixture is carried out. After several iterative calculations the water/cement ratio is kept 0.35(by weight). The total mass of the powder is kept 500 kg/m³. The weight of the coarse aggregate is kept 600 kg/m³. In the process of minimizing the water content for desired stability it can also result into low yield stress concrete with moderate viscosity. Therefore a strong amount of high water reducer is added to obtain a required deformability especially with binding materials being used very less (Brooks et al., 2000). In this case polycarboxylic ether (pH greater than 6) is used as it works just very well in low dosage also, plus it is better compared other bases in terms of effectiveness. Many efforts have been made in order to come up with a single way or a combination of methods to achieve the perfect way to obtain a self concreting mix which characterises all the workability aspects , so in order to get a perfect mix design one should always try different methods and consider their options *(Bonen et al., 2005).* The composition of the mineral admixtures being used and cement is given in the table.

TABLE 1
PROPERTIES OF PORTLAND CEMENT AND MINERAL ADMIXTURES.

Components (%)	Cement	Fly ash	Slag content (GGBS)
Chemical composition (%)			
SiO_2	20	40	10-19
Magnesium Oxide (MgO)	2.5	4	11
$Al2O_3$	4.85	26	1-3
Loss in ignition (LOI)	2.0	2.0	1.2
Fe_2O_3	0.6	6.0	22-30
Calcium Oxide (CaO)	62.56	15	40-52

2.2   Material Properties

In this research The Bureau of Indian Standards (IS) and American Society for Testing and Materials (ASTM) has been adopted to determine the properties of raw materials used in this research.

2.2.1   Cement

Ordinary Portland cement of grade 43 is used corresponding to IS- 8112(1989). The specific gravity of cement is 3.15

2.2.2   Chemical admixture

A polycarboxylate based water reducing admixture was used in the mixes apart from control mixes in order to prevent bleeding

2.2.3   Additive Mineral Admixtures

In this research two mineral admixtures have been used in order to replace the mass of Portland cement, they being Fly ash and Ground Granulated Blast Furnace Slag (GGBS). The chemical composition of both the admixtures is given in Table 1.

Fly ash being industrial by product was obtained from Uttarakhand Power Corporation, Dehradun whereas Ground Granulate Blast Furnace Slag (GGBS) was obtained from local vendors for as cheap as ₹ 4/ Kg.

The specific gravity of fly ash is kept at 2.12 and that of GGBS at 3.44 by weight.

2.2.4   Coarse Aggregate

Coarse aggregates of nominal size of size 12.5mm conforming IS 383-1970 were used. The specific gravity of coarse aggregate being 2.77.

2.2.5   Fine Aggregate

Local rivers were used to obtain the sand lying under zone 2 was used. The specific gravity of the sand is kept 2.65 in oven dry conditions.

2.2.6   Water

Ordinary tap water is used.

2.2.7   Curing

SCC tends to dry faster as compared to conventional concrete this is mainly due to absence of any bleed water at the surface. Therefore it is recommended to start initial curing as soon as practical to avoid shrinkage cracking.

2.2.8   Placing

Though it is quite easy to place SCC but there are certain recommendations that can be kept in mind while placing to minimise the risk of segregation:

- free fall vertical should not be more than 5 m

- the permissible distance of horizontal flow from the point of discharge should not be more than 10 m

Note: the advise is totally conservative as per the research, in suitable circumstances a contractor may demonstrate that the suggested limits can be maximised.

TABLE 2
SPECIFIC GRAVITY OF DIFFERENT COMPONENTS

Different components	Specific Gravity (g/cc)
Sand	2.65
Cement	3.15
Coarse Aggregate	2.77
Fly Ash	2.12
GGBS	3.44

III.   METHODOLOGY

In this paper the compressive strength is evaluated by using the moulds of 150mm×150mm×150mm. 18 cube were tested and casted for each mixture of both fly ash, GGBS and then values of compressive strength is determined. Before studying the strength, the mixture is evaluated for its workability properties by performing tests Slump flow test, L box test, U-box test, V funnel test, T50 test.

3.1   Slump Test

The slump test is a mean of evaluating the consistency of the fresh concrete. It also determines the ability of self compacting concrete to deform under its own weight. It is also used indirectly to check the amount of water added to the mixture. It is also used to evaluate the flowing ability of the concrete with respect to spread diameter, or the horizontal free flow of the SCC under its own weight. On lifting the slump cone, filled from concrete the average diameter of the spread is measured. The results for slump test are given in the table. According to European codes the value of slump should lie in between 650mm-800mm (EFNARC, 2002).

3.2   T 50cm Test

This is the evaluation of filling ability of concrete mixture without any reinforcements. However it does not indicate the ability of the SCC to pass between reinforcements but it does give some indication of resistance to segregation. It is the evaluation of time taken by the slump to reach 50 cm of flow. T 50 test was performed during the slump test flow. Lower time indicates greater flow ability.
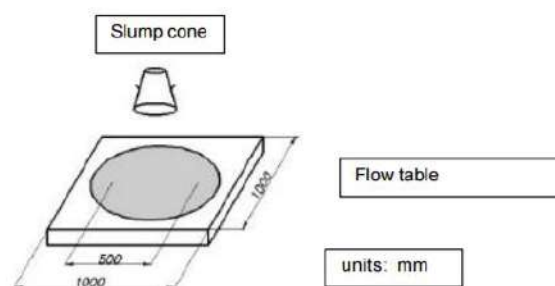
FIG 1. APPARATUS FOR BOTH (I) SLUMP TEST AND (II) T 50 TEST

3.3   L Box Test

It is a test used to assess the flow of the concrete and also the extent up to which it is subjected to blocking due to reinforcements. The apparatus consists of L shaped apparatus with a vertical section and a horizontal section. Both these sections are separated with a movable gate. In this process concrete mixture is poured in from the vertical portion of the apparatus, then suddenly the gates separating the sections is opened and the concrete mix is allowed to flow through to the horizontal section. When the flow is stopped the height of concrete at horizontal section is expressed as a proportion of that remaining in the vertical section (h2/h1). This test determines the passing ability of the concrete through the restricted bars. If flows as freely as water it will be completely horizontal at rest and therefore the ratio is unity. The minimum value of h2/h1 should be 0.8 (EFNARC, 2002).
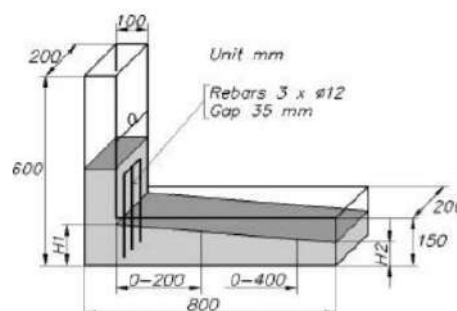
FIG 2. L BOX TEST APPARATUS

3.4   U Box Test

This test is used to determine the filling ability of self compacting concrete. The apparatus consists of U shaped apparatus divided into two compartments with a sliding gate comprising of reinforced bars with adequate spacing. The concrete mixture is poured from one of the compartments, and then after some time the sliding gate is slid causing the concrete mixture to flow into other compartment. Height in both the compartments is noted down as h2 and h1. If concrete is allowed to flow like water the concrete mix in both the compartments will be at same height, the difference in height between both the compartments (h2-h1) will be zero. The nearer the value of h2-h1 to 'zero' betters the flowing ability of the self compacting concrete. The maximum value of the height difference should be maximum 30mm (EFNARC, 2002).
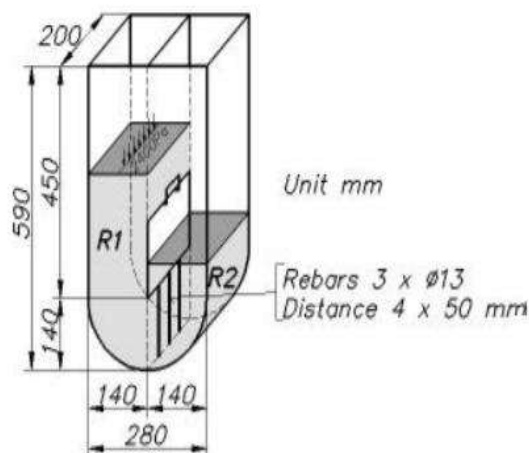
FIG 3. U BOX TEST APPARATUS

3.5   V Funnel Test

The described V Funnel test is used to determine the flow or filling ability of a SCC. The maximum size of aggregate used in mix design should be 20mm. The funnel is a inverted V shaped funnel which is filled with 12 litres of concrete mixture and the time taken for this concrete to flow through the apparatus is measured. Lower the time better the flowing ability of the concrete mixture. If the concrete exhibits segregation the flow time will increase considerably. The inverted shape expose any liability of the concrete to block is easily reflected. For example if there is a high flow time it can be associated with low deformability which is caused due to high paste viscosity, and with high inter particle friction. The maximum time that should be taken by any SCC mix is 10 sec (EFNARC, 2002).
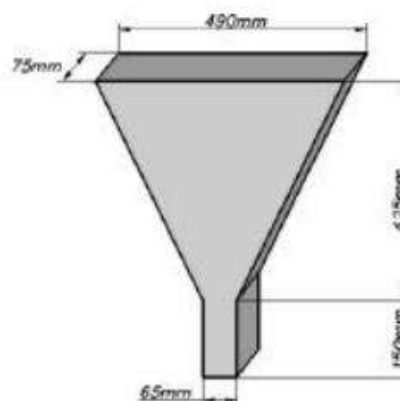
FIG 4. V FUNNEL TEST APPARATUS

IV. RESULTS AND DISCUSSIONS

In these paper properties of self compacting concrete is investigated by using industrial by products such as fly ash and GGBS at three different replacements rates for the cement. The study is done according to the European standards given for Indian conditions. In this paper fresh and hardened properties of a SCC produced by mixing of fly ash and GGBS were performed on fresh concrete, specifically workability tests and strength tests.

4.1   Fresh Properties

Slump test indicates the flowing ability of the concrete mixture under its own weight. All the self compacting mixtures containing fly ash or GGBS showed satisfactory results and the ranges were well within the permissible limits provided by EFNARC 600mm-690mm. This indicates good deformability of the mixtures. The slump flow values for all the self compacting mixtures are given in the table. The higher the value of slump flow it indicates the ability of concrete to fill or flow under its own weight. It is to be noted that as we replace higher amounts of GGBS the blast performance of slag slump increases up to 50%. Whenever cement is replaced by mineral admixture, a small amount of chemical admixture is needed in order to compensate for the water and improve the flow. In comparison to GGBS fly ash requires more amount of chemical admixture to maintain the same slump flow and shown good slump values. In comparison to GGBS fly ash had a more spherical geometry and a coarser particle surface, reducing the surface area. As the density of fly ash is lower in comparison to cement therefore when replaced fly ash causes higher volume of paste, which reduces the friction between the fine aggregates and paste interface, which further increases thee cohesiveness and plasticity, which leads to better workability.

Water/powder ratio is kept between 0.9 to 1.0 by volume depending upon the properties of the powder. With super plasticisers dosage is kept at 2.2%. For constant water/powder ratio and same content of super plasticisers it is observed that an optimum slump is observed at a replacement level of 30% and an increase up to 50% is observed.

In case of T50 test it is a measure of flowing ability of the concrete under no reinforcements. It can also be said as the secondary indication of flow ability. The lower the time the better the flowing ability. As the test is performed during the slump test itself it was influenced with a dosage of water and super plasticisers. It is observed that till 30% replacement the T50 time is reduced, but after replacing more percentage leads to increase in T50 time along with some bleeding and segregation. Various good relationships between T50 time and various mixtures of SCC are shown below. The values for T50 tests for all the self compacting mixtures are also reflected in the table 3 below.

V funnel test is a measure of self flowability and stability of self compacting concrete. The range under which the SCC is considered appropriate is 6-10 sec. We can notice that in both the cases when we increase the percentage of replacement the time decreases which shows the better flowability of the SCC. If the time increases it is sign of segregation or bleeding. In case of severe segregation coarser particles come in the middle part of the apparatus and the mortar and the paste on the outer periphery. All the values for the V Funnel test are given in the table 3 below.

L Box test is a test which assesses the flow of the concrete under the blocking of reinforcements. In here as explained before a blocking ratio h2/h1 is the determining criteria. If concrete flows like water the blocking ratio is unity, therefore the closer the value of the ratio to unity better will be its flowing ability. According to European standards the minimum value obtained should be at least 0.8. It is noticed that the values for SCC are more close to unity than a normal concrete, which shows its tremendous ability to flow under reinforcements. Here in all cases of mixture satisfactory results are obtained. All the values for the tests are given in the table below.

U Box test is used to measure the filling ability of SCC under blockage. It also is a measure of self compatibility of the SCC. In here also a blocking factor of h2-h1 plays a major role. If concrete flow like water in test it will be completely horizontal, hence h2-h1=0. So more the value is near to zero, it signifies better passing and filling ability of the concrete. According to European standards the range for appropriate SCC is set at 0-30mm. All the mixtures were well within the range. All the values for the test are given in the table 4.

TABLE 3
FRESH PROPERTIES OF SELF COMPACTING MIXTURES.

Mixture no	Water/powder	Slump (mm)	T50 (sec)	V funnel (sec)	L Box (h2/h1)	U Box (h2-h1) (mm)
Fly-ash 30%	0.35	660	6.1	10	0.9	26.5
Fly-ash 40%	0.35	675	6.6	9	0.93	26
Fly-ash 50%	0.35	680	7	9.15	0.95	25.7
Blast furnace slag-30%	0.35	680	5	10	0.9	26
Blast furnace slag-40%	0.35	685	5.5	8	0.95	25
Blast furnace slag-50%	0.35	690	6	7	1	24

TABLE 4
ACCEPTANCE CRITERIA FOR SELF COMPACTING CONCRETE.

Method	Unit	Typical ranges of values	
		Minimum	Maximum
Slump flow	Mm	650	800
T50cm	Sec	2	5
V funnel	Sec	6	12
L box	(h2/h1)	0.8	1.0
U box	(h2-h1) mm	0	30

4.2 Mechanical Properties

The compressive strength for all the mixture were taken at 7th and then 28th day. All the measures of compressive strength for each mixture of both the mineral admixture is given in the table below. It is observed when compared the control mix that on increasing the percentage of mineral admixture there is a reduction of strength for both fly ash, GGBS. This happens mainly due to fineness and packing. But on the final day it is noticed that the compressive strengths of both the mixtures of fly ash and GGBS achieved a good value in regard to the control mix. This mainly happens because on initial stages the pozzolanic reactions were not sufficient enough to increase the compressive strengths of both the self concrete mixtures. But in later stages it can be seen from the results that the compressive strength due to slower pozzolanic reactions increases.

TABLE 5
COMPRESSIVE STRENGTH OF FLY ASH AND BLAST FURNACE SLAG MIXES.

Water/ powder	Compressive strength (MPa)					
	Fly Ash			Blast Furnace Slag		
	Mixture no	7 days	28 days	Mixture no	7 days	28 days
0.35	Control	20	30	Control	20	30
0.35	Fly-ash 30%	29.16	37.18	Blast furnace slag- 30%	24.1	32.44
0.35	Fly-ash 40%	28.60	39.13	Blast furnace slag- 40%	21.4	31.8
0.35	Fly-ash 50%	28.73	41.42	Blast furnace slag- 50%	18.2	31.55

V.   CONCLUSIONS

This paper focuses on the freshness as well as mechanical property of a self compacting mixture.

Some conclusions made out his research are:

1.   All the mixes with both the mineral admixtures performed quite well in freshness tests. Out of the both Blast furnace slag had the best results.

2.   With the use of mineral admixture the cost is considerably reduced due to no use of mechanical vibrators, plus viscosity modifying admixtures are also avoided.

3.   It is observed that with a increase in replacement percentage of the mineral admixture the compressive strength is reduced considerably, so 30% replacement is considered the most optimum percentage of replacement.

4. It is observed that to determine the flowing ability of the self concrete mixture slump flow test is the most critical test out of all the tests.

5. Water by cement ratio is kept 0.35. The ratio underneath or beyond this value may cause segregation and develop blocking tendency in the self compacting concrete mixture.

REFERENCES

[1] Ozawa K, Maekawa K, Okamura. H. Development of the high performance concrete. Proc JSI 1989;11(1):699–704.

[2] Skarendahl A, Peterson O. State of the art report of RILEM technical committee 174-SCC, self compacting concrete. S.A.R.L, Paris: RILEM Publications; 2000,. p. 17–22.

[3] Sukumar Binu, Nagamani K, Srinivasa Raghavan R, Chandrasekaran E. Rheological characteristics and acceptance criteria for self-compacting concrete. In: Proceedings of national conference on recent developments in materials & structures, Calicut: National Institute of Technology; 2004.

[4] Jagadish Vengala, Ranganath RV. Effect of fly ash on long term strength in high performance self-compacting concrete. In: Proceedings of the INCONTEST 2003, Coimbatore: Kumaraguru College of Technology; 2003.

[5] Uysal, M. and Sumer, M. (2011). "Performance of self-compacting concrete containing different mineral admixtures." Construction and Building materials, Vol. 25, No. 11, pp. 4112-4120.

[6] Sonebi, M. (2004). "Medium strength self-compacting concrete containing fly ash: Modelling using factorial experimental plans." Cement and Concrete Research, Vol. 34, No. 7, pp. 1199-1208.

[7] EFNARC (2002). Specification and guidelines for self-compacting concrete, UK , p. 32, ISBN 0953973344.

[8] Cement and Concrete Research, Vol. 31, No. 3, pp. 413-420. Brooks, J. J., Johari , M. A. M., and Mazloom, M. (2000). "Effect of admixtures on the setting times of high-strength concrete. " Cement and Concrete Composites, Vol. 22, No. 4, pp. 293-301.

[9] Sahmaran , M., Yaman, I. O., and Tok, M. (2009). "Transport and mechanical properties of self consolidating concrete with high volume fly ash."Cement Concrete Composites, Vol. 31, No. 2, pp . 99-106.

[10] ASTM. Standard test method for sieve analysis of fine aggregate, C136-01. In: Bailey SJ, Baldini NC, McElrone EK, Peters KA, Rosiak JL, Simms ST, Terruso DA , Whealen EA, editors. Annual book of ASTM standards concrete and aggregates, 4 (4.02) ; 2004. p. 84–88.

[11] Performance of self-compacting concrete containing different mineral admixtures; P.Ramanathan, I. Baska, P. Muthupriya, and R. Venkatasubramani,; (2012).

[12] Specification and Guidelines for Self-Compacting Concrete, www.efnarc.org (2002).

[13] Incorporating European Standards for Testing Self Compacting Concrete in Indian Conditions ; Dr. Hemant Sood , Dr.R.K.Khitoliya and S. S. Pathak Dept. of Civil Engineering, N.I.T.T.T.R; Chandigarh, INDIA. (2009).

[14] Evaluation of strength at early ages of self- compacting concrete with high volume fly ash.; Binu Sukumar, K. Nagamani, R. Srinivasa Raghavan, (2007).

[15] Mix Design Procedure for Self Compacting Concrete; 1Krishna Murthy.N, 2Narasimha Rao A.V, 3Ramana Reddy I.Vand 4Vijaya Sekhar Reddy.M Engineering Department , Yogi Vemana University, Kadapa, & Research Scholar of S.V.University ,Tirupati, India (2012).

[16] Bureau of Indian Standards. "Methods of test for aggregates for concrete. Specific gravity, Density, Voids, Absorption and Bulking", IS - 2386 (Part III, 1963).

[17] EFNARC (European Federation of national trade associations representing producers and applicators of specialist building products) , Specification and Guidelines for self- compacting concrete, February 2002, Hampshire, U.K.

[18] EFNARC. "Specification and guidelines for self- compacting concrete. European Federation of Producers and Applicators of Specialist Products for Structures", 2002.

[19] IS: 3812-2003, Specifications for Pulverized fuel ash, Bureau 0f Indian Standards, New Delhi, India.

[20] IS: 8112-1989, Specifications for 43 grade Portland cement , Bureau of Indian Standards, New Delhi, India

[21] IS: 383-1970, Specifications for Coarse and Fine aggregates from Natural sources for Concrete, Bureau of Indian Standards, New Delhi, India

Toxigenic Molds in Different Grains from Albania

Afërdita Shtëmbari

Department of Industrial Chemistry, University of Tirana, Albania

Abstract—*Mycotoxins are secondary metabolites produced by molds, produced by the organism under certain stress conditions, such as drough and high temperatures in field, or high humidity levels in storage facilities. It is well known that their presence may result in hazardous implications in the humans and animals health. The aim of this study was to analyze the presence of mycotoxigenic moulds in cereals harvested in Albania. Microbiological evaluation was accomplished in different media for moulds. Despite the fact that method is conventional, presenting approximate values, it helps to a judgement on the mycotoxigenic molds and other microorganisms.*

The concentration of microorganisms varied 0.5-260 x 10³ cfu/g in wheat and 80-200 x 10⁴ cfu/g in maize. After the identification and classification was found presence of mainly Ascomycete classes; especially Aspergillus, Penicillium and Fusarium species. In conlusion, after comparing the finding with interantional standards was concluded that wheat comodity was within standards, while some of maize samples passed the allowed levels.

Keywords— *Albania, Maize, Toxigenic molds, Wheat.*

I.   INTRODUCTION

The aim of this study was to evaluate the presence of mycotoxigenic fungis in different crops harvested in Albania. The evaluation of the diversity of filamentous molds and investigation of their presence were conducted in wheat and maize samples.

Cereals and cereal products constitute the staple food in the diet of the Albanian population. Their parallel use as to human consumption as well as livestock feed, implicates the importance of food and feed safety issue on cereal grains and cereal products. Microorganisms contaminating the cereal grains may originate from air, soil, water, different living organisms, storage and shipping, as well as processing stages. Many factors, part of the environment, influence microbial contamination, including rainfall, drought, humidity, temperature, sunlight, frost, soil conditions, wind, insect, bird and rodent activity, harvesting equipment, use of chemicals in production versus organic production, storage and handling, and moisture control (Heredia et al. 2009).

According to the stage of fungal contamination, frequently they are grouped into two categories, field fungi and storage fungi (Miller, 1995). The first group invades the grain before harvesting, in field, in climatic conditions when the moisture content during harvesting period vary 18 to 30%, whereas storage fungi, considered as post-harvest invaders, infect grain when they have lower moisture contents (14 to 16%). Field fungi consist primarily of species of *Alternaria*, *Cladosporium*, *Fusarium*, and *Helminthosporium*, while storage fungi include species of *Eurotium*, *Aspergillus*, *Penicillium*, and *Mucor* (Riba *et al.*, 2008).

Finally the fungal growth may affect the grain's quality and have several negative consequences such as appearance alteration, technological properties modification, fungal infections or allergies development, and finally economic losses (Bennett et al. 2003).

Mycotoxigenic fungi presence in grain comodities in certain climatic conditions may indicate for mycotoxin presence, which may have hazardous implications in the humans and animals health. Within a given species, their impact on health is influenced by age, sex, weight, diet, exposure to infectious agents, and the co-occurrence with other mycotoxins through synergic effect manifestation and pharmacologically active substances (Milicevic et al., 2010). The majority of mycotoxins are grouped, according to their toxic activity, under chronic conditions as mutagenic, carcinogenic or teratogenic; while according to site of action they are grouped in: hemo-, hepato-, nephro-, dermato-, neuro- or immunotoxins (Niessen, 2007).

II.   METHOD OF STUDY

Cereals samples were obtained in sterile condition from different regions of the country during harvesting year of 2016. In this study were analyzed 15 samples (6 winter wheat samples and 13 maize samples). An amount of 0.5 kg samples were obtained in order to prepare the sample average with diagonal division.

2.1 Fungal Isolation and Identification

Examination of the contamination to the samples on molds was based on a slightly modified method of the European Feed Microbiology Organization (EFMO) (VDLUFA, 2007). To 20 g of each sample, 180 ml of 0.5% peptone water was added. The mixture was homogenized using a linear shaker for 20 min and then diluted to final concentration of 10^{-2}, 10^{-3} and 10^{-4} (VDLUFA, 2007). 1 ml aliquots of each dilution were spread (in duplicates) on the surface of solid medium. The composition of the medium was (per litre) as follows: 40 g malt extract, 2 g glucose, 1 ml Marlophen 810®, 60 mg Bengal Rose, 60 mg oxytetracycline-HCl (OTC), 12 g agar, 1000 ml distilled water. Plates were incubated for 3 days at 27°C in the dark and normal atmosphere. Afterwards, plates were stored at room temperature for another 3 days. Finally, the colonies were counted and the results were expressed as average colony forming units in thousands per gram of sample (10^3 CFU/g) using the following formula.

$$N = \frac{\sum C}{V \times n \times d} \qquad (1)$$

N = number of colony-forming units per gram of sample (CFU/g)

ΣC = sum of all colonies of the count plates

V = volume of the dilutions pipetted in the count plates in ml

n = number of count plates that can be evaluated

d = dilution factor

Taxonomic identifications of different genera of moulds were made visually and where applicable, by means of a magnifying glass or a stereomicroscope. Closer characterization was possible using a light-optical microscope.

III. RESULTS AND DISCUSSION

The microorganisms, isolated from wheat samples are shown in Table 1, while the results in the maize samples are shown in Table 2, the evidence on molds distribution in the analyzed samples.

TABLE 1
THE PRESENCE OF TOXIGENIC MOLDS IN WHEAT (IN X 10^3 CFU/G)

	Alternaria spp.	*Fusarium spp.*	*Cladosporium spp.*	*Penicillium spp.*	*Aspergillus spp.*
Sample 1	1	0.5	0.5	n.d	n.d
Sample 2	n.d	1	n.d	3.5	2
Sample 3	n.d	n.d	n.d	1	1
Sample 4	0.5	5	n.d	3	1
Sample 5	n.d	1	n.d	10	34
Sample 6	n.d	0.5	1	1	3
Sample 7	n.d	40	n.d	210	10

*n.d.= not detected

The leading contaminants among fungi in the wheat samples were *Aspergillus* spp. and *Fusarium* spp. Which were detected almost in all samples (77.7%) followed by *Penicillium* spp. (66.6%). *Alternaria* spp. and *Cladosporium spp.* were lowest contaminated only 22.2 %. The wheat sample with the highest number of moulds was sample 7 (260 x 10^3).

TABLE 2
TOXIGENIC MOULDS PRESENCE IN MAIZE SAMPLES (IN X 10^4 CFU/G)

	Alternaria spp.	*Fusarium spp.*	*Cladosporium spp.*	*Penicillium spp.*	*Aspergillus spp.*
Sample 1	n.d	2.5	n.d	10	26
Sample 2	n.d	10	n.d	40	140
Sample 3	n.d	8	n.d	12	80
Sample 4	n.d	100	n.d	5	24
Sample 5	n.d	4	n.d	80	14
Sample 6	n.d	82	n.d	11	20
Sample 7	n.d	n.d	1	100	100
Sample 8	25	n.d	n.d	120	32
Sample 9	n.d	11.5	3.5	30.5	2

*n.d.= not detected

The general means of fungi showed that *Penicillium* spp. (92.3%%) and *Fusarium* spp. (84.6%), followed by *Aspergillus* spp. (76.9%) were the most frequently isolated genera, while *Alternaria spp.* and *Mucor spp.* were the least frequently isolated genera (7.7%) from maize samples.

The maize sample with the highest number of moulds was sample 7 (200×10^4).

It is well known, that environmental conditions have great influence on the development and spread of moulds and consequently on the production of mycotoxins. Water stress, temperature stress and insect damage of a host plant are, under field conditions, the major determining factors of mould infestation and toxin production. With stored grain, factors which are likely to affect mycotoxin formation include moisture content and the composition of the substrate, environmental temperature, exposure time, damage to seeds, oxygen availability, carbon dioxide concentrations, fungal abundance, prevalence of toxic strains, spore loads, microbial interaction and invertebrate vectors, particularly insects. Spoilage, fungal growth and mycotoxin formation result from the complex interactions of these factors (Santin, 2005).

IV.   CONCLUSIONS

In this research, moulds, identification and classification, we revealed a high frequency of the genus *Aspergillus*, *Penicillium* and *Fusarium*. The concentration of microorganisms vary $0.5-34 \times 10^3$ cfu/g in wheat samples and vary $80-200 \times 10^4$ cfu/g in the maize samples. In conlusion, wheat samples which have been analyzed were within standards, while maize samples were not within standards. Additional studies incorporating analysis of toxin potential are needed to more fully assess the importance of species and contamination of cereals, in order to protect the population from risks associated with mycotoxin contamination.

REFERENCES

[1]   Bennett, J.W., Klich, M. (2003). Mycotoxins. Clinical Microbiology Review 16:497-516.

[2]   Heredia, N., Wesley, I. and Garcia, S. (2009). Microbiologically Safe Foods, USA.

[3]   Milicevic, D.R., Škrinjar, M. and Baltic, T. (2010). Real and Perceived Risks for Mycotoxin Contamination in Foods and Feeds. Challenges for Food Safety Control.Toxins, 2: 572-592.

[4]   Miller, J.D. (1995). Fungi and Mycotoxins in Grains. Implications for Stored Product Research. Journal Stored Product Research 31:1-16.

[5]   Niessen, L. (2007). PCR-Based Diagnosis and Quantification of Mycotoxin Producing Fungi. International Journal of Food Microbiology, 119:38-46.

[6]   Riba, A., Mokrane, S., Mathieu, F., Lebrihi, A. and Sabaou, N. (2008). Mycoflora and Ochratoxin A Producing Strains of Aspergillus in Algerian Wheat. International Journal of Food Microbiology, 122: 85–92.

[7]   Schmidt, H. L., Bucher, E., Spicher, G. (1981). Microbial Content Determination of Bacteria, Molds and Yeasts in Feed. Nutrient Media and Methodology. Agricultural Research, 34(4): 242-50.

[8]   Smith, M.T., Yarrow, D. (1996). Identification of the Common Food Borne Fungi. In R. A. Samson, E. S. Hoekstra, J. C. Frisvald, O. Filtenborg, Introduction to Food-Borne Fungi 3-232.

[9]   VDLUFA (2007). Standard Operation Procedure for the Enumeration of Micro-organisms Using Solid Culture Media. In VDLUFA Method Book III, Suppl. 7 (ch. 28.1.1., 14 p). Darmstadt: VDLUFA.

The Production Potential of the Olive Oil from Native Cultivars in Albania

S. Velo[1], D. Topi[2*]

Faculty of Natural Sciences, University of Tirana, Blvd Zogu 1, 1010, Tirana, Albania
* Author for correspondence (dritan.topi@unitir.edu.al)

***Abstract*— *Albania has an annual production capacity of ca. 50 000 tons of olive fruits and 6000 tons of olive oil. The corresponding cultivation area covers 41000 ha, distributed over 90 000 small farms. In total, olive trees area covers 6.3% of the total arable land. This paper, presents the characterizes the fatty acid profile and total phenolic content of 6 olive varieties, namely, Kalinjot, Ulli i bardhe Tirana (Bianco di Tirana), Karren, Nisiot, Kotruvs, and Kokerrmadh Berati, all from the same harvesting period.*

Results on fatty acid (FA) profiles exhibit a variation in concentration of oleic acid, 71.53 ± 0.02% (Kotruvs) to 80.07 ± 0.04% (Nisiot). The content of linoleic acid varies from 4.10 ± 0.00% (Nisiot) to 9.31 ± 0.01% (Kotruvs), whereas the content of linolenic acid varies from 0.45 ± 0.01% (Karren) to 0.72 ± 0.02% (Kalinjot). Analysed OO from six olive varieties revealed moderate levels of palmitic acid, between 9.94 ± 0.01% (Nisiot) to 12.21 ± 0.01% (Kotruvs). From a nutritional point of view, it is worth noticing that the Nisiot variety has an n-6/n-3 ratio of 8.11, while the Karren 18.72.

The total phenolic content for the studied olive cultivars varied from 89.74 ± 5.47 (Karren) to 445.03 ± 16.83 mg/kg olive oil (Ulli i bardhe Tirana); such variation may reflects different antioxidant capacity among olive cultivars.

Keywords*— *Native Olive Cultivars; Kalinjot; Ulli i Bardhe Tirana, Kokerrmadh Berati, Nisiot, Fatty acid, Polyphenol content.

I.   INTRODUCTION

The origin of olive trees in Albania is not different from the road of the distribution of this tree in the Mediterranean area. Archaeological evidences on the agriculture activities such as wheat cobs, truss grapes, olive lop are stamped in stones and coins of the Illyrian tribes. Olive tree cultivation is mainly concentrated in the Western Plain of the country, by penetrating the mainland through the river valleys (*[1]; [2]*). Its distribution is diversified according to climate and geography. It is mainly cultivated in the Mediterranean Climatic Zone, which covers 36.2 % of the Albanian territory.

Albania is a country with an actual annual producing capacity of 50 000 tons of olive fruits and 6000 tons of Olive oil. The olive plantations cover an area of 41000 ha, corresponding to 6.3% of the total arable land, where the characteristic is its distribution over 90 000 small farms. The incomes from the olive sector are 16 million Euros (*[3]*).

Recent genetic studies concluded that Albania owns 22 native olive cultivars. All 22 native cultivars are clustered in 7 different groups and the main factor influencing such clustering is the dimension of the olive fruit (*[4]*). In what concerns the region from which the native cultivars in this study have been selected, and based on RAPD methods, cultivars are grouped in three main groups, where the main group belongs to the *Ulli i bardhe Tirana* (UbT) with a coefficient of similarity that varies from 45% to 84%. Hence, scientific studies on the native cultivars are very important, due to their impact in the future of the olive oil industry. Based on their distribution, native olive cultivars are grouped in principal cultivars and secondary cultivars (*[4]*).

Olive oil is the only vegetable oil that can be consumed without prior refining treatment (*[5]; [6]*). Its major components are triglycerides, which represent more than 98% of the total weight. The remaining part belongs to non-saponifiable chemical compounds such as sterols, polyphenols, alcohols, waxes, hydrocarbons etc (*[7];* Servilli, Montedoro, 2003; *[9]*). Virgin olive oil composition depends on numerous factors such as the interaction between the cultivar and the environment, cultivation techniques, fruit ripeness and the oil extraction system (*[6]*). The characterisation of fatty acid profiles of olive oils from different olive cultivars is usually proposed as a methodology to differentiate these products according to their cultivar and geographical origin (*[6]; [10]*).

In this study, are presented the fatty acid composition and total polyphenol content of six olive cultivars. Studied cultivars were *Kalinjot, Ulli i bardhe Tirana (UbT)*, *Karren*, *Nisiot*, *Kotruvs*, *Kokerrmadh Berati*, which belong to different regions of Albania, with different pedoclimatic conditions. The olives from these cultivars are mainly used in the production of oil except to Kokerrmadh Berati used as Table Olive.

Nowadays, an attempt to modify the national fund of olive tree is an ongoing process. The scope of the study presented herein is linked with chemical evaluation of the Monovarietal Virgin Olive Oils. Assessment of quality parameters and nutritional value of olive oils from studied cultivars is presented in this paper. Such pioneering study will allow for the identification of native cultivars that produce good quality olive oil and that are very well adapted to the pedoclimatic conditions in Albania.

II.   MATERIALS AND METHODS

2.1   Sample collection and oil extraction

A total of 6 native olive cultivars, namely, *Kalinjot, Ulli i bardhe Tirana (UbT)*, *Karren*, *Nisiot*, *Kotruvs* and *Kokerrmadh Berati*, were harvested in their main area of Tirana and Kruja Regions, between October and November 2014, and prepared as described in Table 1. The climatic characteristics of the production areas, in terms of temperature, are reported in Figs. 1.
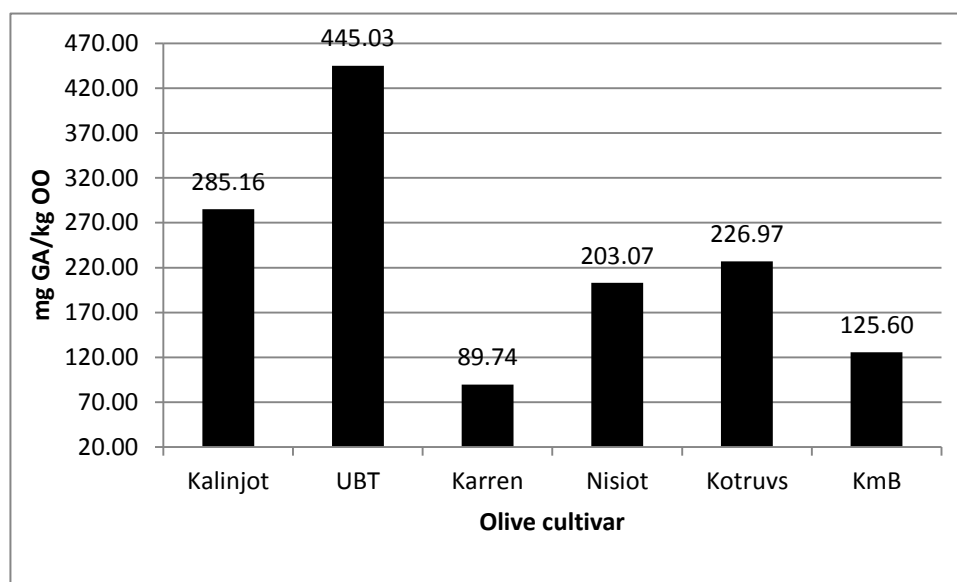
FIGURE 1: TPC OF SIX MONOVARIETAL VIRGIN OLIVE OILS OF NATIVE CULTIVAR. (UBT-ULLI I BARDHE TIRANA; KMB-KOKERMADH BERATI)

TABLE 1
OLIVE VARIETIES, HARVESTING AND EXTRACTION DAY

Code sample	Cultivar name	Harvesting day	Extraction day
Nr. 1	Kalinjot	8/11/2014	8/11
Nr. 2	Ulli Bardhe Tirana	10/10/2014	10/10
Nr. 3	Karren	12/11/2014	13/11
Nr. 4	Nisiot	12/11/2014	13/11
Nr. 5	Kotruvs	13/11/2014	13/11
Nr. 6	Kokerrmadh Berati	13/11/2014	14/11

Oil extraction was performed with a Laboratory press, under cold extraction conditions and mechanical pressing. Once the olives had been properly cleaned and washed, they were poured into the receiving hopper, where a screw activated by hand through a handle fed the crusher that was equipped with a fixed grate and a hollow knife impeller. The paste produced fell into the lower mixer, where a helicoidally shaped stirrer prepared it. A speed change gear sends the paste to the decanter

where separation took place: oil from the front and waste mixed with water from the back of the machine. The oil samples were stored in the dark at 4°C until analysis.

2.2   Chemicals

The chemical reagents were analytical grade, from Sigma-Aldrich Chemie (Steinheim, Germany). Internal standard C15:0 was purchased from Sigma-Aldrich. Gallic acid and Folin-Ciocalteau reagent were supplied by Fluka Chemie GmbH (Buchi, Switzerland).

2.3   Analytical methods

2.3.1   Determination of fatty acid profiles

Fatty acid methyl esters (FAME) were prepared through direct basic transesterification, according to IOOC, using pentadecanoic acid (C 15:0) as Internal Standard. The assay of FAME was carried out with a HP-6890 Gas chromatograph, equipped with a Flame Ionization Detector (GC-FID). Separation was achieved in a SP-2380 capillary column (60 m x 0.25 mm x 0.20 μm) from Supelco. Hydrogen was used as carrier gas at a flow rate of 1.0 ml min^{-1}. Calculations were performed according to Official Method Ce 1b-89 ([11]). Identification of FA was undertaken with pure standards (Sigma-Aldrich, Supelco), based on the comparison of retention times. Fatty acids were named by using the code *i:j(n-k)*, where *i*-indicates the total number of carbons, *j*-the number of double bonds, and *k*-the position of the last double bound counted from the terminal methyl group.

2.3.2   Determination of Total Polyphenol Content

➢   **Fractionation of olive oils**

The method used to perform the fractionation of oils was proposed by *[12]*). Briefly, samples were dissolved in n-hexane (Sigma, Germany) and extracted with a methanol/water mixture (60:40, vol/vol). The insoluble fraction (non-polar) in methanol/water fraction was removed, whereas the polar fraction was used, as it was, for further analysis.

➢   **Colorimetric determination of total polyphenol content**

The Folin-Ciocalteau method was used to determine the total polyphenol content (TPC) of samples, according to method proposed by (*[12]*). The absorbance of mixture was measured after 1 h of reaction with a UV-VIS Mini-1240 Spectrophotometer (Shimadzu) at 725 nm. Results were expressed as Gallic acid equivalent (mg/kg olive oil), calculated from the following calibration curve, determined by linear regression:

$$A_{725} = 3.015 \,[GA] + 0.005 \; (r^2 = 0.999) \tag{1}$$

where [GA] was concentration of gallic acid, expressed as mg/kg oil.

2.4   Statistical analysis

The complete data were evaluated by randomized block design, with three replicates from fatty acid analysis and duplicates for TPC values. Results were displayed as mean values and standard error (n=3). Significance of the differences among the values was determined by analysis of variance using One-way ANOVA test. The level of significance was determined at $P < 0.05$. The employed statistical program was SPSS 17.0 Statistics 2008 (SPSS Inc., Chicago, IL, USA).

III.   RESULTS AND DISCUSSION

Fatty acid profiles of the olive cultivars studied are described in Table 2. One-way ANOVA analysis showed that fatty acid profiles of the seven olive cultivars were statistically significantly different. Results revealed that, in what concerns palmitic acid (PA), the cultivars can be grouped in two groups: (i) those with lower PA content, such as Nisiot (9.94 ± 0.01%), UBT (10.88 ± 0.01%), Kokerrmadh Berati (10.41 ± 0.01%), and Kalinjoti 10.92 ± 0.17%), cultivars, and those with higher PA content, such as Kotruvs (12.21 ± 0.01%) cultivar.

The oleic acid (OA) content was as follows: 71.53 ± 0.02 *%* (Kotruvs), 74.61 ± 0.06 % (UbT), 73.94 ± 0.02% (Karren), 75.1 ± 1.21% (Kalinjot), 80.07 ± 0.04% (Nisiot). Linoleic acid (LA) content showed high variation among the studied cultivars; olive cultivars such as Kalinjot (7.56 ± 0.13%), UbT (8.00 ± 0.07%), Karren (8.35 ± 0.01%), Kotruvs (9.31± 0.01%) and Nisiot (4.10 ± 0.00%), presented low content of LA.

The alpha-Linolenic acid (ALA) was found below 1%, submitting the quality criteria of the Extra Virgin Olive Oils (EVOO). The ALA content varied according to the following ascending order: $0.45 \pm 0.01\%$ (Karren), $0.51 \pm 0.01\%$ (Nisiot and Kotruvs), $0.58 \pm 0.01\%$ (UbT), $0.72 \pm 0.02\%$ (Kalinjot), $0.67 \pm 0.01\%$ (Kokerrmadh Berati).

TABLE 2
TPC OF SIX MONOVARIETAL VIRGIN OLIVE OILS OF NATIVE ORIGIN (MG GALLIC ACID/KG OLIVE OIL)

Variety	Mean±SD
Kalinjot	285.16±3.29
Ulli i Bardhe Tirana	445.03±16.83
Karren	89.74±0.47
Nisiot	203.07±7.51
Kotruvs	226.97±1.40
Kokerrmadh Berati	125.60±6.09

A high content of ALA contributes to the n-6/n-3 ratio, a very important value for the nutritional evaluation of lipids of different origin. Regarding such ratio, the Nisiot cultivar shows a n-6/n-3 ratio of 8.11, followed by 10.31 (Kokrremadh Berati), 10.47 (Kalinjot), and 13.75 (UbT), while the remaining cultivars show higher values, Karren (18.72) and Kotruvs (18.25).

Comparison of the FA profiles of the Albanian native cultivars with those in neighbouring countries (*[7]; [13]; [14]*) and Northern Africa ([15]) gives indication that they are comparable with Italian olive cultivars, but also with other Mediterranean countries (*[7]; [13]*). For example, the level of palmitic acid in the studied native cultivars is comparable with Italian cultivars Leccino (14.3%) and Moraiolo (10.5%); Spanish cultivars Arbequina (14.3%); Lechin (10.5%) and Redondilla (12.5%), and Greek cultivar (13.3%). The level of oleic acid in Albanian cultivars is comparable with Frantoio (78.2%), Arbequina, 75.3% and Koreiniki, 71.9% (*[13]*). Related to the linoleic acid trends is not as even since the Albanian olive cultivars present content differences. The UbT content is comparable with Arbequina, Frantoio, Leccino and Koreiniki. On the other hand, the Boçi cultivar presents high content of linoleic acid comparable to the Spanish cultivars Redondilla and Lechin (*[7], [14]*).

TABLE 3
FATTY ACID PROFILE, TOTAL POLYPHENOL CONTENT (TPC), N-6/N-3 AND 18:1/18:2 RATIOS OF THE SEVEN NATIVE OLIVE CULTIVARS

Formula	Kalinjot	Ulli i Bardhe Tirane	Karre	Nisiot	Kotruvs	Kokerrmadh Berati
14:0	ND	ND	ND	ND	ND	ND
16:0	10.92±0.17	10.88±0.01	11.17±0.02	9.94±0.01	12.21±0.01	10.41±0.00
16:1(n-9)	0.09±0.00	0.07±0.00	ND	0.12±0.00	0.09±0.00	0.13±0.00
16:1(n-7)	0.48±0.01	0.35±0.01	0.36±0.00	0.41±0.00	0.82±0.00	0.61±0.00
17:0	0.04±0.05	0.13±0.00	0.14±0.00	ND	ND	ND
17:1 (n-7)	0.14±0.01	0.19±0.00	0.18±0.00	ND	ND	ND
18:0	2.31±0.03	2.83±0.01	3.22±0.01	2.56±0.01	1.96±0.01	2.10±0.01
18:1(n-9)trans	ND	ND	ND	ND	ND	ND
18:1(n-9)cis	75.11±1.21	74.61±0.06	73.94±0.02	80.07±0.04	71.53±0.02	76.26±0.07
18:1(n-7)	1.88±0.02	1.53±0.00	1.45±0.01	1.55±0.00	2.87±0.00	2.20±0.01
18:2 (n-6)cis	7.56±0.13	8.00±0.07	8.35±0.01	4.10±0.00	9.31±0.01	6.92±0.00
20:0	0.36±0.01	0.43±0.01	0.50±0.01	0.45±0.02	0.37±0.01	0.40±0.01
18:3 (n-3)	0.72±0.02	0.58±0.01	0.45±0.01	0.51±0.00	0.51±0.01	0.67±0.01
20:1 (n-9)	0.31±0.01	0.28±0.01	0.24±0.02	0.31±0.01	0.34±0.01	0.33±0.01
22:0	0.08±0.04	0.07±0.00	ND	ND	ND	ND
n-6/n-3	10.47	13.75	18.72	8.11	18.25	10.31
ΣΣSFA	13.36	14.34	15.04	12.95	14.54	12.92
ΣΣMUFA	78.01	77.05	75.94	82.46	75.65	79.53
ΣΣPUFA	8.29	8.59	9.03	4.60	9.82	7.59
18:1/18:2	9.93	9.33	8.86	19.54	7.68	11.02
MUFAs/SFAs	5.84	5.37	5.05	6.37	5.20	6.16
MUFAs/PUFAs	9.42	8.97	8.41	17.92	7.71	10.48

The ratio between monounsaturated and saturated fatty acids of the studied cultivars had an average value of 5.05 - 6.37, whereas the ratio between monounsaturated and polyunsaturated fatty acids presented an average value of 7.71-17.92 (Table 3), which are relatively low; however, the high phenol content could indicate that oil quality was maintained without lipid deterioration.

Analysis of the ratio 18:1/18:2 is another indication that refers to the oil oxidation stability. The limit value proposed is 18:1/18:2 ≥ 7.00 (*[17]*). The results show that the Monovarietal olive oils from 7.68 (Kotruvs) to 9.33 (UbT) and 19.54 (Nisiot) have acceptable oxidation stability. In conclusion all the OO from studied cultivars are above the limit value of 7.00.

Quantitative determination of phenolic compounds in olive oil was performed according to the colorimetric method Folin-Ciocalteu (*[12]*). The amount of phenolic compounds in olive oil varies from 50 to 1000 mg/kg and depends on several factors such as: climate, and extraction technology (*[6]*), cultivar (*[19]*) and degree of maturation (*[18]*).

The results for the six olive cultivars (Table 3) reveal that the highest value belongs to UbT, 445.03 ± 11.90 mg GA/kg olive oil, and the lowest value belongs to Karren, 63.02 ± 3.9 mg GA/kg olive oil. The results show that the polyphenol content of the studied olive oils had significant differences (*p*<0.05) among the cultivars. According to the classification for the olive oils proposed by Montedoro et al (*[19]*) regarding to the Total Polyphenol Content, the Karren and Kokermadh Berati cultivars can be classified in group of "low" content (50-200 mg/kg); while the next four cultivars, Kalinjoti, UBT, Nisioti and Kotruvs can be classified in the group of "medium" content (200-500 mg/kg). The obtained results from the studied cultivars can be related mainly to the cultivar differences. The geographical and pedo-climatical conditions are relatively comparable among regions were collected the olive fruits. The TPC results for UBT are comparable with Koreiniki (Greece), Picual (Spain) and Frantoio (Italy) cultivars (*[7], [13]*).

IV.   CONCLUSION

The results on the chemical composition of the studied cultivars give for the first time a comprehensive analysis of the Albanian olive cultivars. The variations, observed in fatty acid composition and phenolic compounds, are probably due to both genetic factors and environmental conditions. By comparison with results from literature, it can be concluded that the levels of fatty acids in the oils of the studied cultivars are similar to those found in the group of olive cultivars typical from Northern Mediterranean regions. In general referred to the 18:1/18:2 ratio an index of the oxidative state to the monovarietal olive oils give good consistency. The nutritional profile of *Nisioti* cultivar is highly interesting, as well as the *Kokerrmadh Berati* cultivar. The total phenolic content of the UBT is particularly of interest, with potential to be expanded beyond its territory.

REFERENCES

[1]   Kafazi, N., Muço, Dh. (1984). *Olive Culture*. Tirana. Albania: ILB, p. 0 (In Albanian).

[2]   Thomaj, F., Panajoti, Dh. (2003). *Olive cultivars*. Tirana, Albania: ILB, p 350 (In Albanian).

[3]   MAFCP. *Study on Actual Olive cultivation and its developing perspectives*. Ministry of Agriculture, Food and Consumer Protection. Tirana, (2009) p. 484.

[4]   Thomaj, F., Panajoti, Dh. (2005). Variability of Olive varieties according to the multivariate methods. *Revista Shqiptare e Shkencave Bujqesore. 6(4),* (In Albanian).

[5]   EUC. (1991). Characteristics of olive oil and olive pomace oil and their analytical methods. Reregulation EEC/2568/91. *Official Journal of European Communities, L248, 1-82.*

[6]   Boskou, D. (2006). *Olive Oil: Chemistry and Technology*. Champaign, IL, USA: AOCS Press.

[7]   Aparicio, R., Luna, G. (2002). Characterization of Monovarietal virgin olive oils. *European Journal of Lipid Science and Technology, 104,* 614–627.

[8]   Servilli, M., Montedoro, G. (2003). Contribution of phenolic compounds to virgin olive oil quality. *European Journal of Lipid Science and Technology. 105,* 403-408.

[9]   Pirisi, F. M., Cabras, P., Falqui, C., Migliorini, M., Muggelli, M. (2000). Phenolic Compounds in Virgin Olive Oil. 2. Reappraisal of the Extraction, HPLC Separation, and Quantification Procedures. *Journal of Agriculture and Food Chemistry. 48,* 1191-1196.

[10]   Mannina, L., Dugo, G., Salvo, F., Cicero, L., Ansanelli, G., Calcagni, C. (2003). Study of the cultivar –composition relationship in Sicilian Olive oils by GC, NMR, and statistical methods. *Journal of Agriculture and Food Chemistry. 51,* 120-127.

[11]   Official Method Ce 1b-89. (1994). In: *Official Methods and Recommended Practices of the American Oil Chemists' Society*, 4th edition; AOCS Press: Champaign, IL, USA.

[12]   Kalantzakis, G., Blekas, G., Pegklidou, K., Boskou, D. (2006). Stability and radical scavenging activity of heated olive oil and other vegetable oils. *European Journal of Lipid Science and Technology. 108,* 329-335.

[13] Pinelli, P., Galardi, C., Mulinacci, N., Vincieria, F. F. Cimato, A. Romani, A. (2003). Minor polar compound and fatty acid analyses in monocultivar virgin olive oils from Tuscany. *Food Chemistry. 80,* 331-336.

[14] Paz Aguilera, M., Beltran, G., Ortega, D., Fernandez, A., Jimenez, A., Uceda M. (2005). Characterization of virgin olive oil of Italian olive cultivars: 'Frantoio' and 'Leccino', grown in Andalusia. *Food Chemistry. 89,* 387–391.

[15] Haddada, F. M., Krichène, Dh., Manai, H., Oueslati, I., Daoud, D., Zarrouk, M. (2008). Analytical evaluation of six Monovarietal virgin olive oils from Northern Tunisia. *European Journal of Lipid Science and Technology. 110,* 905–913.

[16] Maestri, D. M., Labuckas, D. O., Meriles, J. M., Lamarque, A. L., Zyagadlo, J. A., Guzman, C. A. (1998). Seed composition of soybean cultivars evaluated in different environmental region. *Journal of Agriculture and Food Chemistry. 77,* 494-498.

[17] Kiritsakis, A. K., Nauos, G. G., Polymenoupoulos, Z., Thomai, T., Sfakiotakis, E. Y. (1998). Effect of fruit storage conditions on olive oil quality. *J. Amer. Oil Chem. Society, 75,* 721-724.

[18] Servilli, M., Montedoro, G. (2002). Contribution of phenolic compounds to virgin olive oil quality. *European Journal of Lipid Science and Technology. 104,* 602–613.

[19] Brenes, M., Garcia, A., Garcia Prios, J. J., Garrido, A. (1999). Phenolic compounds in Spanish olive oil. *Journal of Agriculture and Food Chemistry. 47,* 3535–3540.

[20] Montedoro, G., Servilli, M., Miniati, E. (1992). Simple and hydrolysable Phenolic Compounds in Virgin Olive oil. 1. Their extraction, separation and quantitative and semi quantitative evaluation by HPLC. *Journal of Agriculture and Food Chemistry. 40,* 1571-1576.

Probabilistic Completion Time in Project Scheduling

Min Khee Chin[1], Sie Long Kek[2], Sy Yi Sim[3], Ta Wee Seow[4]

[1]Department of Mathematics and Statistics, Universiti Tun Hussein Onn Malaysia
[2]Center for Research on Computational Mathematics, Universiti Tun Hussein Onn Malaysia
[3]Department of Electrical Engineering Technology, Universiti Tun Hussein Onn Malaysia
[4]Department of Construction Management, Universiti Tun Hussein Onn Malaysia

Abstract— *There are two common used methods to find the minimum completion time for a project scheduling. These methods are Critical Path Method (CPM) and Program Evaluation Review Technique (PERT). In CPM, a network diagram, which is Activity on Node (AON), is drawn and the slack time for every activity is calculated such that the project's critical path could be found. It is important that the critical path can suggest the shortest possible completion time. On the other hand, PERT concerns on uncertainty and risk in a project. It has three time estimates, which are optimistic, pessimistic and most likely, and all the time estimates mentioned follows the beta distribution. Besides, the probability in completing the project within certain duration is calculated by using the standard normal distribution. As the risk cannot be avoided in a project, it is important to keep track on any changes and to minimize the completion time for a project. Both of the methods are used to calculate the shortest possible completion time, slack and critical path. The difference between these methods is CPM has only one determined time estimate, while PERT has three time estimates, which shows the uncertainty in the duration of an activity in a project. For illustration, the data used for the construction of a three-room house was studied. The results show that the minimum completion time for the project is 44 days with a success probability 0.91. In conclusion, CPM and PERT are practical tool in the project scheduling.*

Keywords—Activity on Node, Critical Path Method, Program Evaluation Review Technique, Probabilistic Completion Time, Slack Time.

I. INTRODUCTION

Project scheduling is a complicated process of planning, scheduling and controlling a progressing event. The problem that deals with a project is always related to risk, which its occurrence will affect the project objective, scope, time, budget and quality [1]. Since variability is unavoidable, a project manager shall determine the risk and uncertainty before executing a project. A good estimation of project completion time is one of the solutions in diminishing uncertainty. On this basis, the project manager will be able to gauge the uncertainty and quickly adapt to any problem that might occur. The project manager should also figure out the shortest completion time in order to minimize the cost incurred. By virtue of this, two popular methods, which are critical path method (CPM) and program evaluation review technique (PERT), are applied to find the shortest completion time with consideration of risk factors and uncertainty [2]. Duration on a critical path is the possible shortest time to complete critical activities, and any delay of a critical activity will cause the impact on the project completion. Thus, critical path, which is having the least amount of scheduling flexibility, is identified by using the network diagram, that is, Activity on Node (AON) [3]. The probability of completing a project by certain time is calculated by using the standard normal distribution. Here, SAS University Edition is employed for the calculation.

The rest of the paper is organized as follows. In Section 2, the problem of scheduling for a project is described, where the activities and the corresponding time estimates are presented. In Section 3, the methods used, which are CPM and PERT, are clearly discussed. The forward and backward passes are considered in calculating the slack time such that the critical path of the activities could be determined. In Section 4, Gantt chart and network diagram AON are shown. The results show the critical path and the probabilities of the certain duration are given. Finally, some concluding remarks are made.

II. PROBLEM STATEMENT

Uncertainty is inevitable in most of the project scheduling and even an excellence project manager has difficulty to deal with the uncertainty. Every uncertainty is bringing a risk of money loss and time wastage. This situation will eventually overrun the project budget and make a project fail if it is not managed properly [4], [5]. Therefore, the project minimum completion time at a high probability to be completed should be chosen so as a target for completing a project could be set. In practice, the time estimates for construction of a three-bed room house at Nkronsa, Off the Santasi-Obuasi Road, Kumasi [6], which

are provided by the project manager from Angel Estates and Construction Ltd, are shown in TABLE 1. In order to ensure there is no budget overrun and time wastage, the project completion time must within the estimated duration.

TABLE 1
ACTIVITIES DESCRIPTION WITH THEIR PREDECESSOR AND TIME ESTIMATES

Activity	Activity Description	Immediate Predecessor	Estimated Duration (x)	Optimistic Estimate (a)	Most Likely Estimate (m)	Pessimistic Estimate (b)
A	Site clearing	-	2	1	2	3
B	Foundation	A	4	2	3.5	8
C	Block laying	B	10	6	9	18
D	Roofing	C	6	4	5.5	10
E	Plumbing	C	4	1	4.5	5
F	Electrical work	E	5	4	4	10
G	Plastering	D	7	5	6.5	11
H	Fixing up the doors and windows	E, G	9	5	8	17
I	Ceiling	C	7	3	7.5	9
J	Flooring	F, I	8	3	9	9
K	Interior Fixtures	J	4	4	4	4
L	Exterior fixtures	J	5	1	5.5	7
M	Painting	H	2	1	2	3
N	Landscaping	K, L	6	5	5.5	9

The data consists of 14 activities with their immediate predecessors and estimated durations. This project is having only an estimation of completion time including risks. Hence, the project manager should always keep tracking and setting a minimum time as a target of the completion time.

III.   CPM / PERT APPROACH

In finding a project's minimum completion time, Gantt chart is drawn to show all activities that are displayed over time. The list of activities is transferred in network diagram AON for a better understanding in terms of their duration in an order. Thus, CPM is used to calculate earliest start time (ES), late start time (LS), earliest finish time (EF) and late finish time (LF) for each activity. During the calculation, the critical path, which is the path with the shortest possible completion time, is determined. In computing ES, EF, LS, and LF, two nodes, which form a pass, need to be considered. For a forward pass,

$$ES = \max\{EF_i\}, \text{ for } i > 1 \tag{1}$$

is considered if there are more EF values from predecessors. Similarly, for a backward pass,

$$LF = \min\{ES_i\}, \text{ for } i > 1 \tag{2}$$

is considered when there are more than one of ES values from the successor. After this, slack time for each activity is computed using the following formula:

$$Slack = LF - EF = LS - ES. \tag{3}$$

Every activity's slack time is listed and those with zero slack are a critical activity. The succession path that is formed by critical activity is regarded as the critical path. The duration on the critical path is calculated and identified as minimum completion time of the project.

PERT is more advanced with three time estimations, which are optimistic (a), most possible (m) and pessimistic (b), are considered in completion time of scheduling the project. PERT is more suitable for large project with more uncertainties if compared with CPM. In PERT, the expected time TE and the variance σ are calculated by:

$$TE = \mu = \frac{a + 4m + b}{6} \qquad \text{and} \qquad \sigma^2 = \left(\frac{b - a}{6}\right)^2 \tag{4}$$

Furthermore, the probability of the completion time is then calculated by using the standard *z*-score with considering the expected time and the variance calculated. The *z*-score formula, where *d* value is any duration that the project manager desires to complete a project, is given by:

$$Z = \frac{d - \mu}{\sigma}$$

(5)

On the other hand, SAS University Edition is used in calculating the completion time and the corresponding probability as well as drawing Gantt chart, while RF Flow is used for drawing network diagram as it is a very user-friendly software and free for all users.

IV. RESULT AND DISCUSSION

Gantt chart is shown in Fig. 1, where a clear display of activities with the respective time used in managing the project, is presented.
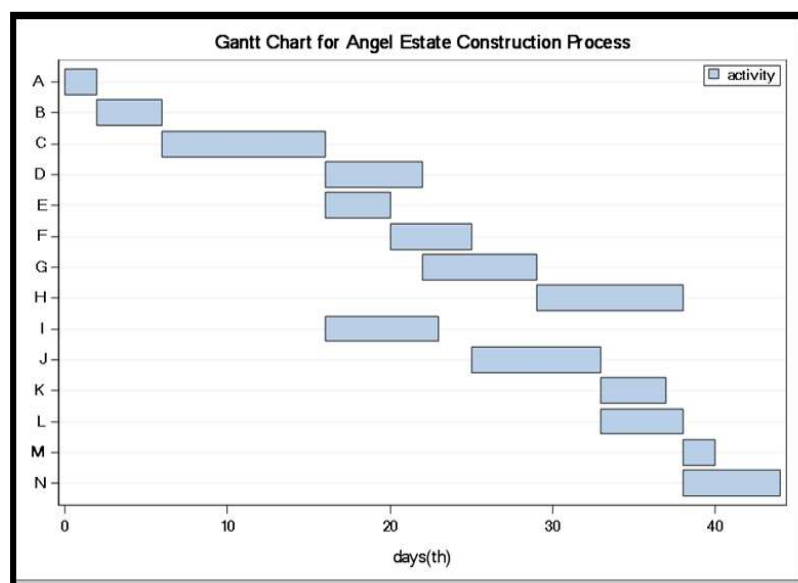

FIG. 1 GANTT CHART FOR ANGEL ESTATE CONSTRUCTION PROCESS

The network diagram AON is simpler and easy to understand. As such the duration of each activity is expressed in Fig. 2.
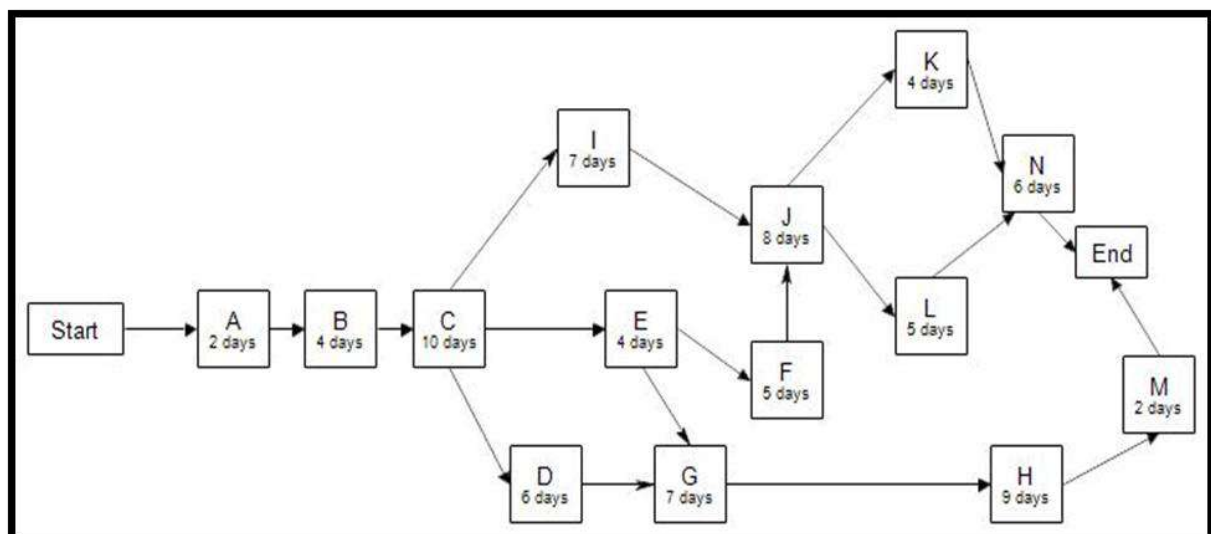

FIG. 2 AON FOR ANGEL ESTATE CONSTRUCTION PROCESS

Next, CPM is used to calculate all the ES, LS, EF and LF for determining the path with zero slack. TABLE 2 shows the calculation of ES, LS, EF, and LF. The results show that the critical path is

$$A - B - C - E - F - J - L - N$$

as these activities have a zero slack. This path has a completion time of 44 days, which is the shortest completion time in the whole project.

TABLE 2
ACTIVITIES CODE WITH THEIR ES, EF, LS, LF AND SLACK

Activity Code	Earliest Start (ES)	Earliest Finish (EF)	Latest Start (LS)	Latest Finish (LF)	Slack (LS-ES)	Critical
A	0	2	0	2	0	Yes
B	2	6	2	6	0	Yes
C	6	16	6	16	0	Yes
D	16	22	20	26	4	No
E	16	20	16	20	0	Yes
F	20	25	20	25	0	Yes
G	22	29	26	33	4	No
H	29	38	33	42	4	No
I	16	23	18	25	2	No
J	25	33	25	33	0	Yes
K	33	37	34	38	1	No
L	33	38	33	38	0	Yes
M	38	40	42	44	4	No
N	38	44	38	44	0	Yes

PERT could be used to find the probability of a project which can be accomplished within 44 days. Mean and variance for every activity that are computed by using (4) is shown in TABLE 3.

TABLE 3
ACTIVITY CODE AND THE CALCULATION OF MEAN AND VARIANCE

Activity	Optimistic Estimate (a)	Most Likely Estimate (m)	Pessimistic Estimate (b)	Critical	Mean	Variance
A	1	2	3	Yes	2	1/9
B	2	3.5	8	Yes	4	1
C	6	9	18	Yes	10	4
D	4	5.5	10	No	6	1
E	1	4.5	5	Yes	4	4/9
F	4	4	10	Yes	5	1
G	5	6.5	11	No	7	1
H	5	8	17	No	9	4
I	3	7.5	9	No	7	1
J	3	9	9	Yes	8	1
K	4	4	4	No	4	0
L	1	5.5	7	Yes	5	1
M	1	2	3	No	2	1/9
N	5	5.5	9	Yes	6	4/9

The mean is calculated by adding up all the mean values of the critical activities, as given below:

$$\mu = 2 + 4 + 10 + 4 + 5 + 8 + 5 + 6 = 44.$$

The variance is calculated by adding up all the variance values of the critical activities as follows:

$$\sigma^2 = \frac{1}{9} + 1 + 4 + \frac{4}{9} + 1 + 1 + 1 + \frac{4}{9} = 9.0.$$

By substituting the mean and the variance that are calculated from (4) into (5) to calculate the z-value, the probability that the project will be done in 44 days is 0.91.

Besides finding the probability of a given duration of the project, the corresponding duration of the project can be known by giving the probability of the time estimated. For this purpose, five values of probability and the duration are randomly selected as shown in TABLE 4. Their respective duration and probability are calculated to show the best minimum completion time for the project, where the results with some given probabilities can be obtained by calculating the duration and vice versa.

TABLE 4
CALCULATION RESULTS OF GIVEN PROBABILITY AND DURATION

Given Probability	Duration Calculated		Given Duration	Probability Calculated
0.90	50		40	0.84
0.50	40		42	0.50
0.88	50		44	0.91
0.75	50		47	0.98
0.60	40		48	0.25

(a) Duration Calculated   *(b) Probability Calculated*

As a result, the shortest completion time, which close with mean and high probability (higher than 90%), is selected. That is, the shortest completion time is 44 days with 91% completion.

V.   CONCLUDING REMARKS

In this paper, the probabilistic completion time of a project scheduling was discussed. The minimum possible completion time for the project mentioned is 44 days with the probability of 0.91. Uncertainty in the project can be minimized by applying CPM and PERT. The project manager will be able to cope with these methods as they know the use of these two approaches. CPM is more suitable for construction process as the project has fairly accurate in the time estimation. However, if it is dealing with large and high capital construction project, PERT would be a better choice. For the future usage, it is more challenging if it is including the cost in the project and taking the real data from the real-world implementing projects. This suggestion would be more practical if the knowledge can be applied in more challenging environment and increasing the value of the study.

ACKNOWLEDGEMENTS

REFERENCES

[1] Project Management Institute, The Practice Standard for Scheduling," 2008.

[2] M.T. Pich, C.H. Loch, and A.D. Meyer, "On uncertainty, ambiguity and complexity in project management," Management Science, vol. 48, iss.8, pp. 1008-1023, 2002.

[3] A. Goksu, and S. Catovic, "Implement of critical path method and project evaluation and review technique," The 3rd International Symposium on Sustainable Development, 31th May-1st June 2012, Sarajevo, Bosnia and Herzegovina.

[4] P.W.G. Morris, and G.H. Hugh, The Anatomy of Major Projects, Wiley, Chichester, U.K, 1987.

[5] M.V. Tatikonda, and S.R. Rosenthal, "Technology novelty, project complexity and product development execution success," IEEE Transaction Engineering Management, vol. 47, pp. 74-87, 2000.

[6] A. Wallace, "Project planning and scheduling using PERT and CPM techniques with linear programming: case study," International Journal of Scientific and Technology Research, vol. 1, 2015.

Investigation on Performance of Jia Bharali River Bank Protection Measure Using Geotextile Bags

Mayank Kumar Gupta

Department of Civil Engineering, University of Petroleum and Energy studies, Dehradun, Uttrakhand, India

Abstract— River bank erosion is one of the major natural disasters being faced by the state of Assam, located in the North-eastern part of India. With the increasing popularity of geotextile materials in construction industry several pilot projects to control bank erosion of major rivers of Assam have recently been executed with the application of geotextile bags, geotextile tubes. But very little scientific study on the post-construction performance of these works is available. In this paper the findings of a study on the post construction performance of one of these recently completed bank protection works is presented. In order to ascertain the erodibility of the bank soil characterisation of geotechnical properties of the bank soil is carried out. The bore log obtained by adopting a simplified method of boring suitable for this investigation is presented along with detailed laboratory test results and analysis. The change in river flow pattern near the bank after installation of the bank protection work and the resultant siltation is studied in this work. In order to predict progressive development of sand bar due to the induced siltation during the first 1 year after installation of the protection work the siltation area is surveyed and the contours are prepared. The resultant flow pattern is reasonably determined from the siltation area contours. Satellite images of the study area for a period of 3 years after installation of the protection work are analysed and presented before arriving at a final conclusion on the performance of the protection measure.

Keywords— Jia Bharali, Geotextile Bag, erodibility, river sand.

I. INTRODUCTION

Stream bank disintegration is one of the significant catastrophic events being confronted by the condition of Assam, situated in the North-eastern piece of India. In the course of the most recent 100 years compelling waterway Brahmaputra, which runs 740 km through the State of Assam, has demonstrated a general pattern of enlarging wiping out more than 4500 towns. The Brahmaputra which possessed around 4000 km2 in 1920 has extended to around 6000 km2 in 2010 along the surge fields of Assam [1]. Brahmaputra and the vast majority of its tributaries in its north bank have begun for the most part from the Himalayan range. A sudden lessening in slants of these streams as they enter its surge fields in Assam result in a lot of dregs statement, offering ascend to improvement of plaiting example of the waterway. With the initiation of surge season, the silt transport in these waterways increment, the thalweg begins to change position and geometry and area of mid-channel bars change. As the stream subsides, affidavit over the bed happens as bars and islands. The waterways stream in a few twisted directs in the middle of these sandbars.

Kotoky et al. from their review on nature of bank disintegration of the interlaced Brahmaputra waterway channel confirm noteworthy disintegration on both banks amid the period 1914–1975, while amid 1975–1998 the stream saw a prevailing period of statement.

Jiyabharali and Subansiri are two noteworthy tributaries of Brahmaputra in its northern bank. Both the two tributaries have started from the Himalayan range and have comparable plaiting trademark in the surge fields of Assam. Subansiri has drawn more consideration of scientists than Jia Bharali because of its hydro-electric power potential. Gogoi and Goswami in their investigation of bank-line movement example of Subansiri stream utilizing satellite symbolism of 1995 and 2010 found that the aggregate disintegration (82 km2) on both banks is twofold that of statement (43 km2) amid this 15-year time of study. The Subansiri stream is portrayed by substantial stream amid surge season, tremendous volume of dregs load, constant change in channel morphology, bankline relocation and horizontal changes in channels which additionally causes extreme bank disintegration prompting an impressive loss of good fruitful land each year. The immense seismic tremor that hit Assam in 1950 bothered the harmony between dregs supply and transportation of Subansiri waterway and this extra residue brought about mid-channel bar development, bank disintegration and broadening. The normal suspended silt heap of Subansiri and Jia Bharali are accounted for as 1776 and 2013 ha m, individually.

Development of goads, utilization of porcupines and stone pitching of banks are the normal measures taken up to contain bank disintegration in these waterways of Assam. Government organizations take up the essential duty of executing and

keeping up these security measures. With the expanding fame of geotextile materials in development industry a few pilot activities to control bank disintegration of significant waterways of Assam have as of late been executed with the utilization of geotextile sacks, geotextile tubes, and so on.

Mondal et al. through a contextual analysis on bank rupturing in Moyna waste bowl range of West Bengal, India, examined the physical, mechanical and geotechnical properties of the dike material and assessed existing outline system for dike dependability examination. As locally accessible soil was utilized as a part of development of the earthen banks the review found that the geotechnical properties of dike materials should have been enhanced by utilizing added substances or strengthening materials like soil–cement, characteristic or geosynthetic fiber. It was additionally recommended utilization of geotextile packs, bond composites with support for dike incline assurance.

Geotextile tubes, Geotextile packs are likewise being tested in chosen extends of banks of waterway Brahmaputra and its real tributaries. Maurya et al. have given a definite record of the current surge security and against disintegration works composed and executed utilizing geotextile to give insurance of the overnight boardinghouse disintegration of the Brahmaputra stream. Bank security taken after by a reasonable bed insurance was completed utilizing geotextile packs put on geotextile channel layer. Steel Gabions loaded with geotextile sacks were put at standard interims to confer assist steadiness to the scour assurance measure. Maurya et al. concentrated the material properties of the geosynthetics utilized as a part of stream preparing works of waterway Dibang, a tributary of Brahmaputra, and talked about the benefits of utilizing these geotextile packs over regular materials and techniques.

Very little study on the post-construction performance of these bank protection measures using geotextile bags in flood plains of river Brahmaputra is available in literature. In this work a study on the effects of Jia Bharali river bank protection work, executed by Water Resources Department of Assam under one of its pilot projects using geotextile bags, on the induced siltation and flow pattern of the river is taken up.

Research has shown that differential physical properties of cohesive and non-cohesive bank materials result in marked differences in erosion rates, erosion processes and failure modes. Although fine-grained materials are resistant to fluid shear, they tend to have low shear strength and are susceptible to mass failure. To acquire appropriate understanding of mass failure problem like erosion the characterization geotechnical properties of the bank soil is also undertaken in this work.

II.   THE STUDY AREA

A stretch of western bank of Jia Bharali river near Tezpur town of Assam had continuously been subjected to erosion every year during the floods since last several years. The progression of the river into the land due to erosion resulted in breaching of an existing embankment and was perceived as a threat to the Tezpur Central University, situated about 1.5 km away. The Water Resource Department, Assam, in the year 2012, had taken up a pilot project for protection of this stretch of the river bank. The measure consisted of installation of a launching apron up to low water level (LWL) and boulder pitching of river bank above LWL. Application of geotextile was made in the form of geotextile bags for construction of the launching apron. A satellite map of the location is shown in Fig. 1.

FIGURE 1: A SATELLITE MAP OF THE JIA BHARALI RIVER
Length of this bank protection work is 650 m, located from Lat. 26°42'53" Long. 92°51'2" to Lat. 26°43'21" Long. 92°50'58", about 12 km upstream from the point of confluence of this tributary and river Brahmaputra.

2.1   Field and Laboratory Studies

Portrayal of geotechnical properties of the stream bank soil is embraced in this work in a geotechnical examination of the Jia Bharali waterway bank soil at an area close to the insurance work under review.

The field work constituted of field soil examination up to ground water table amid the dry season. Since the profundities of disappointments because of disintegration are by and large shallow the dirt stratification in fine detail should have been gathered for suitable incline strength examination. Both wash exhausting and twist drill drilling, the most usually received subsurface drilling strategies, give very aggravated soil tests and it is hard to distinguish more slender strata of subsoil. Keeping in mind the end goal to acquire the dirt stratification information in better detail an option and rearranged system was received in this examination. In this strategy an empty aroused iron pipe of 2.5 m length, 70 mm inward measurement and 3 mm thickness was utilized and the borehole was brought around rehashed upward–downward development of the pipe into soil with the assistance of manual exertion. The pipe was removed from the borehole after each 30 cm entrance and the dirt was deliberately removed from the pipe by tenderly tapping its external body. Tests of soil were than gathered, fixed in checked holders and transported to the geotechnical designing research center of the Dept. of Civil Engineering, Tezpur University for research facility testing. The technique could be viably used to gather soil tests for profundities up to ground water table. The in situ shear quality of the bank soil at various profundities were measured utilizing field vane shear instrument. The test strategy was taken after as set down in Indian standard code of practice.

The soil samples collected from field were tested in laboratory for determination of the geotechnical properties of the river bank soil. The shear strength was determined from laboratory testing of remoulded samples prepared at field density. For determination of the shear strength direct shear test was conducted under undrained condition.

2.2   Field Surveying

In the principal year after establishment of the assurance measures new siltation was seen in the review zone shaping sand bars. Keeping in mind the end goal to concentrate the example and degree of this instigated siltation and arrangement of the sand bars field reviewing was done in the siltation range. Electronic Theodolite was utilized as a part of this looking over work. The study zone was partitioned into 20 m × 20 m matrix and diminished levels at the lattice focuses were resolved with a point of setting up a form drawing of the sand bars.

2.3   Properties of the River Bank Soil

The borehole log obtained from the field borehole is shown in Fig. 2. It shows a surface layer of silty sand soil up to a depth of 0.9 m beyond which the soil is predominantly clayey sand.

* Diameter at which soil moulded in field moisture content crumble when rolled in thread

FIGURE 2: BOREHOLE LOG OBTAINED FROM THE FIELD BOREHOLE

The ground water table was encountered at 1.46 m depth. The stratification of the bank soil could be obtained in finer detail due to adoption of the simplified method of boring.

Table 1 gives the geotechnical properties of the bank soil obtained from laboratory testing of the soil collected from field at different depths.

<div align="center">

TABLE 1
GEOTECHNICAL PROPERTIES OF THE RIVER BANK SOIL AT FIVE DIFFERENT DEPTHS

</div>

Depth from ground level (m)	Dry Density (g/cc)	Atterberg limits			Specific gravity	% Finer than (particle size)		Classificati
		LL	PL	PI		2 mm	0.075 mm	
0.3	1.33	22.8	19.8	3.0	2.70	100	30	Silty sand
0.6	1.26	36.1	30.6	5.5	2.71	97	21	Silty sand
0.8	1.45	29.5	23.3	6.2	2.76	98	33	Silty sand
1.1	1.45	32.9	23.3	9.7	2.76	92	34	Clayey sand
1.6	1.50	31.0	24.1	6.9	2.75	93	30	Clayey sand
2.7	–	–	–	–	–	–	–	–

III.   DESCRIPTION OF THE RIVER-BANK AND INSTALLED BANK PROTECTION WORKS

The detail of the protection work designed and installed at the river bank by the Water Resources Department (WRD) is shown in Fig. 3 and Table 2.
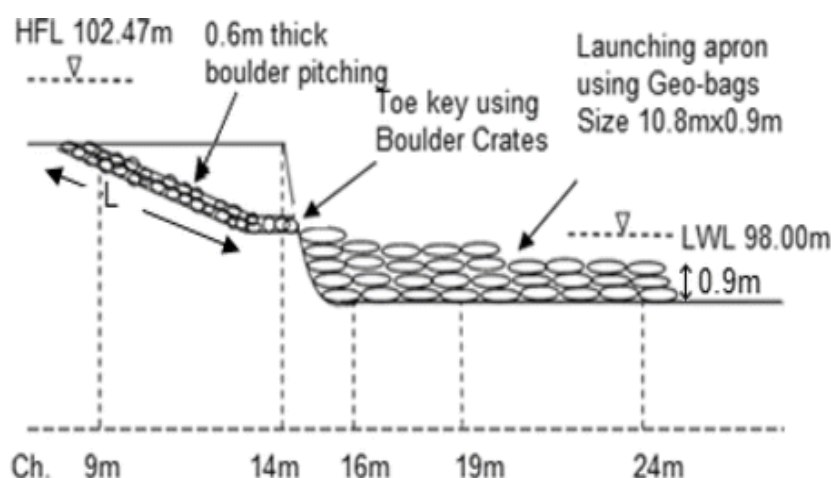

FIGURE 3: TECHNICAL DETAILS OF THE BANK PROTECTION WORK INSTALLED BY WATER RESOURCES DEPARTMENT ASSAM

TABLE 2
TECHNICAL DETAILS OF THE BANK PROTECTION WORK INSTALLED BY WATER RESOURCES DEPARTMENT ASSAM

Site: Jiyabharali river embankment at Dikoraijan near Tezpur University

Length of mitigated area: 650 m

Type of mitigation measures: boulder rip-rap and geotextile bags

Year of work: 2012–2013

Boulder pitching	Launching apron with geotextile bags
Slope of pitching: 2H:1 V	Length of launching apron: 10.80 m
Pitching thickness: 0.60 m	Thickness of apron: 0.90 m (3 layers of geotextile bags each 0.3 m thick)
0.075 m of thick metal filter bed	
Average pitching length (*L* in Fig. 3): 5.4 m	Geotextile bag filling: local sand packed to density 1.90 g/cc.

IV.   PROPERTIES AND PHYSICAL CONDITION OF GEO-TEXTILE BAG MATERIAL

Tests of unused geotextile sacks from a similar parcel of packs utilized as a part of the above venture were gathered for testing. A couple geotextile sacks, sand-filled in the year 2012, were discovered unused in the filling site in the waterway bank and were gathered for surveying their physical condition following 3 years of presentation to handle condition. The geotextile materials were tried in the research center for assurance of mass per unit territory, thickness, rigidity and cut quality. The cut quality and rigidity were tried in the CBR instrument utilizing 50 mm distance across plunger. The CBR test setup was reasonably altered as appeared in Fig. 4 to do these tests. The elasticity of the geotextile and resist disappointment was resolved from the CBR cut test utilizing the accompanying relations [14].

FIGURE 4 CBR TSSTING

$$\text{Tensile force per unit width} = \frac{\text{CBR puncture breaking force}}{2 \times \pi \times \text{radius of CBR puncturing plunger}},$$

$$\text{Strain at failure} = \frac{(x - a)}{a} \times 100 \%,$$

where x = diagonal length of the geotextile at failure; a = horizontal distance between the outer edge of the plunger and the inner edge of the mould.

The geotextile material used in the project is of nonwoven type. A general inspection of the used and unused samples of the geotextile showed that the geotextile, after 3 years of exposure to field condition, has not shown any significant deterioration. The laboratory test results are shown in Table 3.

<div align="center">

TABLE 2
RESULT OF LABORATORY TESTS CARRIED OUT ON THE GEOTEXTILE BAG MATERIALS

</div>

Properties	Test results of the geotextile bag material used in the project[a]	
	Unused material samples (stored in room condition)	**Material used in field in the year 2012 (3 years of field exposure)**
Mass per unit area (g/m²)	326	300
Thickness (mm)	2	2
CBR puncture strength (N)	1400	1200
Tensile strength (kN/m)	8.9	7.6
Strain at failure (%)	33	27

[a]Project executed in year 2012–2013 and materials tests conducted in March 2016

The results show that the nonwoven geotextile bag material used in this work, even after 3 years of field exposure, has not shown signs physical deterioration with only 15 % drop in its strength.

V. EFFECT OF THE PROTECTION MEASURES AND SILTATION AND FLOW DEFLECTION OF THE RIVER

The waterway Jiyabharali in the year 2012 ruptured around 500 m of an earthen dyke built in the western bank. The dyke was basically in charge of security of the Tezpur University and its abutting territories from waterway Jiya Bharali surge. The WRD, alongside works for shutting the rupture of the dyke, completed a stream bank insurance work utilizing geotextile packs in the area. The adjustment in waterway stream design close to the bank because of the bank security work and the resultant siltation was considered in this work.

Because of establishment of the starting cover in the waterway bed the speed of stream gets diminished close to the bank and sediment testimony begins. With the expansion in volume of the residue store the standard stream heading of the waterway continuously makes tracks in an opposite direction from the bank and siltation territory gradually augments. As the water level retreats after surge the ranges encountering most astounding residue store seem first as a sand bar over the waterway water surface. Stream water keeps on streaming around these little sand bars. As the water subsides advance the following level of sediment store zones develop over the water surface. More siltation zones develop as the waterway water level keeps on subsiding until it achieves LWL. In this way, the diverse ground heights of bars in the waterway speak to various phases of their arrangement concerning time. The profile of this dynamic development of sand bars subsequently of actuated siltation can by implication be utilized to evaluate the adjustment in stream example of the waterway after establishment of the bank assurance works.

In order to estimate the extent of this progressive sand bar formation contour drawing of the char area was prepared through detailed ground surveying. The sand bar which was formed after installation of bank protection measures in 2013

was surveyed in January 2014 in this work. The surveying was done using digital theodolite by dividing the entire area into 20 m grids. The contour map was drawn adopting the method of interpolation with a contour interval of 25 cm. Contours at elevations 99.25, 99.00, 98.75, 98.50, 98.25 and 98.00 m (LWL) are shown in Fig. 5a–f.
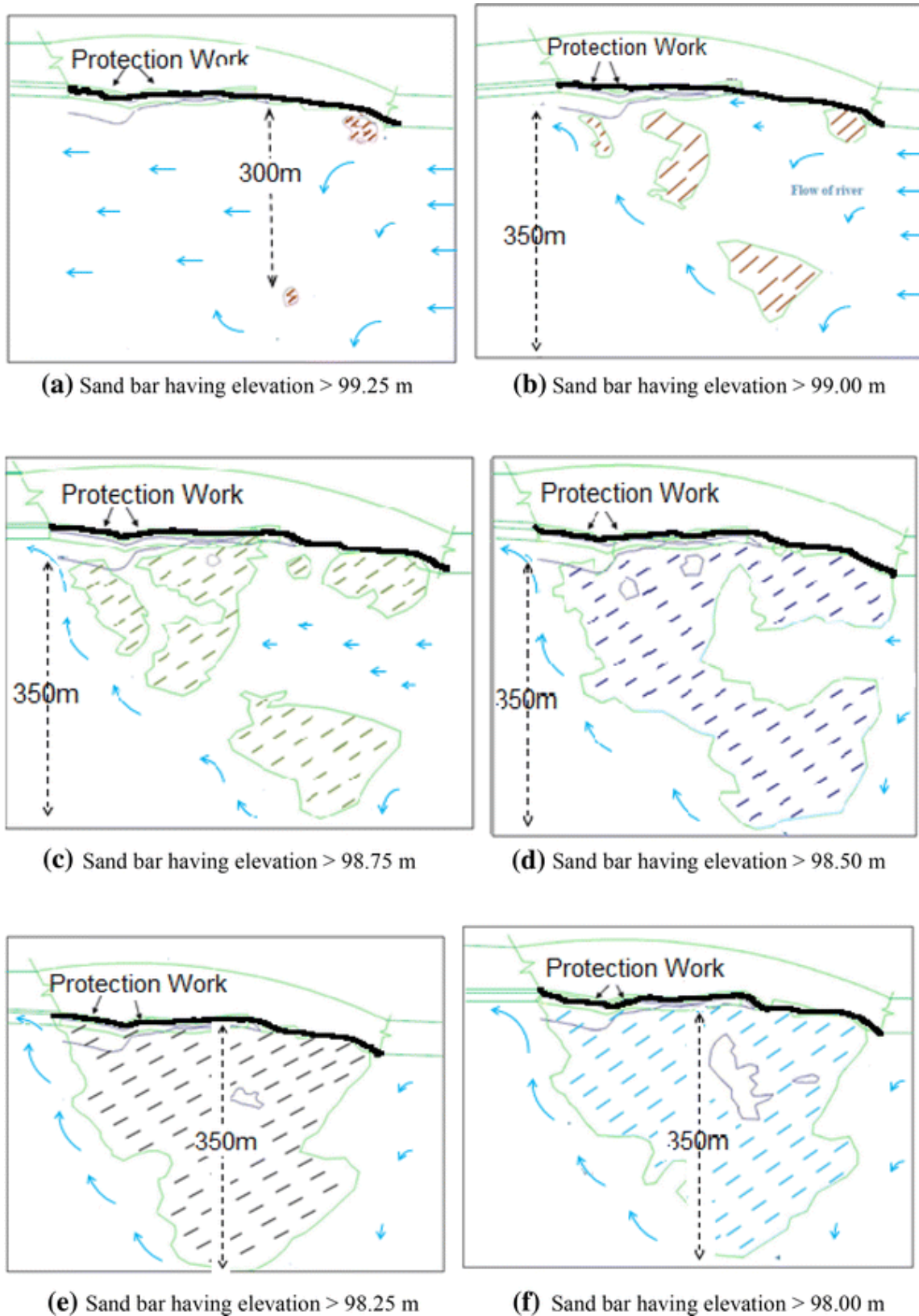

(a) Sand bar having elevation > 99.25 m

(b) Sand bar having elevation > 99.00 m

(c) Sand bar having elevation > 98.75 m

(d) Sand bar having elevation > 98.50 m

(e) Sand bar having elevation > 98.25 m

(f) Sand bar having elevation > 98.00 m

FIGURE. 5

SAND BAR HAVING ELEVATION A >99.25 M; B >99.00 M; C >98.75 M; D >98.50 M; E>98.25 M; F >98.00 M

VI.   CHANGE IN RIVER FLOW DIRECTION AFTER INSTALLATION OF PROTECTION MEASURES

The adjustment in stream example of Jia Bharali waterway in the review territory amid the period after establishment of the insurance measure is considered with the assistance of satellite photographs of the waterway accessible in Google Earth. With the assistance of Google Earth satellite photographs taken in March 2013 and March 2015 the stream example of the waterway stations and the sand bars as existed in March 2015 and March 2013 are followed out in Fig. 6a, b, individually. A correlation of Fig. 6a, b indicates new disintegration amid the period together with development of new sand bars. The degree of the zones influenced by crisp disintegration because of alter in stream course of the waterway channels and new siltation zones amid the period from 2013 to 2015 are resolved and appeared in Fig. 6c. The matrix in the figures demonstrates the latitude–longitude of the review range.
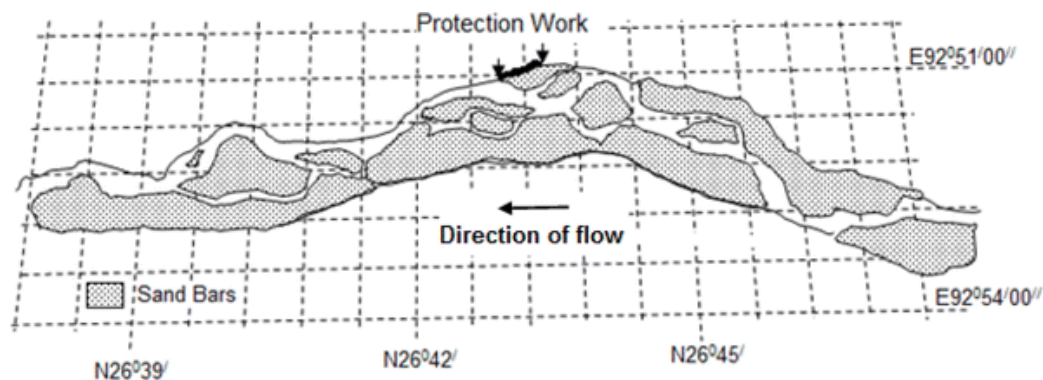
(a) Flow pattern and sand bars of Jia Bharali river in the study area as on March 2015
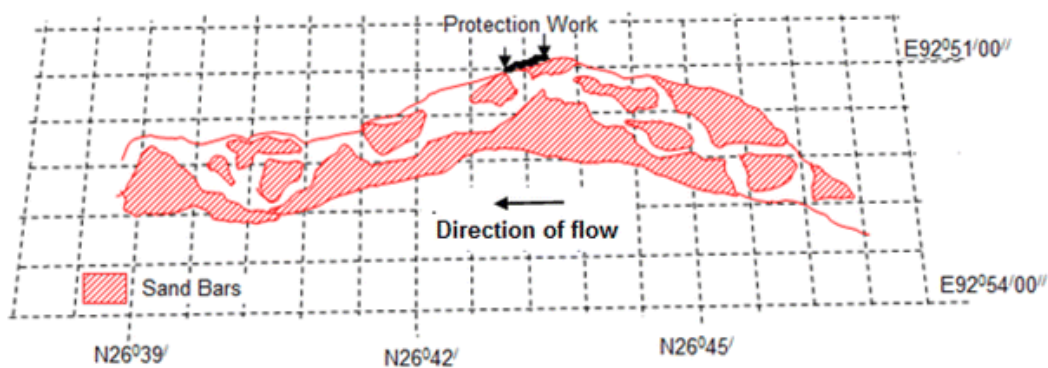
(b) Flow pattern and sand bars of Jia Bharali river in the study area as on March 2013
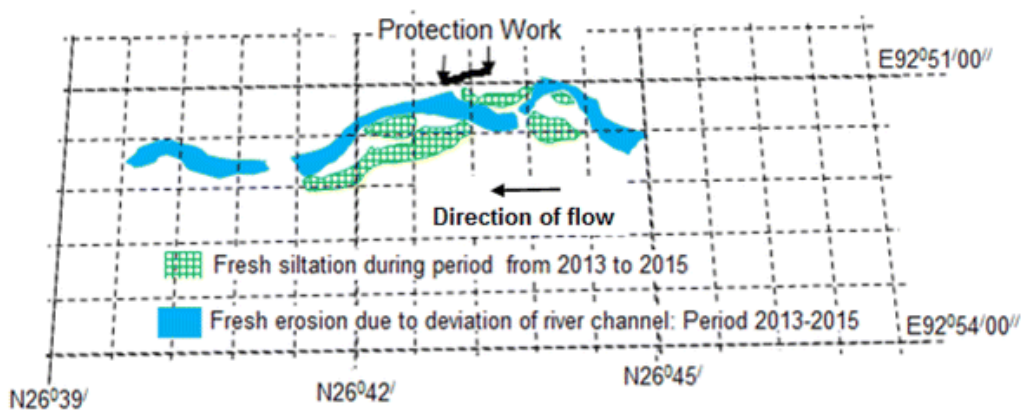
(c) Fresh change in flow direction and siltation areas during the period from 2013 to 2015

FIG. 6
FLOW PATTERN AND SAND BARS OF JIA BHARALI RIVER A IN THE STUDY AREA AS ON MARCH 2015; B IN THE STUDY AREA AS ON MARCH 2013. C FRESH CHANGE IN FLOW DIRECTION AND SILTATION AREAS DURING THE PERIOD FROM 2013 TO 2015.

VII. DISCUSSION

Two essential parts of stream bank material quality are erodibility and shear quality of the bank soil. Bank soil with low union and low versatility list (PI <15) are more vulnerable to disintegration [15]. The bank under review is constituted of soil having low PI (<10) and attachment esteem making it erodible. The shear parameters are likewise observed to be low. The in situ vane shear tests indicate marginally higher shear quality. The purpose behind this might be loss of quality because of remolding of the dirt example. The vane shear quality record demonstrates a sharp fall in the shear quality as the dirt winds up noticeably immersed. This shows the sharp loss of strength of the bank soil in the submerged condition amid surge occasions.

As the speed of stream is diminished after establishment of the bed cook's garment the primary indication of siltation is seen close to the upstream end of the bed smock (Fig. 5a). Figure 5a likewise demonstrates start of mid-channel siltation at an area around 300 m far from the bank showing redirection of the waterway stream bearing far from the insurance work. As the surge water retreats the siltation territory develops around the underlying mid-channel sand bar and furthermore close to the downstream side of the starting smock (Fig. 5b–d). It demonstrates progressive redirection of the waterway water stream channel far from the bank. Figure 5 demonstrates that the zone of impact of the bed assurance work through propelling overskirt stretches out up to remove 350 m from the bank into the stream which is about 30 times that of the 10.5 m width of the starting cover.

As the surge water subsides the stream of water is bit by bit diverted far from the bank, the reroute additionally starts siltation in the upstream of the assurance measure and the sand bar logically grows much past the upstream end purpose of the insurance measure.

Figure 5e, f demonstrates that in spite of the fact that the starting smock effectively redirected the stream water stream channel far from the bank close to the upstream end of the insurance measure and brought about advancement of another sand bars no siltation happens quickly past the downstream end of the assurance measure and the waterway channel returns strongly towards the bank just past the downstream end of the bed cook's garment. Since the bank soil is erodible, as obvious from the geotechnical testing, this sharp stream of the waterway towards the bank downstream of the security work has made it profoundly powerless against impinging stream disintegration.

Figure 6 plainly demonstrates that the waterway channel has strongly returned into the bank. This channel has begun new bank disintegration in the prompt downstream of the insurance work.

Jia Bharali stream, after establishment of the assurance measure in the western bank, has logically come nearer to a similar bank in the downstream of the security work. It, consequently, has additionally expanded the powerlessness of the bank to disintegration in quick downstream of the security measure. In this downstream segment of the stream, amid the time of 2 years from 2013 to 2015, the waterway has changed course towards the western bank bringing about bank disintegration and arrangement of mid-channel sand bars. This has made an earnest need to ensure the waterway bank facilitate downstream of the assurance work under review.

VIII. CONCLUSION

The study on the effect of installation of river bank protection measure along with bed protection using geotextile bags in river Jia Bharali has revealed the following important conclusions:

1. The protection work has successfully diverted the river from the protected bank and resulted in siltation creating a sand bar extending to a distance nearly 30 times that of the width of the launching apron.
2. Although flow of the river is diverted from the bank in the protected stretch the diverted steam has sharply come back towards the bank just beyond the downstream end of the protection work, thus, rendering the bank downstream of the protection work vulnerable to erosion.
3. The poor geotechnical properties of the bank subsoil has made it further susceptible to erosion.
4. The protection work in its downstream has adversely affected the very river bank causing erosion and gradual shifting of the major stream of the river into the bank within a period of 3 years.

From this review it is presumed that short length bank security measures with bed overskirt utilizing geotextile packs, albeit viable in ensuring a planned zone, has the capability of driving the disintegration issue towards the downstream

zone of a similar bank. Such venture arranging needs to incorporate measures to lessen downstream bank disintegration especially if the geotechnical properties of the bank soil in the downstream extend are observed to be poor.

REFERENCES

[1] Mitra AK (2010) Brahmaputra river—flood and erosion management in Assam. In: Proceeding of 26th National Convention of Civil Engineering organized by the Institution of Engineers (India), Guwahati, pp 59–73

[2] Kotoky P, Bezbaruah D, Baruah J, Sarma JN (2005) Nature of bank erosion along the Brahmaputra river channel, Assam, India. Curr Sci 88(4):634–640Google Scholar

[3] Gogoi C, Goswami DC (2013) A study on bank erosion and bank line migration pattern of the Subansiri river in Assam using remote sensing and GIS technology. Int J Eng Sci 2(9):1–6

Quantitative Study of Hydration of PPC-FA Based using Powder X-Ray Diffraction

Diptendu Roy[1], Susanta Kr. Sethy[2]

[1]Student, M.Tech/Structural Engineering, Department of Civil Engineering, UPES, Bidholi, Dehradun, 248001, India
[2]Professor, M.Tech/Structural Engineering, Department of Civil Engineering, UPES, Bidholi, Dehradun, 248001, India.

Abstract— *Pozzolana is the most commonly used mineral in cement industry. Pozzolana doesn't possess cementitious property on its own but derives its strength by reacting in the presence of moisture with calcium hydroxide formed as a result of hydration. The pozzolanic reaction is slow and required high pH and calcium ion content. This paper deals with study the PPC-FA based cement conforming to IS 1489 Part 1:2015. The LSM, AR, SR, Degree of sulphurization, Burnability Index, Burnability Factor and Percentage Liquid is obtained for the cement using X-Ray diffraction analysis. The hydration of the cement is also studied for 1 day,3 days,7 days,14 days,21 days,28 days and 56 days of curing. The samples for initial setting and final setting of cement obtained as per IS 4031 Part 5:1988 were also analysed for X-Ray diffraction analysis. The paper presents a procedure for sample preparation, X-Ray analysis of cement and cement slurries, identification of phases in cement, identification of silicate hydrates, AFm and AFt phases, percentage variation of these phases and rate of change. The changes in the phases occurring are checked by performing physical tests on cement and cement mortar cubes.*

Keywords— *pH, LSM, AR, SR, AFm, Aft, X-Ray diffraction.*

I. INTRODUCTION

The most commonly used mineral mixture cement industry is pozzolans. The pozzolans are defined as the siliceous and aluminous materials which by themselves possess very little or no cementitious property but in finely divided form in the presence of moisture, they react chemically with calcium hydroxide at ordinary temperatures to form compounds possessing cementitious properties. Chemically speaking, the pozzolanic reaction occurs between calcium hydroxide (CH) also known as portlandite and silicic acid (H_4SiO_4 or $Si(OH)_4$), their crystal structure details are given in Table 1.

$$Ca(OH)_2 + H_4SiO4 \rightarrow CaH_2SiO_4.2H_2O$$
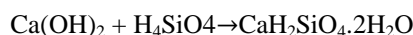
Many pozzolans also contain Aluminate $Al(OH)^-_4$,that will react with calcium hydroxide and water to form hydrates such as C_4AH_{13},C_3H_6 or hydrogarnet or in combination of silica forming stratlingite (C_2ASH_6) given in Table1.In the presence of anionic group such as sulphates, carbonates or chlorides, Afm phases and Aft phases or ettringite phases can form. The process is a long term process, sufficient amount of free calcium ion and pH of 12 and above is necessary for the solubility silicon and calcium ions and to support pozzolanic reaction.The pozzolans are classified into natural and man-made. Natural pozzolans include trass, certain pumicites and perlite which are generally of volcanic origin. The man made pozzolans include flyash, blast furnace slag and silica flume. Flyash is the most frequently used man-made pozzolan in concrete. The name flyash came from being finely divided residue that results from the combustion of ground or powdered coal.

1.1 Cement Minerals

Alite (C_3S-tricalcium Silicate) it forms the major part in cement composition about 50%.Alite has polymorphs belonging to three different families viz. Triclinic (T_1,T_2,T_3) , Monoclinic (M_1,M_2,M_3) and Rhombohedral (R) depending upon the temperature . Alite hydrated rapidly and hardens the cement slurry and provides high initial (1-3 days) and final mechanical strengths . Monoclinic (M_3) alite is similar to the mineral named Hatrurite.Belite (C_2S-dicalcium silicate) exhibits three to four polymorphs and it reacts with water and forms hydrated dicalciumsilicate . It hydrates slowly and is responsible for the strength of cement after 7 days and is responsible for providing ultimate strength of the cement. Larnite is the naturally occurring mineral similar to belite. Aluminate (C_3A-tricalcium aluminate) is the least abundant phase in a Portland cement. This phases reacts the fastest with water exothermally releasing maximum heat about 207 cal/g. If not controlled, it on immediate hydration with water is responsible for flash set and thereby making the cement paste unworkable. So, retarder such as gypsum is used.C_3A can incorporate Na^+ by substitution of Ca^{2+} ion in an otherwise vacant site, thus giving solid solutions ofgeneral formula $Na_{2x}Ca_{3-x}Al_2O_3$.Its crystal structure is cubic(x=0) but monoclinic(x=0.4375) and orthorhombic(x=0.75) aluminate also exist.

Ferrite (C_4AF-tetracalcium-aluminoferrite) phase is very similar to aluminate phase with orthorhombic crystal structure. Like Aluminates this phase is formed from the melt during cooling. At clinkering temp it facilitates the formation of silicates by increasing the ion mobility. At ordinary pressures in the absence of oxide components other than CaO , AI_2O_3 and Fe_2CO_3,

the ferrite phase can be prepared with any composition in the solid solution series $Ca_2(Al_xFe_{1-x})_2O_5$, Where $0<x<0.7$. The mineral similar in composition to ferrite is called Brownmillerite. Other minor phases present in cement include oxides such as Na_2O, K_2O, SO_3, MgO, loss on ignition, insoluble residueetc. These oxides are not present in cement in their pure form but exist in combined forms . The minerals resembling these combined phases include aphthitalite, langbeinite , arcanite, thenardite, periclase, syngenite(responsible for lumps formation in storedcement) ,calcite, anhydrite and lime (free lime).

1.2   Hydrated Products

C-S-H gel (calcium silicate hydrate) is not only the most abundant about 50% of the hydration product but is also responsible for the most of the engineering properties of the cement. Generally two different types of C-S-H gel structures has been observed found in researches done by Viehland et al[1], Slegers et al [2],Jenning et al [3] and other chemists. These two forms are in close resemblance with 1.4nm tobermorite and Jennite. A gelatinous calcium silicate hydrate, called plombierite, occurs in nature. Calcium Hydroxide (CH) is also know by mineral name portlandite. It forms form C3S and to a lesser extent form C2S. It occupies around 15-20% of the volume of the hydrated cement paste. It forms as a crystal with wide range of shapes and sizes depending upon the space available for growth.AFm are shorthand for a family of hydrated calcium aluminate phases structurally related to hydrocalumite and occurring mainly in hydrated cement paste. A representative formula is $[Ca_2(Al,Fe)(OH)_6] \cdot X \cdot xH_2O$ where X equals an exchangeable singly charged (e.g. chloride) or half of a doubly charged anion (e.g. sulfate, carbonate and aluminosilicate) . Some Fe(III) may also substitute for aluminium. The term 'mono' relates to the single formula unit of CaX_2 in another way of writing the formula, viz. $C_3(A,F).CaX_2.yH_2O$ [or $C_4(A,F)X_2.yH2O$], where $y = 2 (x + 3)$. Many different anions can serve as X, of which the most important for Portland cement hydration are OH^-, SO_4^{2-} and CO_3^{2-}. The AFm phases consists of hydroy–Afm ,hemi-carboaluminates, mono-carbo aluminate , mono-sulpho aluminate, stratlingite, vertumnite, kuzelite and Friedel's salt found in cement concrete exposed to chlorine. AFt (Al_2O_3-Fe_2O_3-tri) phases have the general constitutional formula $[Ca_3(Al, Fe)(OH)_6 \cdot 12H_2O]2 \cdot X_3 \cdot xH_2O$, where x is, normally at least, ≤ 2 and X represents one formula unit of a doubly charged, or, with reservations, two formula units of a singly charged anion. The term Aft refers to the three units of CX in an alternative way of writing the formula, C3(A, F). 3CX.yH$_2$O [or C_6 (A,F)X$_3$.yH_2O], where $y =x+30$. The most important Aft phase is ettringite, $[Ca_3Al(OH)_6.12H_2O]2-(SO_4)3-2H_2O$ or $C_3A \cdot 3CaSO_4 \cdot 32H_2O$; a phase of or near this composition is formed during the early hydration of most Portland cement. Ettringite is trigonal, with a=1.123nm, c = 2150nm, Z = 2, D_x=1775kgm^{-3}; the space group is P31c.

II.   LITERATURE REVIEW

Tomislav Matusinovic et al[4] paper deals with the environmental degradation of the concrete infrastructure.Concrete from a hydro-electric power plant's pipeline 30 years old was characterised with X-ray diffraction (XRD), and thermogravimetric analysis (TGA/DTA). The study highlights the capabilities of the methods for the analysis of concrete towards the determination of hardened cement paste degradation. XRD results showed small quantity of ettringite, calcium carbo-aluminate hydrate and Friedel's salt, and a complete leach of portlandite, while TGA results indicated small quantities of hydrates. Samples taken from flawless inside of concrete layer showed expected quantities of hydrates for the concrete.

F.Guirado et al[5] paper present the quantitative Rietveld analyses of twenty samples of CAC from four different manufacturers over the world, one synthetic mixture and a NIST standard were performed using synchrotron radiation. As compared with conventional XRD, synchrotron powder diffraction permitted to find new minor phases, improve the characterization of solid solutions of iron rich CAC phases and reduce preferential orientation and micro absorption effects

Jumate Elena et al[6] paper presents a study performed on type I Portland cement with respect to the cement hydration processes performed at various time intervals. The methods used concern X-ray diffraction and electronic microscopy applied to define materials and to understand the changes occurring in mineral compounds (alite, belite, celite and brownmillerite) during their modification into hydrated mineral compounds (tobermorite, portlandite and ettringite).

T. Matschei, B. Lothenbach and F.P. Glasser et al [7] studied the solubility and stability of AFm phases in Portland cement. The paper also gives an idea of the thermodynamic stability of the mono sulphate phases and the amount of substitution. The paper helped my research immensely in choosing the AFm phases for the study of hydration of ordinary Portland cement.

III.   EXPERIMENTAL PROGRAM

3.1   X-Ray Diffraction

The X-Ray diffraction analysis was done with Bruker's D8 Advance diffractometer. The CuKα radiation of wavelength 1.5418740 Å,theta range of 10-90 degrees, 25kV voltage and Bragg-Brentano arrangement was employed in the study. The phase quantification was done using Match software with maximum of 20 entries.

3.2   Sample Preparation

About 10 g of cement was taken out of the bag, sieved using 75 microns IS sieve, the amount passing were oven dried at 55°C for 10 minutes to remove any absorbed moisture. The cement is then enclosed and sent to the laboratory for XRD testing. 3 samples of the cement were analysed. ASTM C1365-06[8] was also referred. For the hardened cement slurries, the cement cubes were made by adding water required for standard consistence calculated as per IS:4031 Part 4-1988[9], placing in a mould, unmoulded after 24 hours and placing it in the curing tank. The cubes are then taken out of curing tank at their respective ages of curing, surface water was removed by sun drying for about 15 minutes, and then the samples were crushed to smaller bits using ball mill. Samples obtained for ball mill were further crushed and sieved using 75 micron IS sieve. The fine particles passing through 75 micron sieve were further grounded using a mortar and pestle. The ground samples are then enclosed and sent to lab for testing.

The samples for initial and final setting times as per IS 4031,Part 5-1988[10] were prepared in a slightly different manner. The samples were plastic and thus had to be oven dried at 110°C for 15 mins. Rest of the procedure is same only ball mill is not required in this case. The figure below shows an enclosed sample prior to testing. The sampling for compressive test on cement mortar was done as per IS:3535-1986. Phase selected for analysis of cement and hydrated cement pastes are given in Table 1 below. The table also gives the mineral names of the phases. The phase given in the table is chosen carefully and fully represents the various types of cement compounds formed.

TABLE 1
PHASES SELECTED FOR ANALYSIS

PHASE TYPE	PHASE		MINERAL NAME	CHEMICAL FORMULAE	CRYSTAL STRUCTURE
MAJOR CEMENT PHASES	**ALITE**		Hatrurite(M3)	$3(CaO).SiO_2$	Monoclinic
			T1-C3s	$3(CaO).SiO_2$	Triclinic
	BELITE		B-C2S/LARNITE	$2(CaO).SiO_2$	Monoclinic
			ϒ-C2S/Calcio Olivine	$2(CaO).SiO_2$	Orthorhombic
	ALUMINATE		Cubic-Aluminate	$3(CaO).Al_2O_3$	Cubic
			Orthorhombic-A	$Al_{5.175}Ca_{8.393}Fe_{0.45}Na0_{.875}O_{18}Si_{0.375}$	Orthorhombic
			Monoclinic-B	$Al_6Ca_{8.25}Na_{1.5}O_{18}$	Monoclinic
	FERRITE		Brownmillerite-A	$Al_{0.909}Ca_2Fe_{1.091}O_5$	Orthorhombic
			Brownmillerite-B	$Al_{1.346}Ca_2Fe_{0.654}O_5$	Orthorhombic
			Brownmillerite-C	$AlCa_2FeO_5$	Orthorhombic
MINOR CEMENT PHASES	**APHTHITALITE**			$K_3NaO_8S_2$	Trigonal
	LANGBEINITE			$Ca_2K_2O_{12}S_3$	Cubic
	THENARDITE			Na_2O_4S	Orthorhombic
	ARCANITE			K_2O_4S	Orthorhombic
	GYPSUM			$CaSO_4.2H_2O$	Monoclinic
	LIME			CaO	Cubic
	ANHYDRITE			$CaSO_4$	Orthorhombic
	PREICLASE			MgO	Cubic
	CALCITE			$CaCO_3$	Trigonal
	SYNGENITE			$CaH_2K_2O_9S_2$	Monoclinic
HYDRATED PRODUCTS	**C-S-H GEL**		Tobermorite	$Ca_2H_3O_{11}Si_3$	Trigonal
			Jennite	$Ca_9H_{22}O_{32}Si_6$	Triclinic
			Plombeirite	$Ca_{2.5}H_{11}O_{12.5}Si_3$	Monoclinic
	AFt		Ettringite	$Al_2Ca_6H_{64}O5_0S_3$	Trigonal
			Thaumasite	$CH_{30}Ca_3O_{25}SSi$	Hexagonal
	CH		Portlandite	CaH_2O_2	Trigonal
	Afm		Hemi Carbo Aluminate	$C_{0.25}AlCa_2O_{9.5}$	Trigonal
			Mono Carbo Aluminate	$CH_{22}Al_2Ca_4O_{20}$	Triclinic
			Stratlingite	$Al_{2.11}Ca_2H_{18}O_{16.25}Si_{1.11}$	Trigonal
			Vertumnite	$Al_{2.126}Ca2H_{22}O_{15.72Si1.434}$	Hexagonal

3.3   Phase Analysis of PPC-FA Based and PPC-FA Based Paste

The raw xrd patterns are obtained from the D8 advance spectrometer and these raw data is analysed using the Match Software. The software gives output in terms of mass percentages of the selected phases. The results obtained from the software are represented up to two decimal places. The minor phases were also identified and the results are presented in Table 2. The oxide composition of the cement was found out calculated based on the chemical formulae of the selected phases. The chemical requirements for PPC-FA based cement are given in IS 1489-Part 1:2015[11]. Cement parameters like Lime Saturation Factor (LSF), Alumina Ratio (AR), Silica Ratio (SR), Alkali content expressed as Na_2O equivalent, SO_3 content were obtained. The values of these parameters are given in Table 3.In addition to the above parameters Percentage liquid, Burnability Index and Burnability Factor is obtained. The LSF controls the ratio of alite to belite in the clinker.

A clinker with a higher LSF will have a higher proportion of alite to belite than will a clinker with a low LSF. This determines the potential relative proportions of aluminate and ferrite phases in the clinker. In ordinary Portland cement clinker, the AR is usually between 1 and 4. A high silica ratio means that more calcium silicates are present in the clinker and less aluminate and ferrite. SR is typically between 2.0 and 3.0. The degree of sulphurization for a cement as the ratio between $C3A_{cubic}/C3A_{orthorhombic}$.The degree of sulphurization depends on the percentage of alkali percent in the cement. The water consumption is greater by orthorhombic C3A and thus its rate of hydration is high.

The phase composition of hydrated cement paste was done for initial setting, final setting,1 day,3 days,7 days,14 days,21 days,28 days and 56 days of curing. The initial and final setting time of the cement was found out to be 55 minutes and 235 minutes obtained as per IS 4031-Part 5-1988.The composition in percentage by mass is given in Table 3 with varying ages of curing .The raw XRD data of samples taken at various ages of curing were analysed using Match software .

The gamma-belite is similar to olivine group which does not participate in hydration and are mostly absent in cement. For the purpose of study, it is included as one of the phases similarly monoclinic and orthorhombic aluminate are rare in cement. The background radiation for different output, diffraction peaks and unidentified peak area is also given below
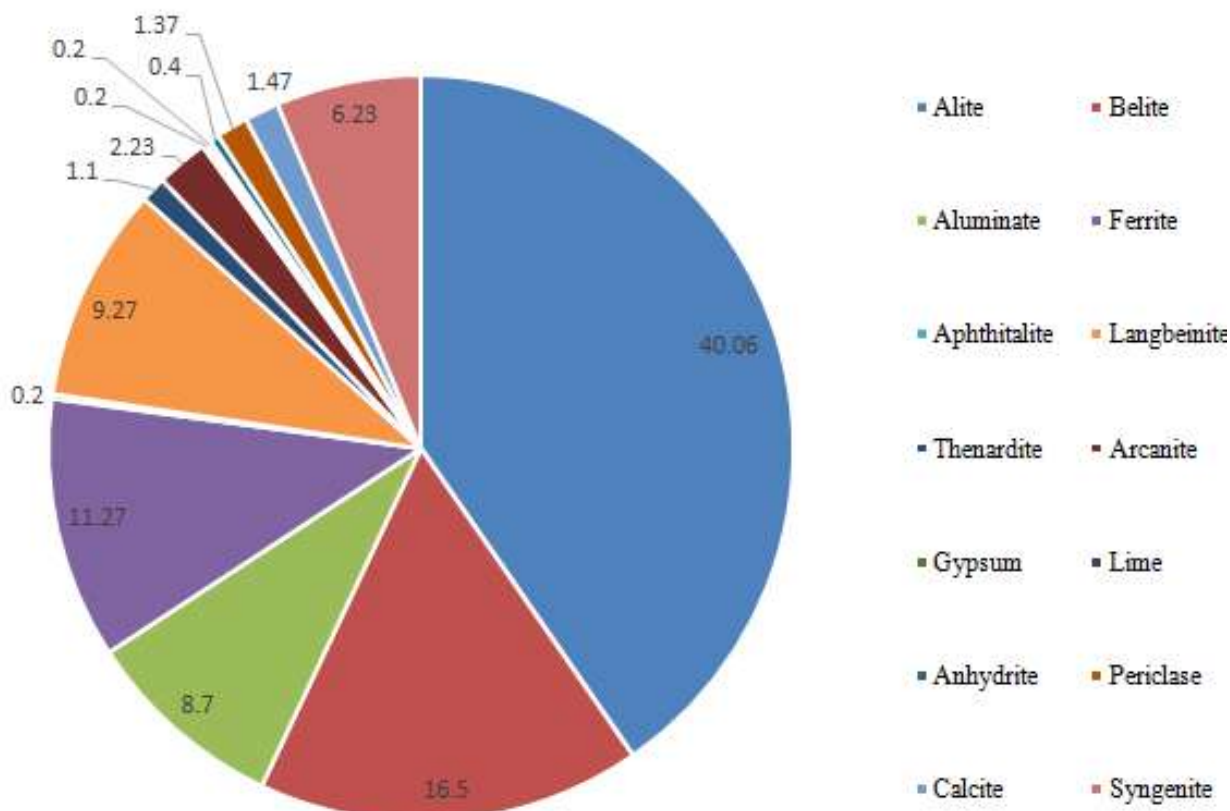
IV.   RESULTS AND DISCUSSIONS

FIGURE 1- PHASE COMPOSITION OF CEMENT

TABLE 2
PHASE COMPOSITION OF CEMENT ALONG WITH CEMENT PARAMETERS

PHASES	PERCENTAGE BY MASS	CEMENT PARAMETERS	VALUES	CODAL PROVISION
Alite(M_3+T_1)	40.06	Lime Saturation Factor(LSM)	1.1	
Belite($\beta+\gamma$)	16.5			
Aluminate (cubic+ortho+mono)	8.7	Alumina Ratio(AR)	2.48	
Ferrite	11.27	Silica Ratio(SR)	3.08	
Aphthitalite	0.2	Magnesia	1.37	6
Langbeinite	9.27	SO3	8.89	3
Thenardite	1.1	Alkali Content	4.38	
Arcanite	2.23	Percent Liquid	28.59	
Gypsum	0.2			
Lime	0.2	Burnability Index	2.25	
Anhydrite	0.4			
Periclase	1.37	Burnability Factor	14.63	
Calcite	1.47	Degree of Sulphurization	0.622	
Syngenite	6.23			

NOTE:
- M3 stands for monoclinic alite and T1 stands for triclinic alite.
- β-C2S stands is also called as larnite and γ-C2S is similar to olivine group and it doesn't participate in hydration and is rarely present in cement.
- Cubic aluminate is similar to Cyclohexa-aluminate, ortho is shorthand for orthorhombic aluminate and mono stands for monoclinic aluminate.
Both monoclinic as well as orthorhombic forms are Na^+ doped aluminates.

The *Lime Saturation Factor* (LSM) was found out to be 1.1. The LSM limits are not given in IS:1489, Part 1 , 2015.*The Alumina Ratio* (AR) is 4.8,*Silica Ratio* (SR) 3.08, *Magnesia* is 1.37 which is with the limiting value 6 as per standards, SO_3 is 8.89 which much greater than that mentioned in the code and the alkali content is 4.38.

TABLE 3
OXIDE COMPOSITION OF CEMENT

OXIDES	MASS PERCENT
CaO	60.036
SiO_2	15.552
Al_2O_3	3.604
Fe_2O_3	1.45
Na_2O	0.739
K_2O	5.529
SO_3	8.892
MgO	1.37
H_2O	1.379

The mass percent of M3 alite is39.2 while for T1alite it is 0.83. The β-C2S is 8.83% and γ-C2S is 7.67%. The mass percent of cubic aluminate is 1.2, ortho-aluminate is 1.93 and mono-aluminate is 7.67.The degree of sulphurization which is the ratio between cubic-C3A to orthorhombic-C3A is 0.622.The smaller the ratio more is the water consumption by aluminates.

TABLE 4
PHASE DATAS IN MASS PERCENTAGE WITH AGE OF CURING

PHASES	MINERAL NAME	AGE OF CURING (HOURS)									
		0^1	0.916^2	3.916^3	24	72	168	336	504	672	1344
Alite	M$_3$-Alite/ Hatrurite	39.2	7.2	7.33	9.5	7.87	3.17	5.27	2.93	3.7	1.3
	T$_1$-Alite	0.83	18.2	10.03	5.23	6.73	5.1	5.63	9.9	9.53	6.67
Belite	β-C$_2$S o/Larnite	8.83	1.3	1.87	1.83	0.13	5.33	3.83	3.8	0.17	0.87
	γ-C$_2$S /Olivine	7.67	2.07	5.43	1.63	3.47	5.5	0.9	2.53	3.1	3.63
Aluminate	Cubic-a	1.2	0	0	0	1.4	1.2	0.27	0	0.33	0.33
	Ortho-b	1.93	13.83	8.97	17.6	7.43	7.63	8.07	7.47	10.4	7.33
	Mono-c	5.57	0	0	0	0	0	0	0	0	3
Ferrite	Brownmillerite	11.3	5.07	6.03	5.77	6.57	7.23	6.23	5.97	5.33	3.8
C-S-H GEL	Tobermorite	0	6.33	4.57	5.8	9.57	8.3	9.5	5.8	7.97	8.03
	Jennite	0	19.2	23.03	21.7	21.9	19.53	24.4	21.9	18.8	24.43
	Plombeirite	0	5.17	8.57	5.57	10.7	8.37	9.77	10.2	9.03	4.7
Aft	Ettringite	0	6.57	5.5	6.73	7.73	6.33	4.87	6.93	5.93	8.13
	Thaumasite	0	0.23	0.4	0.3	0.37	0.37	0.33	0.3	0.33	4
CH	Portlandite	0	0.23	0.23	2.3	0.43	3.97	5.13	6.9	6.13	3.77
Afm	Hemicarbo-Aluminate	0	0.17	0.13	0.2	0.2	0.2	0.3	0.2	0.23	1.23
	MonoCarbo-aluminate	0	2.7	2.77	3	3.57	3.67	4.13	3.27	4.43	2.5
	Stratlingite	0	5.07	3.8	5.8	3.93	9.03	2.27	7.63	6.83	8.07
	Vertumnite	0	6.63	11.33	7.13	7.47	5.1	8.7	3.7	7.8	9.23
Diffraction Peak		98.083	96.33	96.333	96.3	96.3	96.11	96.12	94.8	95.1	96.035
Background Radiation		1.917	3.67	3.667	3.67	3.66	3.887	3.88	5.17	4.85	3.965
Unidentified Peak Area		20.823	13.54	29.923	13.4	30.1	31.22	30.59	28.5	30.2	31.005
Note:1.Composition of cement,2.Composition for initial set,3.Composition of Final set											

The Jennite phase has maximum percentage by mass in the C-S-H group, the ettringitic is the dominant phase in Aft group and the Stantlingitic and Vertumnite phases comprised almost 85% of the Afm phase for most of the ages of curing.
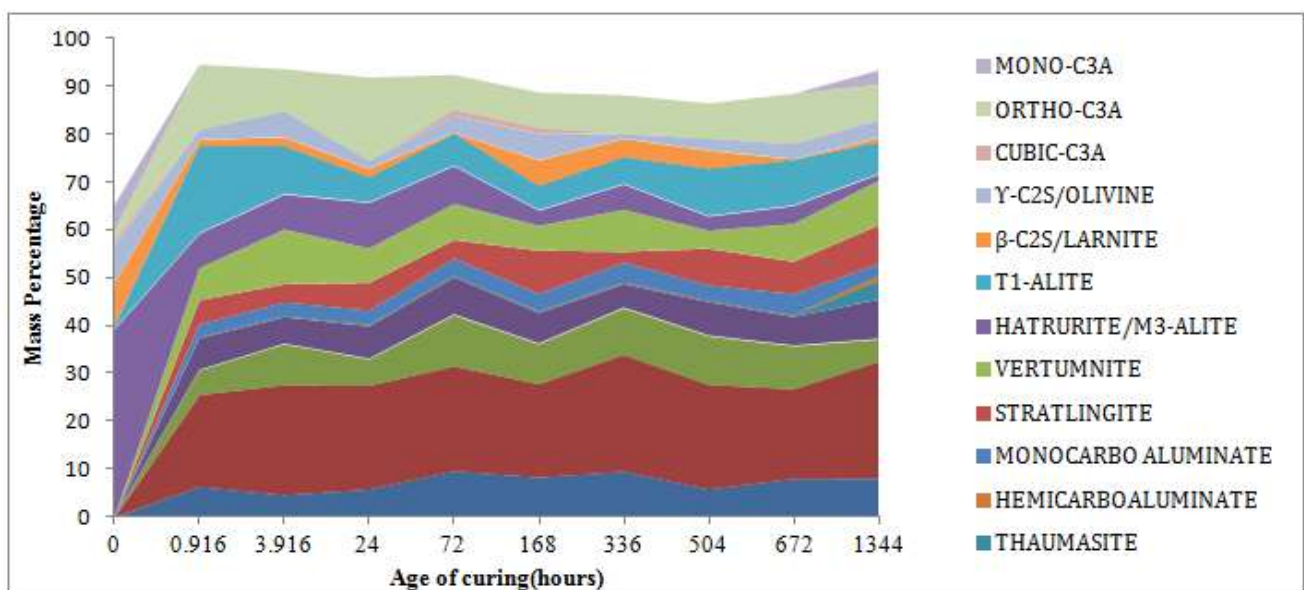

FIGURE 2- VARIATION OF PHASES WITH AGE OF CURING

The maximum value of C-S-H was obtained on 14 days of curing about 13.67% (Tobermorite = 8.03 %, Jennite =24.43% and Plombierite = 47%) by mass. The maximum value of Aft is 12.13 % (Ettringite = 8.13 % and Thaumasite = 4%) by mass on 56 days of curing. Calcium Hydroxide CH is maximum on 21 days of curing which is 6.9 % by mass and Afm phase was maximum on 56 days of curing and its value is 21.03% (Hemicarbo aluminate = 1.23 % , Monocarbo aluminate =2.5 %, Stratlingite = 8.07 % and Vertumnite =9.28%) by mass.

TABLE 5
HYDRATION INDEX VARIATION WITH INTERVALS OF 7 DAYS.

HI (Hydration Index)	1st 7 days	2nd 7 days	3rd 7 days	4th 7 days
C-S-H	0.215	0.044	-0.035	-0.013
Aft	0.04	-0.009	0.012	-0.006
CH	0.024	0.007	0.011	-0.005
Afm	0.107	-0.015	-0.004	0.027
Hydrated Products	0.386	0.027	-0.016	0.003

The *Hydration Index* (HI) is a parameter used in tis paper to define the rate of increase of phase percentages divided by the duration of 168 hours or 7 days. The HI has units *% by mass/hr* .HI also denotes the slope of curve drawn between mass percent of phases with age of curing at 168 hours of intervals. This parameter gives the slope of plot between mass percentages of phases with age of curing in hours. The Hydration Index(HI) is the most for 1st 7 days which is around 0.386 and the second most is during the 2nd 7 days of 0,027 .In the 3rd 7 days the HI is -0.016 which can be attributed due to fall in HI of C-S-H by -0.035 and fall in HI of Afm by –0.004.During the 4th 7 days, there is a marginal increase of 0.003 in the HI of the hydration products. This is due to decrease in HI of C-S-H by -0.013,Aft by -0.006,CH by -0.005 and increase of HI by Afm by 0.027.
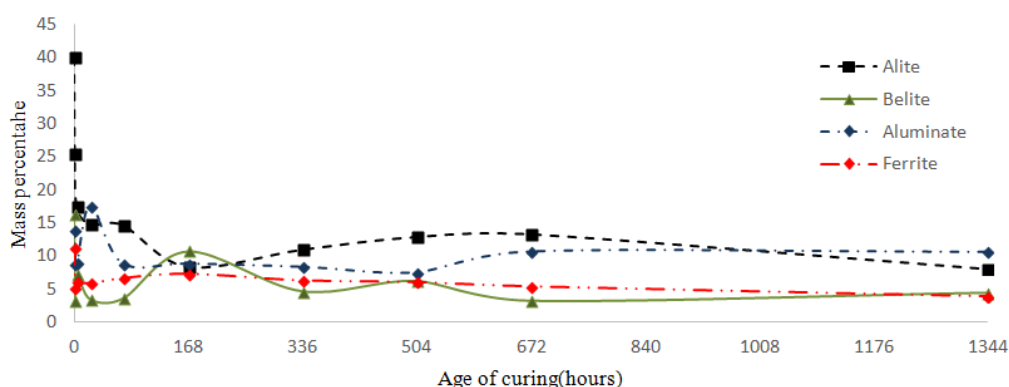

FIGURE 3-VARIARTION OF MAJOR PHASES WITH AGE OF CURING

The Figure 3 shows the variation of four major phases with the age of curing as the hydration progresses. The curves for Alite, Belite and Aluminate shows a zig-zag pattern which the Ferrite phase shows a very little variation minimum being -0.26 and maximum being -6.2 during initial setting.
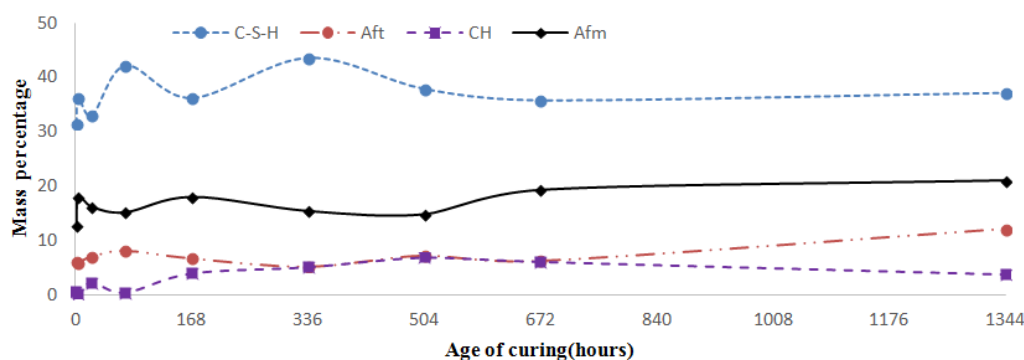

FIGURE 4- VARIATION OF HYDRATED PRODUCTS WITH AGE OF CURING

In the Figure 4, the hydration products vary rather randomly with age of curing. The most of the calcium hydroxide in lost by leaching of the sample when in water. The C-S-H gel at the end of 56 days of curing comprises of 37% of the products while there has been a jump in Aft percentage during this phase of 5.87 which is nearly its double. Afm value saw a marginal rise of 1.27 but its composition in quite high as compared to Aft. After 21 days of hydration the plot of Afm and Aft is more like a mirror image upto 56 days of curing with Afm increasing at a HI 0.027 while Aft decreasing an HI of -0.006 from 21days to 28 days.
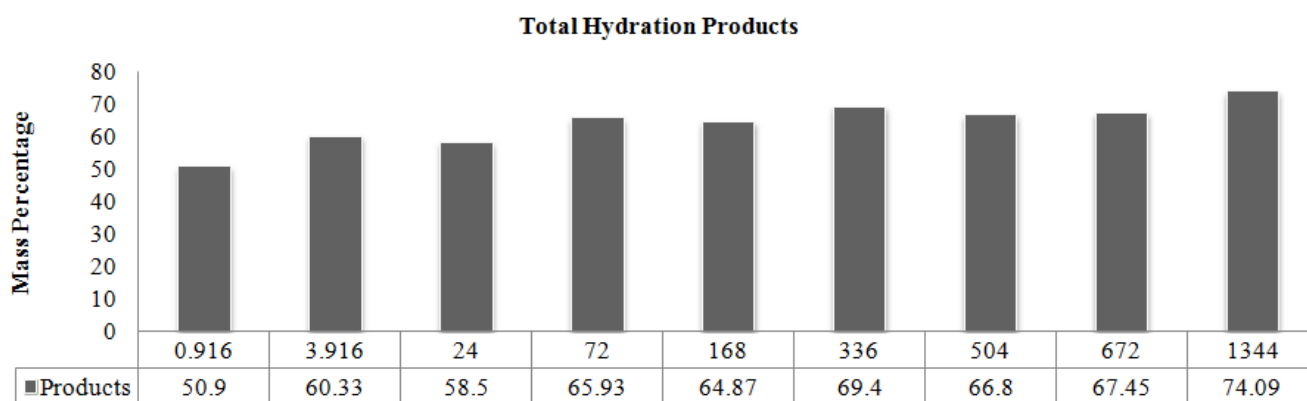

Total Hydration Products

	0.916	3.916	24	72	168	336	504	672	1344
■Products	50.9	60.33	58.5	65.93	64.87	69.4	66.8	67.45	74.09

FIGURE 5- TOTAL HYDRATION PRODUCTS FORMED WITH AGE OF CURING

There is a decrease in hydration products on day 1 by 3.033% (C-S-H=-8.65% ↓,Afm=-10.54% ↓, Aft = 19.15% ↑ and CH=900% ↑),on day 7 by 1.608% (C-S-H=-14.28% ↓,Aft=-17.28% ↓,CH = 823.26 % ↑ and Afm = 18.66% ↑) and on day 21 by -3.746%(C-S-H =-13.28% ↓, Aft=39.04% ↑, CH= 34.5% ↑ and Afm= -3.9% ↓).

The variation of the total mass percent of hydration products in given in Figure 5 .The most of the products are formed during initial setting as this is the phase of maximum heat release. The percentage increase in hydration products form initial set to final set which is about 18.527%.

The percentages are obtained taking products formed during the initial set as reference. The 2nd most and 3rd most increase was observed during period of 1 day to 3 days of 12.701 and 9.844% during 28 to 56 days. At the end of 56 days of curing the total amount of hydration products formed is 74.09% which comprises of 37.16% C-S-H , 12.13% Aft , 5.77% CH and 21.03% Aft. At the time of initial setting the total amount of hydration products were 50.9%.
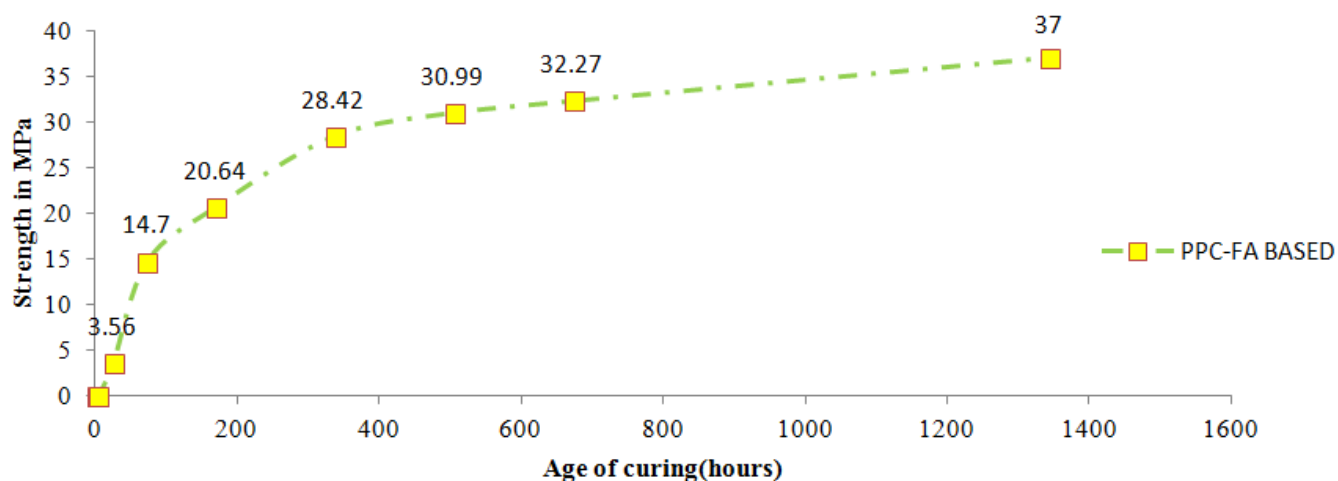

FIGURE 6- STRENGTH INCREASE FOR PPC-FA BASED

A parameter called *Strength Index* (SI) was used which gives the rate of increase in strength of the cement during the period of 168 hours or 7 days. Thus, the strength index is calculated by considering the compressive strengths obtained during the course of 1-7 days, 7-14 days, 14-21 days and 21-28 days dividing by 168 hrs. The unit being *MPa/hr*. The SI for the 1st 7 days is 0.123, 2nd 7 days is 0.022, 3rd 7 days is 0.015 and for the 4th 7 days is 0.01756.

TABLE 5
SI VARIATION WITH INTERVALS IN 168 HRS.

SI (Strength Index,MPa/hr)	1st 7 days	2nd 7 days	3rd 7 days	4th 7 days
PPC-FA Paste	0.1228	0.0463	0.0153	0.0076

The maximum increase in strength was obtained during the period 1 day to 3 days of about 312.92% followed by 40.41% during the period 3 days to 7 days and 37.39% during 7 days to 14 days.
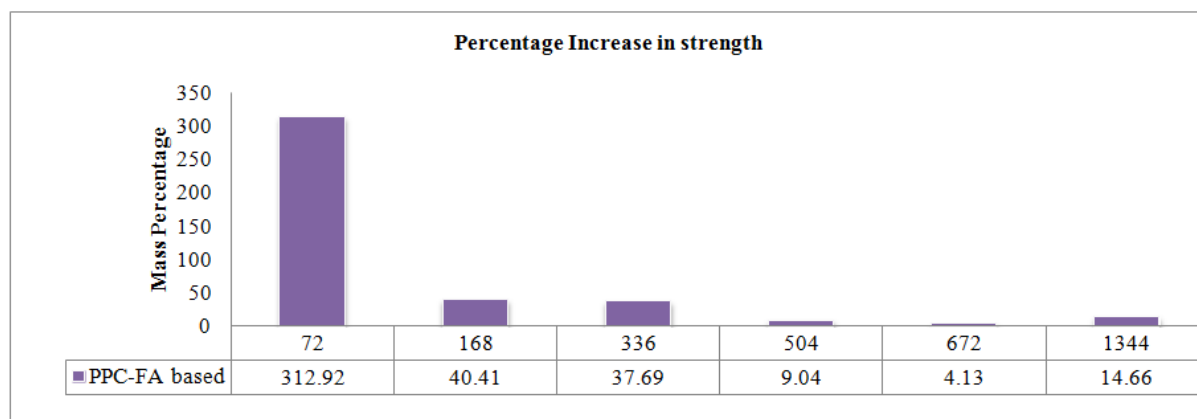

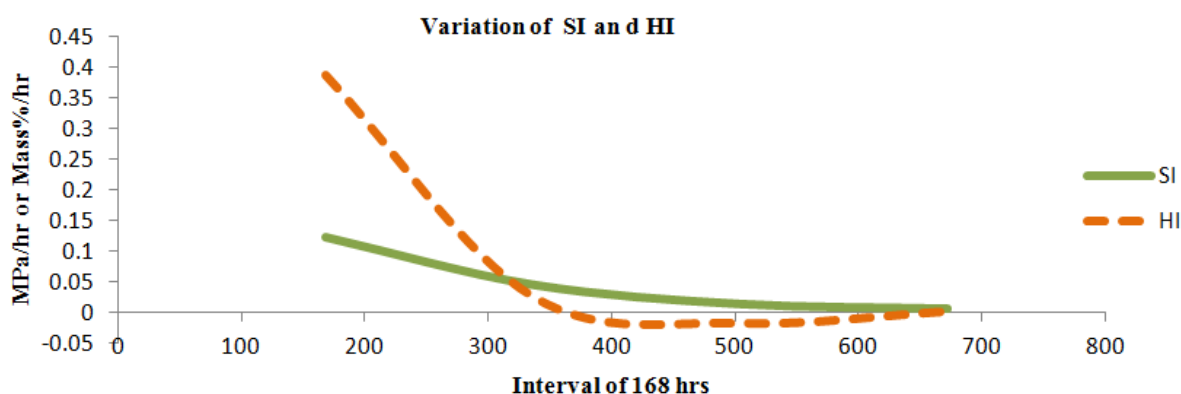FIGURE 7- PERCENTAGE INCREASE IN STRENGTH WITH AGE OF CURING

FIGURE 8- COMPARISON BETWEEN SI AND HI FOR PPC- FA BASED.

The unhydrated products percentages include, Alite=7.97% , Belite = 4.5% , Aluminate = 10.66% (the cubic aluminate is around 0.33% which the orthorhombic aluminate is 7.33% and monoclinic aluminate is 3%).The Figure: shows the plot between values for HI and SI with the interval of 168 hrs. The curves meet somewhere in between 7 and 14 days.

V.   CONCLUSION

The *Lime Saturation Factor* (LSM) was found out to be 1.1. *The Alumina Ratio* (AR) is 4.8, *Silica Ratio* (SR) 3.08, *Magnesia* is 1.37 which is with the limiting value 6 as per standards, SO_3 is 8.89 which much greater than that mentioned in the code and the alkali content is 4.38. The degree of sulphurization is about 0.62 at MgO content of 1.37.

The HI is the most for 1st 7 days which is around 0.386 and the second most is during the 2nd 7 days. In the 3rd 7 days the HI is -0.16 which can be attributed due to fall in HI of C-S-H by -0.035 and fall in HI of Afm by −0.004. During the 4th 7 days, there is a marginal increase of 0.003 in the HI of the hydration products. This is due to decrease in HI of C-S-H by -0.013,Aft by -0.006,CH by -0.005 and increase of HI by Afm by 0.027.

There is a decrease in hydration products on day 1 by 3.033%, on day 7 by 1.608% and on day 21 by -3.746%. The most of the products are formed during initial setting as this is the phase of maximum heat release. The percentage increase in hydration products form initial set to final set which is about 18.527%.

There is increase in compressive strength of the cement with age of curing. The chage being drastic during the initial stages which smoothes with passage of time. The maximum increase in strength was obtained during the period 1 day to 3 days of about 312.92% followed by 40.41% during the period 3 days to 7 days and 37.39% during 7 days to 14 days. The SI for the 1st 7 days is 0.123, 2nd 7 days is 0.022, 3rd 7 days is 0.015 and for the 4th 7 days is 0.01756.

At the end of 56 days of curing the total amount of hydration products formed is 74.09%.At the time of initial setting the total amount of hydration products was 50.9%.The unhydrated products percentages include, Alite =7.97% , Belite = 4.5% , Aluminate = 10.66% (the cubic aluminate is around 0.33% which the orthorhombic aluminate is 7.33% and monoclinic aluminate is 3%).

REFERENCES

Book Chapters

[1]   H.F.W Taylor, " Cement chemistry" 2nd Edition , Chapter 3.1.3,Page 57-60.

[2]   H.F.W Taylor, " Cement chemistry" 2nd Edition , Chapter 3.1.3,Page 57-60.

[3]   H.F.W Taylor, " Cement chemistry" 2nd Edition , Chapter 5.3.5,Page 128.

Journal Articles

[4]   Neven Ukrainczyk , Marko Ukrainczyk , Juraj Šipušić , Tomislav Matusinović "XRD and TGA investigation of Hardened Cement Paste Degradation , "Conference on Materials , Processes, Friction and Wear , MATRIB'06 , Vela Luka, 22-24.06.2006.

[5]   F.Guirado , S.Galí ," Quantitative Rietveld analysis of CAC clinker phases using synchrotron radiation", Elsevier Journals,Cement and Concrete Research 36 (2006) 2021-2032

[6]   Jumate Elena, Manea Daniela Lucia "Application of X-Ray Diffraction (XRD) and Scanning Electron Microscopy (SEM) methods to the Portland Cement Hydration processes," Journal of Applied Engineering Sciences,Volume 2(15), Issue 1/2012,PP 35-42.

[7]   T.Matschei ,B.Lothenbach ,F.P.Glasser,"AFm phases is Portland Cement " ,Elsevier Jornals ,Cement and Concrete Research 37(2007)118-130.

Standards

[8]   ASTM C 1365-06 "Determination of the proportion of phases in Portland Cement and Portland Cement Clinker using X-Ray powder diffraction Analysis.

[9]   IS 4031, Part 4:1988, " Methods of Physical Tests for Hydraulic Cement - Part 4 , Determination of Consistency of standard cement paste.

[10] IS 4031, Part 5:1988, " Methods of Physical Tests for Hydraulic Cement Part 5, Determination of Initial and Final Setting times".

[11] IS 1489(Part 1)-2015," PPC-FA specifications".

[12] IS 4031, Part 6:1988 , " Methods Of Physical Tests For Hydraulic Cement Part 6 Determination of compressive strength of hydraulic cement other than masonry cement.